UNIVERSIDADE ESTADUAL DE CAMPINAS
Faculdade de Engenharia Mecânica

MARINA WEYL COSTA

Physicochemical properties and numerical study on combustion of n-decane - ethanol - methyl-decanoate blends

Propriedades físico-químicas e estudo numérico da combustão de misturas de n-decano - etanol - metil decanoato

CAMPINAS
2016

MARINA WEYL COSTA

Physicochemical properties and numerical study on combustion of n-decane - ethanol - methyl-decanoate blends

Propriedades físico-químicas e estudo numérico da combustão de misturas de n-decano - etanol - metil decanoato

Dissertation presented to the School of Mechanical Engineering of the University of Campinas in partial fulfillment of the requirements for the degree of Master in Mechanical Engineering, in the area of Thermal and Fluid Engineering.

Dissertação apresentada à Faculdade de Engenharia Mecânica da Universidade Estadual de Campinas como parte dos requisitos exigidos para obtenção do título de Mestra em Engenharia Mecânica, na Área de Térmica e Fluidos.

Advisor: Prof. Dr. Rogério Gonçalves dos Santos
Co-advisor: Prof. Dr. Dario Alviso

ESTE EXEMPLAR CORRESPONDE À VERSÃO FINAL DA DISSERTAÇÃO DEFENDIDA PELA ALUNA MARINA WEYL COSTA, ORIENTADA PELO PROF. DR ROGÉRIO GONÇALVES DOS SANTOS E COORIENTADA PELO PROF. DR DARIO ALVISO.

CAMPINAS
2016

Ficha catalográfica
Universidade Estadual de Campinas
Biblioteca da Área de Engenharia e Arquitetura
Luciana Pietrosanto Milla - CRB 8/8129

Informações para Biblioteca Digital

Título em outro idioma: Propriedades físico-químicas e estudo numérico da combustão de misturas de n-decano - etanol - metil decanoato
Palavras-chave em inglês:
Combustion
Chemical kinetics
Ethanol
Surrogate
Petroleum as fuel
Área de concentração: Térmica e Fluídos
Titulação: Mestra em Engenharia Mecânica
Banca examinadora:
Rogério Gonçalves dos Santos [Orientador]
Waldir Antonio Bizzo
Amir Antônio Martins de Oliveira Junior
Data de defesa: 14-07-2016
Programa de Pós-Graduação: Engenharia Mecânica

UNIVERSIDADE ESTADUAL DE CAMPINAS

FACULDADE DE ENGENHARIA MECÂNICA

COMISSÃO DE PÓS-GRADUAÇÃO EM ENGENHARIA MECÂNICA
DEPARTAMENTO DE ENERGIA

DISSERTAÇÃO DE MESTRADO ACADÊMICO

Physicochemical properties and numerical study on combustion of n-decane - ethanol - methyl-decanoate blends

Propriedades físico-químicas e estudo numérico da combustão de misturas de n-decano - etanol - metil decanoato

Autora: Marina Weyl Costa

Orientador: Prof. Dr. Rogério Gonçalves dos Santos
Coorientador: Prof. Dr. Dario Alviso

A Banca Examinadora composta pelos membros abaixo aprovou esta Tese:

Prof. Dr. Rogério Gonçalves dos Santos, Presidente
UNICAMP/FEM

Prof. Dr. Waldir Antonio Bizzo
UNICAMP/FEM

Prof. Dr. Amir Antônio Martins de Oliveira Júnior
UFSC/CTC/EMC

A Ata da defesa com as respectivas assinaturas dos membros encontra-se no processo de vida acadêmica da aluna.

Campinas, 14 de julho de 2016.

Dedication

To my parents, Merce and João, who always supported me. Even when I decided I didn't want to go to med school. Even when I changed my major after two years in college. Even when I left that job. Even hating my tattoos and my blue-green hair.

You always believed in me, and gave me wings to fly and a place to come back. I really love you.

... And to my sister, Livia, who was jealous because her name was not in the first version of this dedication. And then she threatened me not to visit me never more. Love u, sis <3

Acknowledgments

This work would not be possible without the contributions of some people and entities, to whom I would like to thank:

- My advisor, Rogério. Thank you for all the support and motivation: from the first understanding of the problem to be solved to the careful reading of this work. Thank you for always being gentle and attentive. Thank you for being a great teacher and human being.

- My co-advisor, Beto. Thank you for all the academic help, especially in the understanding of REGATH operation and combustion modeling. Thank you for being a great host for me and Rodolfo during our internship in FIUNA, always trying to improve our stay. I miss the chipas.

- FIUNA team. Thank you for make the internship possible. It was an important experience and I learned a lot.

- Professor Darabiha, from EM2C/Centrale Supelec. Thank you for not only allow us to use REGATH, but also for being very kind spending time teaching us how to do it.

- Lab Extrae (FEA-Unicamp), especially Professor Guilherme and the technician Patrícia. Thank you for allowing me to use the lab equipment, for the suggestions of how to develop the experimental part of this work and for the training.

- My colleague Rodolfo, who shared the study room with me. Thank you for the exchange of ideas, that helped the progress of both our works. Also, thank you for all the non-academic talk: thank you for our political disagreements, for the "crushes" stories and for all the laughs.

- My friends. Thank you for kidnapping me from the lab or from the front of the computer and making me remember that there is a world outside. Thank you for the talks and drinks and ice-creams and more drinks. Thank you for believing in my capacity even don't understanding what my job was. Thank you for saving me from loneliness and boredom.

- My family. Thank you for the love and support.

- The members of the examining board and Professor Gustavo Valença, who was in the qualification examining board. Thank you for the interest in this work and the improvement suggestions.

- CNPq. Thank you for financing my scholarship.

Don't let anyone rob you of your imagination, your creativity, or your curiosity. It's your place in the world; it's your life. Go on and do all you can with it, and make it the life you want to live.

Mae Jemison, the first African-American woman to travel in space.

Resumo

Foram estudados três combustíveis: n-decano (apresentado na literatura como simulacro de querosene, ou como o principal componente de simulacros de diesel), etanol e metil decanoato (apresentado na literatura como um simulacro de biodiesel) e suas misturas (base mássica). Ensaios de solubilidade foram feitos para todas as misturas possíveis, passo 10%, com etanol anidro e etanol hidratado. Todas as misturas de etanol anidro são estáveis em $T = 25°C$ e $T = 5°C$. A mistura máxima de etanol hidratado solúvel em $T = 25°C$ foi 10% etanol + 40% metil decanoato + 50% de n-decano. Nenhuma mistura com 50% ou mais n-decano foi estável em $T = 5°C$. Os testes de densidade foram feitos para as misturas E10 (80% n-decano + 10% etanol + 10% metil decanoato); E20 (70% n-decano + 20% etanol + 10% metil decanoato) e E30 (60% n-decano + 30% etanol + 10% metil decanoato) em três temperaturas. Tanto a adição de etanol quanto o aumento de temperatura diminuiram as densidades. Um novo modelo de cinética química com 258 espécies e 1586 reações foi desenvolvido combinando três modelos dos combustíveis estudados encontrados na literatura. Velocidade laminar de chama simulada em uma chama 1D pre-misturada foi o parâmetro escolhido para validar o novo modelo. O novo modelo estava mais próximo de dados experimentais encontrados na literatura do que os modelos originais de n-decano e metil decanoato. Para o etanol (usado como esqueleto do novo modelo), o novo modelo estava próximo dos dados da literatura e do modelo original. Depois da validação, a velocidade laminar de chama simulada dos simulacros foi comparada com dados experimentais dos combustíveis alvo encontrados na literatura. N-decano reproduziu o comportamento do querosene, mas não do diesel. O metil decanoato aproximou-se pouco do biodiesel. As misturas E10, E20 e E30 foram comparados com combustíveis puros. Os resultados para velocidade laminar de chama se aproximaram do n-decano. A configuração contracorrente foi simulada variando velocidades de injeção e relações de equivalência para os combustíveis puros e misturas. O aumento de ϕ aumenta a temperatura máxima da chama e a geração de CO e $HCOOC$ para n-decano e misturas. Nas misturas, a produção de CH_2O e CH_3CHO também aumenta com ϕ. A geração de H_2O e CO_2 não varia com ϕ. O aumento da velocidade de injeção muda velocidade axial máxima, mas não o perfil de velocidade. Nas mesmas condições de operação, temperatura máxima e perfis de velocidade, HCO, CO e CO_2 foram os mesmos para n-decano e misturas. A adição de etanol aumenta a formação $HCOOC$. Metil decanoato aumenta a produção de CH_3CHO e tanto etanol quanto metil decanoato aumentam a produção de CH_2O.

Palavras-chave: Combustão, Cinética Química, Etanol, Simulacro, Petróleo com combustível.

Abstract

Three fuels and their blends (weight basis) were studied: n-decane (presented in literature as a kerosene surrogate, or as the main component of diesel surrogates), ethanol and methyl decanoate (presented in literature as a biodiesel surrogate). Solubility tests were made for all possible blends, 10% step, using anhydrous ethanol and hydrated ethanol. All anhydrous ethanol blends were stable at $T = 25°C$ and $T = 5°C$. Maximum soluble blend of hydrated ethanol at $T = 25°C$ was 10% ethanol + 40% methyl decanoate in 50% n-decane. No blend with 50% or more n-decane was stable at $T = 5°C$. Density tests were made for blend E10 (80% n-decane + 10% ethanol + 10% methyl decanoate) ; E20 (70% n-decane + 20% ethanol + 10% methyl decanoate) and E30 (60% n-decane + 30% ethanol + 10% methyl decanoate) at three temperatures. The addition of ethanol and the increase of temperature decreased densities. A new chemical kinetic model with 258 species and 1586 reactions was developed by the combination of three models found in literature for the studied fuels. Laminar flame speed simulated in a 1D premixed flame was the parameter chosen to validate the New Model. The New Model simulation was closer to experimental data found in literature then the original models for n-decane and methyl decanoate. For ethanol (used as New Model skeleton), New Model simulations were close to original model simulation and experimental data. After validate the model, laminar flame speed simulated for surrogates was compared with experimental laminar flame speed data of target fuels found in literature. N-decane reproduced kerosene behavior, but not diesel. Methyl decanoate simulation approached little biodiesel experimental data. Blends E10, E20 and E30 were compared with pure fuels. Blends laminar flame speed are close to pure decane. The counterflow configuration was simulated at different injection velocities and equivalence ratios for pure fuels and blends. The increase of ϕ increases maximum flame temperature and the generation of CO, $HCOOC$ for both n-decane and blends. In blends, CH_2O and CH_3CHO production also increases with the increase of ϕ. H_2O and CO_2 generation do not varies ϕ. The increase of injection speed changes maximum axial velocity, but not change the velocity profile. Blends maximum temperature, velocity profile, HCO, CO and CO_2 profile were the same observed for n-decane at same ϕ and injection velocity. The addition of ethanol increases $HCOOC$ formation. Methyl decanoate increases CH_3CHO production and both ethanol and methyl decanoate increase CH_2O production.

Keywords: Combustion, Chemical Kinetics, Ethanol, Surrogate, Petroleum as fuel.

List of Figures

List of Tables

List of Abbreviations and Symbols

a	Polynomial coefficient
A	Pre-exponential factor
ANP	National Petroleum Agency
bhp	brake horsepower
bsfc	brake specific fuel consumption
CI	Compression ignition
C_p	Specific heat
$D_{k,j}$	Binary diffusion coefficient
e	Internal energy
E	Activation energy
e_t	Total energy
E10	Blend of 10% ethanol + 80% n-decane + 10% methyl decanoate (weight basis)
E20	Blend of 20% ethanol + 70% n-decane + 10% methyl decanoate (weight basis)
E30	Blend of 30% ethanol + 60% n-decane + 10% methyl decanoate (weight basis)
f_v	Forces acting on the body
H	Enthalpy
i	Subscript relative to each reaction
J	Radial pressure
k	Subscript relative to each specie
k_f	Rate constant of a chemical reaction
MD	Methyl decanoate
n	Number of moles o
Superscript relative to standard-state 1atm	
OPEC	Organization of Petroleum Exporting Countries
p	Pressure
PROÁLCOOL	National Alcohol Program
PM	Particulate matter

q	Heat flux
Q	Energy brought by a heat source
R	Ideal gas constant
RIF	Representative Interactive Flamelet
S	Entropy
SCTP	Standard Conditions for Temperature and Pressure
t	Time
T	Temperature
v	Velocity
V	Diffusion velocity
W	Molar mass
X	Molar concentration
Y	Mass fraction
β	Temperature exponent
λ	Thermal conductivity of the mixture
μ	Dynamic viscosity
ν	Stoichiometric constant (integer)
ρ	Density
σ	Surface stress tensor
τ	Viscous stress tensor
ϕ	Equivalence ratio
ω	Molar production rate

Summary

1 INTRODUCTION

In the present work, three pure substances were studied: n-decane, ethanol and methyl decanoate. The aim of this introduction is to justify the importance of the developed study. Section 1.1 presents the past and current use of diesel and kerosene in Brazil and in the world, and explains why n-decane was studied instead of the real fuels. Section 1.2 reports ethanol history and present its role in Brazilian energy matrix and the advantages in expand its use to another types of engines. Section 1.3 explains why studies of blends of diesel and ethanol are also interested in biodiesel, and why methyl decanoate is used in the place of biodiesel in several works. Finally, section 1.4 presents which objectives were achieved in this study and its layout.

1.1 Diesel, kerosene and n-decane

The current compression ignition (CI) engines were developed using original diesel cycle, conceived by Dr Rudolf Diesel; and some concepts created by the engineer Herbert Akroyd-Stuart, who presented in 1891 the first oil engine to run without a spark for ignition. It needed an external heat source to start. CI engines invented by Diesel used a higher compression rate in order to achieve a higher thermal efficiency in comparison with spark-ignited engines. Original Diesel's CI engines would be able to use several types of fossil fuels: oil derived from bituminous coal, crude oil, kerosene, pulverized coal and even gasoline. In fact, gasoline was the fuel used in the initial tests, in 1893. It succeed in starting combustion by compression, but this caused some mechanism pieces to dismantle (Owen and Coley, 1995).

First CI engines using diesel were heavy and slow, and were used mainly in marine, industrial and railway installations. Diesel road vehicles development started in Europe after a gasoline shortage in 1918. Diesel trucks and buses already were common by the mid-1930s. Diesel passenger cars became common after World War II. After 1960, the number of passenger cars powered by diesel increased significantly in Europe and Japan, due to their better fuel economy (Owen and Coley, 1995). Now days, diesel engines are widely used worldwide.

The increase of power-weight ratio made increased oil refinement necessary, reducing fuel viscosity and the levels of hard combustion residues. The improvement in engines output, efficiency and reliability increased the ignition quality requirements. Cetane number became a fundamental diesel characteristic, and several tests to measure it were developed. Since the 1960s, viscosity range, sulfur and contaminants specifications became important parameters. In cold countries, weather resistance became fundamental as well (Owen and Coley, 1995). These physicochemical characteristics of diesel are discussed in chapter 2.

Diesel has an important role in Brazilian energy matrix. Figure 1.1 presents an evolution

of Brazilian domestic energy supply over the years since the 1970s. Figure 1.2 presents Brazilian domestic energy supply in 2014. Figures 1.1 and 1.2 reveal that petroleum and oil products are the most abundant Brazilian energy source since the 1970s, when the record started. Diesel is the most produced and used oil product in Brazil. It was responsible for 39% of total oil products made in Brazil in 2014, meaning that diesel alone is responsible for 15.4% of total Brazilian energy supply (Empresa de Pesquisa Energética, 2015). Figure 1.3 presents different activities that used diesel in Brazil in 2013. Total domestic consumption of diesel was 57 783 000 m^3, a 6.3% increase compared to 2012. Since the 1970s oil crisis, Brazil has a legislation that prohibits diesel passenger cars. Yet, diesel is the most used fuel in transportation. In 2013, 46.2% of Brazilian transportation energy came from diesel and 82.9 % of final energy consumption of diesel was in this sector, of which 75.8% were used on highways. Diesel is also used in railroads and waterways (Empresa de Pesquisa Energética, 2014).
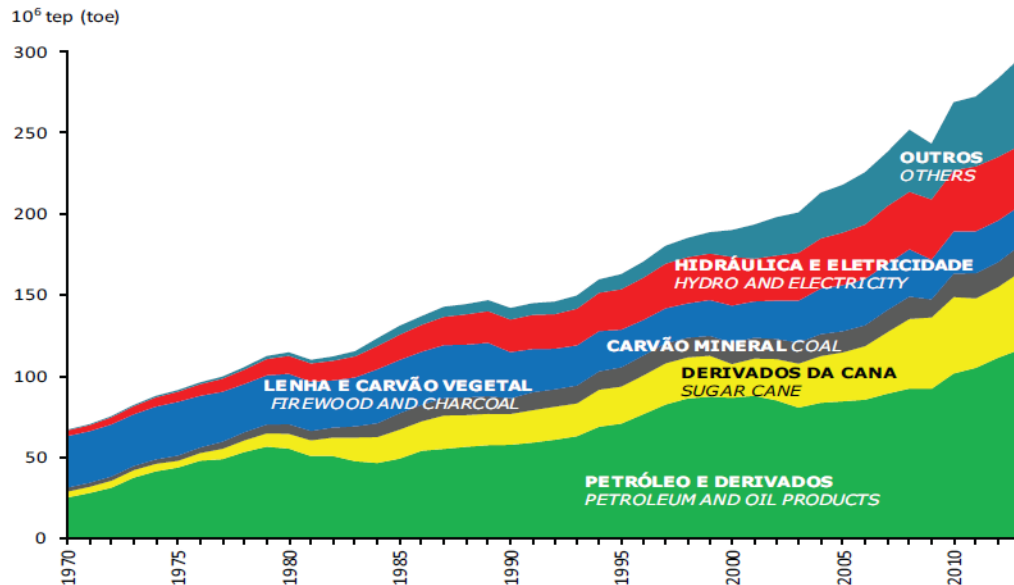
Figure 1.1: Brazilian domestic energy supply over the years. Source: Empresa de Pesquisa Energética (2014)

The percentage of oil in world energy supply and world final energy consumption are similar to Brazils's percentage, as can be seen in figures 1.4 and 1.5.

Oil is not renewable, and its price and availability can be highly influenced by geopolitics. The emissions of oil products combustion cause environmental and health damages. Replacing fossil fuels by renewable fuels, even in small proportions, increases energy security and can reduce emissions. Brazilian diesel has a compulsory addition of 7% of biodiesel, made mainly of soybean oil and tallow (Empresa de Pesquisa Energética, 2015)
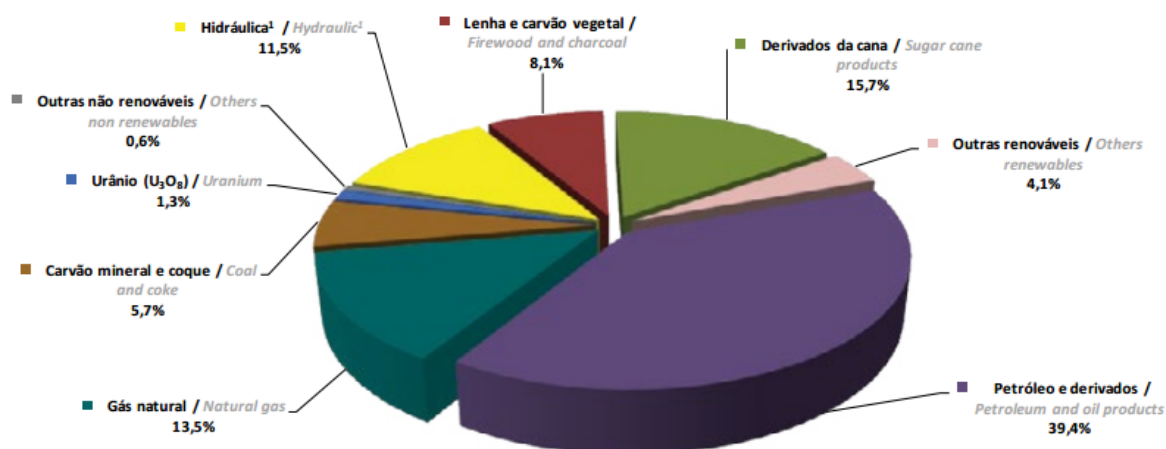
Figure 1.2: Brazilian domestic energy supply in 2014. Source: Empresa de Pesquisa Energética (2015)
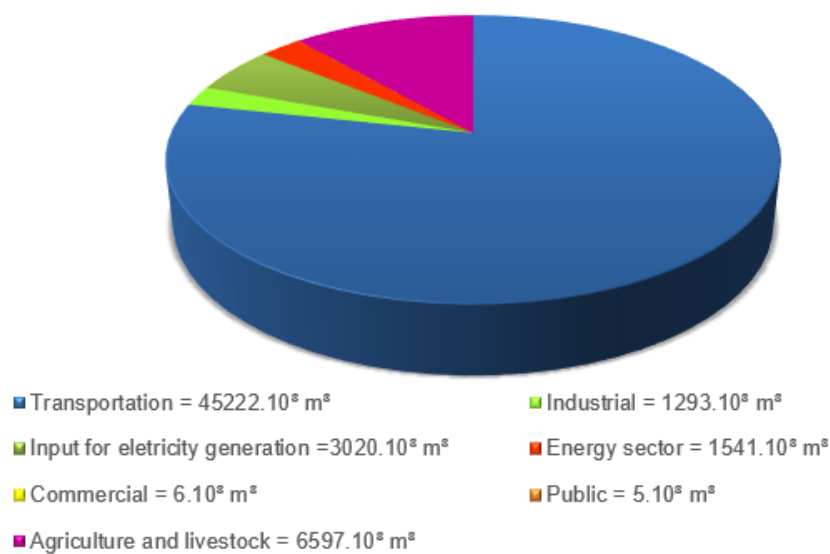
Figure 1.3: Brazilian diesel use in 2013. Source: own elaboration, using data from Empresa de Pesquisa Energética (2014)
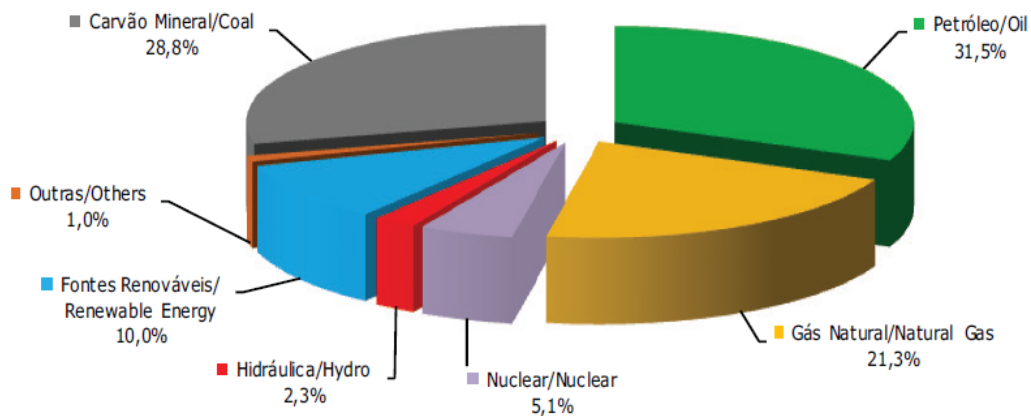
Figure 1.4: World Energy Supply in 2011. Source: International Energy Agency (2011) apud Empresa de Pesquisa Energética (2014)
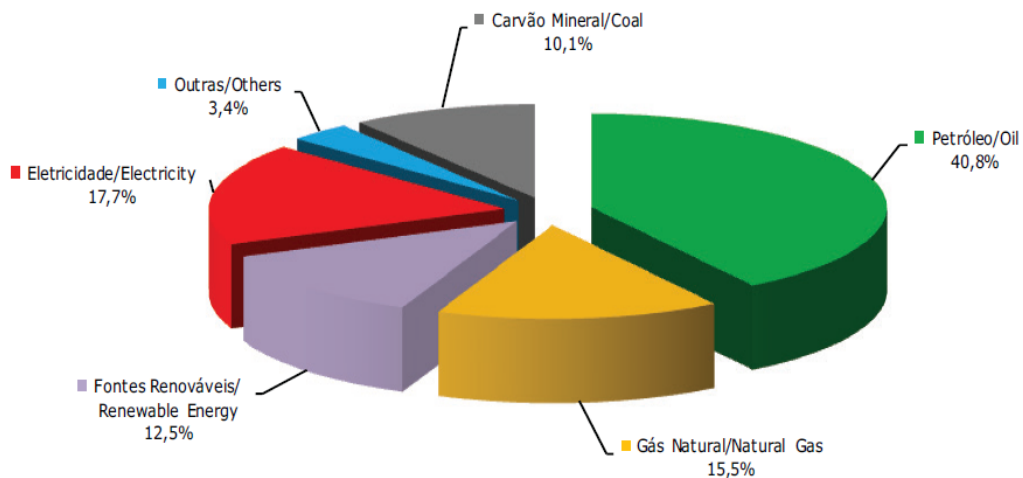
Figure 1.5: World Final Energy Consumption in 2011. Source: International Energy Agency (2011) apud Empresa de Pesquisa Energética (2014)

Kerosene is the middle distillate fraction of crude oil, between the gasoline fraction and the diesel fraction. It was chosen to be used as jet fuels in the 1940's, replacing gasoline, that was the first jet fuel due to its availability. Kerosene's lubricity is higher than gasoline's, which is better for pumps. It also have higher volumetric heating values (Maurice *et al.*, 2001). In Brazil, kerosene energy use has increased 40.66% from 2005 to 2014. It was responsible for 1.4% of Brazil's final energy consumption in 2014. Almost all kerosene consumed in the country (99.7%) was used in airways (Empresa de Pesquisa Energética, 2015). There are several types of jet fuels. They need to meet operational specifications, meaning that they can have different chemical composition as long as the application requisites are guaranteed (Maurice *et al.*, 2001).

Kerosene and diesel are composed of hundreds of different chemical compounds and, due to their complexity, it is not possible to develop a computational chemical model that describes those real fuels. A surrogate fuel can be used instead. It is a simpler representation of a composite fuel, consisting in a small number of pure compounds that have combustion characteristics similar to the target real fuel. N-decane has been used as major component of diesel surrogates in several studies. It has also being studied as a kerosene surrogate, or as the main component of jet fuels surrogates. N-decane is a colorless liquid obtained mainly from the refining of petroleum, and it is used as solvent and to make other chemicals (NNOAA's Ocean Service, 2016). It occurs naturally in natural gas and in the paraffin fraction of petroleum. Combustion of oil derivatives, vulcanization and extrusion operations, waste incinerator and several materials release n-decane into the atmosphere (Toxicology Data Network, 2016). Its modeling also helps the understanding of more complex alkanes.

1.2 Ethanol

Although the exact origin of the alcohol distillation process is not registered, it is known that ethanol is consumed by mankind since ancient times. It first use was as psychotropic and as medicine (Dietler, 2006). Its use as a fuel dates back to the nineteenth century, initially being used in lamps and then as the first fuel in internal combustion engines (Sarathy *et al.*, 2014). Ethanol came to be considered the best option for these engines; but fossil fuels were preferred in the early twentieth century because oil products were cheaper and easier to operate with the materials known at the time (Raheman, 2007). Interest in alternative fuels started to grow again only after the 1970s, primarily due to embargoes promoted by OPEC (Organization of Petroleum Exporting Countries) and the product supply problems; and then from the 1990s by environmental concerns (Instituto de Pesquisa Econômica Aplicada, 2010; Raheman, 2007).

The first oil embargo occurred in October 1973, as retaliation of Middle East to United States

and the European countries that supported Israel in the Yom Kippur War against Syria and Egypt. Such an embargo generated supply crises and caused the price of oil to increase 400% in about three months, forcing rich countries to reduce public spending and oil imports and raise their exchange rates. In Brazil, oil purchases at very high prices were maintained, but the country turned its attention to the production of ethanol as an alternative fuel, which culminated in the creation of National Alcohol Program (PROÁLCOOL) (Instituto de Pesquisa Econômica Aplicada, 2010).

PROÁLCOOL was created in 1975 by presidential decree, encouraging the domestic production of alcohol from sugar cane, cassava or any other input. Sugar cane has been one of the most important agricultural activities in Brazil since colonial times, so it became the main source of ethanol. In addition to increased agricultural production, PROÁLCOOL encouraged the modernization and expansion of existing distilleries and the installation of new production units. PROÁLCOOL's first phase was focused in increase the production of anhydrous ethanol, which was used mixed with gasoline (Rosillo-Calle and Cortez, 1998).

In 1979 Islamic Revolution in Iran resulted in the stoppage of oil production and generated a new oil shock. In Brazil, the PROÁLCOOL partially cushioned the crisis (Instituto de Pesquisa Econômica Aplicada, 2010). That year, the PROÁLCOOL entered its second phase, which increased production of hydrated ethanol for use in vehicles fueled only by ethanol. Between 1980 and 1986, ethanol fueled vehicle sales almost tripled, reaching 95.8% of domestic sales (Rosillo-Calle and Cortez, 1998).

In 1986 oil prices have stabilized and the sugar price in the international market has increased, making ethanol production less profitable. The use of ethanol started to reduce and at the end of the 1980s, ethanol-powered cars almost stopped being produced (Instituto de Pesquisa Econômica Aplicada, 2010).

Environmental and health problems caused by fossil fuel emissions made research in renewable energy sources increase after 1990s. In Brazil, ethanol has returned to prominence only in the 2000s, when the first flex cars went on sale. Soon all automakers began to manufacture these engines, whose sales rose from 90% of all cars sold in the country in 2009. The sugarcane cultivation grew; however, alcohol production is still subject to variations due to the international price of sugar (Instituto de Pesquisa Econômica Aplicada, 2010). Figure 1.6 presents total ethanol consumption over the years. Figure 1.7 presents ethanol balance in 2013.

Despite being renewable, there are environmental concerns about the devastation of forests to create areas of sugarcane cultivation to produce ethanol (Instituto de Pesquisa Econômica Aplicada, 2010). There are studies showing that ethanol can be seen as an alternative to fossil fuels, but both its supply chain needs to be evaluated in a case-by-case basis as its combustion in different types of engines still need to be better understanding to determine their real advantages and disadvantages.
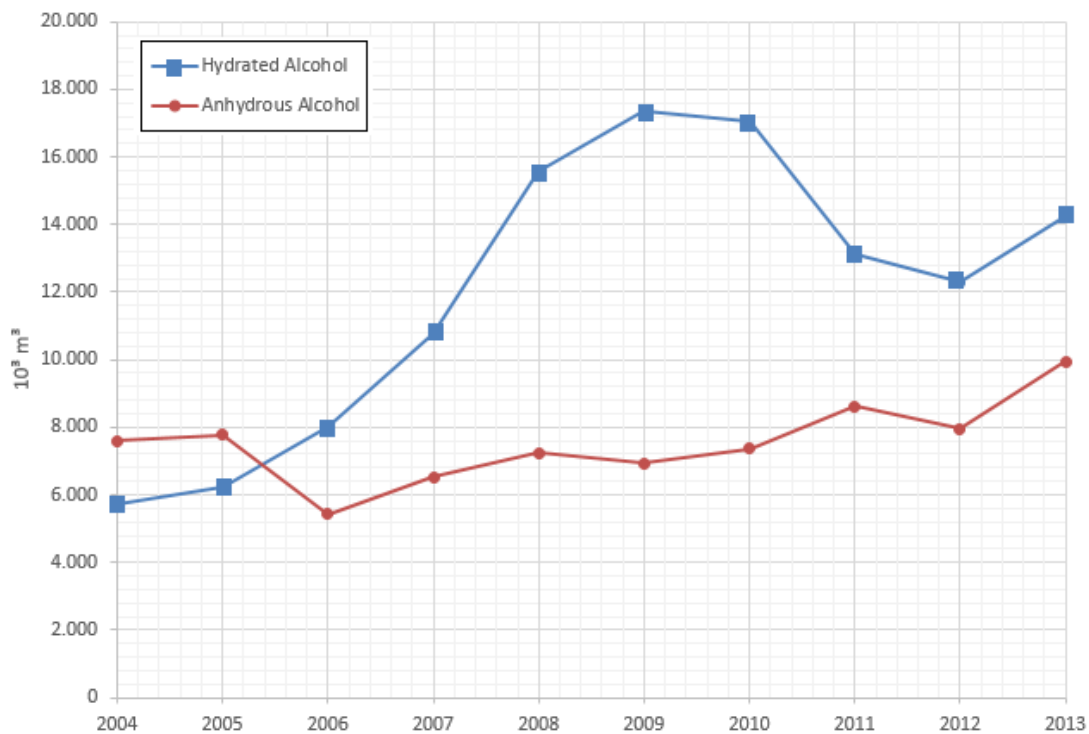
Figure 1.6: Brazilian ethanol comsumption over the years. Source: own elaboration, using data from Empresa de Pesquisa Energética (2014)
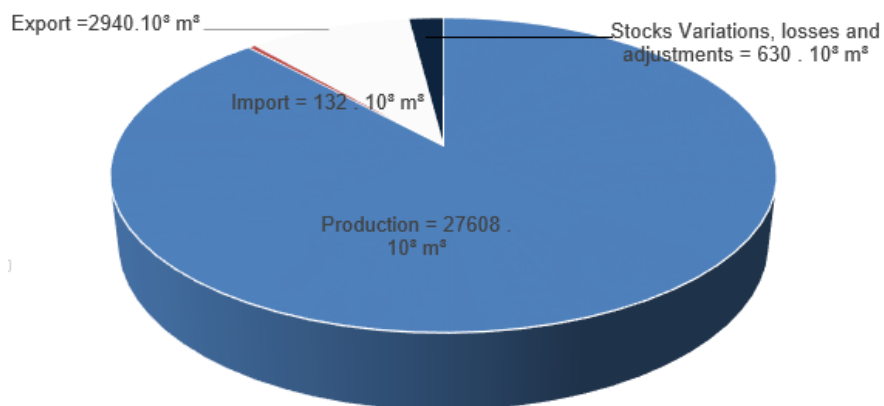
Figure 1.7: Brazilian total ethanol ethanol balance in 2013. Adapted from Empresa de Pesquisa Energética (2014)

1.3   Biodiesel and methyl decanoate

Ethanol solubility in diesel and kerosene is small. An additive can be used to increase the percentage of ethanol in diesel-ethanol blends. Biodiesel is one possible choice, and that is why it was studied in the present work.

Biodiesel is used worldwide blended with diesel in order to reduce fossil fuel consumption. It can be obtained from vegetable oils, waste oils, animal fats, waste greases or any other raw material that contains free fatty acids and/or triglycerides. Biodiesel is a mixture of saturated and unsaturated fatty acid alkyl esters. It has less components then fossil fuels; still, it is not possible to model its combustion. Methyl decanoate can be studied as a biodiesel surrogate (Alviso, 2013). Brazilian diesel has a mandatory addition of 7% of biodiesel.

1.4   Objectives and Layout

Studies of diesel + ethanol blends use in diesel motors started in 1980 in order to reduce fossil fuel dependence and emissions (Hansen *et al.*, 2005). Nevertheless, there are few studies in basic characterization of diesel + ethanol blends combustion. The interest in the use of renewable fuels in jet engines has increased, and the addition of ethanol to jet fuels is considered a possible alternative (Chen *et al.*, 2014). N-decane can be used as a major component of diesel or kerosene surrogates in computational combustion modeling. The kinetic mechanism describes combustion in molecular level, and can be used to predict several combustion properties: ignition properties, heat release rates, emissions, and intermediate species. Turbulent combustion modeling is stiff and have a high computational cost. So a laminar flame is studied instead, because it's mechanism can be used as a start to study turbulent flame mechanism (Turns *et al.*, 1996).

Several physicochemical characteristics need to be evaluated in order to use blends of diesel and ethanol or kerosene and ethanol. Biodiesel cans be used to increase the percentage of ethanol in those blends. No previous study of basic physicochemical characterization of n-decane - ethanol -methyl decanoate blends was found in literature, neither any chemical kinetic model that described the combustion of those three fuels.

The objectives of this work are:

1. To characterize two physicochemical properties of n-decane - ethanol - methyl decanoate blends, and compare these blends properties with diesel + ethanol blends properties found in literature. The characteristics evaluated were solubility (using anhydrous ethanol and hydrated ethanol), density and flash point;

2. To develop a chemical kinetic model that describes the laminar combustion of n-decane -

ethanol - methyl decanoate blends in two geometries: a 1D premixed flame and a counterflow flame.

3. To use the developed new model to find fundamental combustion parameters: flame speed, maximum temperature, flame and species profile and emissions.

The structure of this work is:

○ Chapter 2 presents the physicochemical properties of the real target fuels regulated by Brazilian legislation and which characteristics need to be evaluated in order to use diesel-ethanol blends. It also explains the importance of the study of surrogate fuels, how they are chosen and which is the state-of-art in chemical modeling of n-decane, ethanol and methyl decanoate combustion.

○ Chapter 3 explains how the work was developed. It presents the reagents and equipments used to measure the physicochemical properties, the measuring process and how the results were analyzed. It also presents the computational package used, explaining which equations it solves and which thermodynamic and transports properties it needs and how they are obtained. The process of development of the chemical kinetic model is detailed, and the experimental literature data used to validate it is summarized.

○ Chapter 4 reveals the findings of this work. The physicochemical properties of the blends are presented and compared with the ones of the real fuels. The simulations that validate the chemical kinetic model developed are presented. The ability of the surrogates to reproduce real fuels behavior is evaluated. Finally, the effect of the addition of ethanol and methyl-decanoate in n-decane basic combustion is unveiled.

○ Chapter 5 ends this work by presenting its main conclusions and some perspectives of possible future works in the subject.

2 LITERATURE REVIEW

The importance of physicochemical characterization of fuels and the state-of-art in n-decane, ethanol and methyl decanoate combustion modeling are presented in this chapter. Section 2.1 explains the difficulties in modeling real combustion and why the study of surrogates is important. Section 2.2 presents the physicochemical characteristics of real diesel and kerosene and compares it with the ones of n-decane. It ends by presenting a summary of n-decane's chemical kinetic models available in literature. Section 2.3 presents the physicochemical characteristics of ethanol and the chemical kinetic models available in literature for this fuel. Finally, section 2.4 explains why biodiesel is added to diesel-ethanol blend. It also presents methyl decanoate chemical kinetic models existing and explains which parameters need to be evaluated in target fuels blends.

2.1 Chemical kinetic models and surrogates

Combustion is a complex process composed of series of chain reactions: first, the dissociation of the reactants into free radical species. Then, free radicals react with stable compounds, resulting in more free radical species. In the end, free radicals recombine and form new stable species (Glassman *et al.*, 2014). Each intermediate reaction has its own set of chemical kinetic parameters, and the development of a chemical kinetic model that properly describes a fuel combustion at a molecular level is a challenging task because there are hundreds or even thousands of intermediate species and reactions. But the effort is justified: chemical kinetic models can be used to describe energy release rate, soot and pollutant formation, ignition behavior, knocking limits and cool flame characteristics (Westbrook and Dryer, 1984). The prediction of combustion characteristics by chemical kinetic models allows computational design and optimization of real devices (Pitz and Mueller, 2011).

Chemical kinetic models are usually validated in simpler geometries, in order to avoid physical aspects that could interfere in kinetics measurements, such as evaporation, diffusion, etc. After the detailed chemical kinetic model is validated comparing experimental and computational data, it can be simplified in order to generate a reduced chemical kinetic model that can be used in more complex combustion systems (Alviso, 2013).

The development of a model that exactly describes all reactions of real fuels derived from petroleum (such as diesel, gasoline or jet fuels) is not possible using current computational resources, because those fuels are too complex: they are made of hundreds of compounds; the radicals product from those compounds react together; fuels composition varies between different refineries; and fundamental properties are not available. The solution is to study a surrogate fuel instead. A surrogate is a simpler fuel, made of a small number of pure chemical compounds, that behaves

similarly to the real target fuel (Pitz and Mueller, 2011).

Besides contributions in computational modeling, studies of surrogate fuels are also important for two other reasons: First, they allow the development of standardized fuels that can be used to increase engine experiments reproducibility worldwide, as long as fuel variability may not be an issue anymore. Finally, the efforts to match critical performance characteristics of surrogates and target fuels also helps the understanding of the relationship between fuel properties and engine performance, because the surrogate fuels are chosen based on their characteristics with the intention of mimic some engine behavior and if it does match, it proves that specific fuel property leads to the engine behavior (Pitz and Mueller, 2011).

The choice of the surrogate fuel depends on the intend use of it. Farrell *et al.* (2007) presents 3 types of target characteristics of the real fuel that a surrogate can mimic:

1) Property Targets: these are the basic physicochemical fuel characteristics, such as density, hydrogen/carbon ratio, gross chemical composition, phase behavior, molecular transport properties, viscosity, surface tension, etc. Some of these properties (e.g: density) are easily reproduced by a single-component surrogate; others need more components to be reached (e.g: phase behavior). Matching then do not necessarily mean that combustion behavior of the surrogate and the target fuel will match as well, and generally it is not possible to match a wide range of properties. Those "unmatches" may or may not interfere in desired analysis.

2) Development targets: these are the kinetic-related phenomena and the fluid dynamic processes important to the surrogate behavior validation. For example: auto ignition delay, burn rate, species evolution histories, emissions, multi-component spray vaporization, droplet size distribution, etc. These properties are evaluated in controlled conditions devices, and it is difficult to a surrogate to match a broad range of development targets.

3) Application targets: these are the properties obtained from engine experiments, such as combustion phasing and duration, combustion efficiency and primary emissions. These properties may be obtained in steady-state or in transient operation, and can be only used to evaluate the quality of a surrogate fuel if relevant property targets matches.

Furthermore, there are some fuel characteristics used to validate chemical kinetic models. For example, laminar flame speed. It is the propagation speed of a adiabatic laminar flame and depends on fundamentals fuel properties: thermal diffusivity, reactivity and exothermicity (Zhao *et al.*, 2004).

The steps of the development of a chemical kinetic model are described in chapter 3. In the present work, the blend of three pure fuels was studied: n-decane, that is the main component of some diesel or kerosene surrogates; methyl decanoate, that is studied as a biodiesel surrogate; and ethanol. Physicochemical properties and combustion of ternary blends were studied as well.

2.2   N-decane as a component of diesel and kerosene surrogates

Real fuels derived from petroleum, such as diesel and kerosene, are complex blends of different hydrocarbons. Due to oil variability and to variabilities in refining processes, diesel and kerosene composition and properties change from refinery to refinery, as said in chapter 1. Figure 2.1 presents the average composition of kerosene Jet A1 and North American diesel.
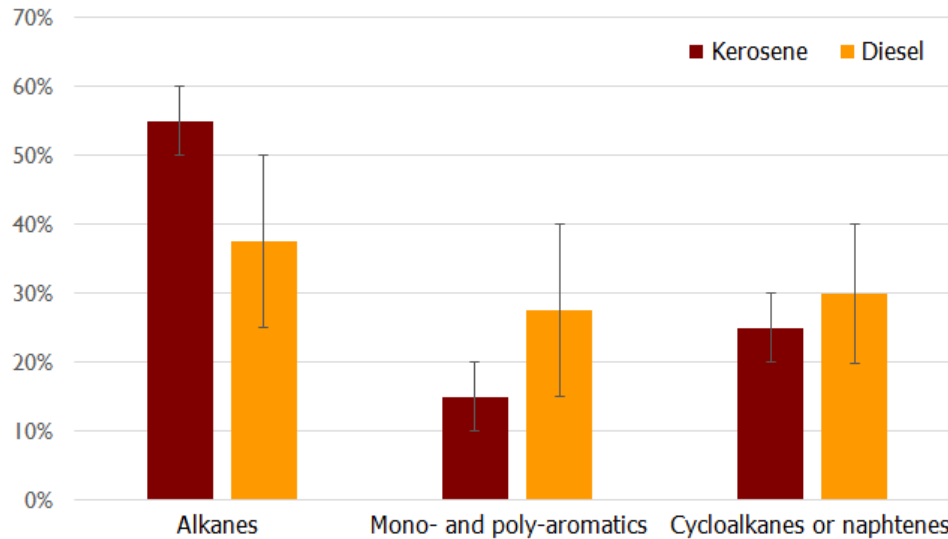
Figure 2.1: Average composition of kerosene Jet A1 and North American diesel. Source: Own elaboration, using data from Dagaut *et al.* (2006) and Farrell *et al.* (2007)

Different types of kerosene are used as jet fuel. Kerosene Jet A1, for example, is composed of alkanes (50-60 % vol.) mono- and poly-aromatics (10–20% vol.) and cycloalkanes or naphtenes (mono- and polycyclic, 20–30% vol.) (Dagaut *et al.*, 2006). It is the jet fuel used in turbine aircrafts in Brazil (Nacional Oil Agency, 2009).

Diesel is composed of medium-high molecular-weight hydrocarbons. Figure 2.2 presents some representative examples of the major classes of molecules contained in it. The proportion of the components are highly variable. North American diesel is composed for alkanes (25-50 % vol.) mono- and poly-aromatics (15–40% vol.) and cycloalkanes or naphtenes (mono- and polycyclic, 20–40% vol.) (Farrell *et al.*, 2007).

In order to assure diesel properties, there are laws that vary worldwide. Brazilian diesel is regulated by ANP resolution N° 50, from 12/23/2013 and ANP resolution N° 69, from 12/23/2014 that make small modifications on it. ANP resolution N° 50 classifies diesel for road use in two kinds:
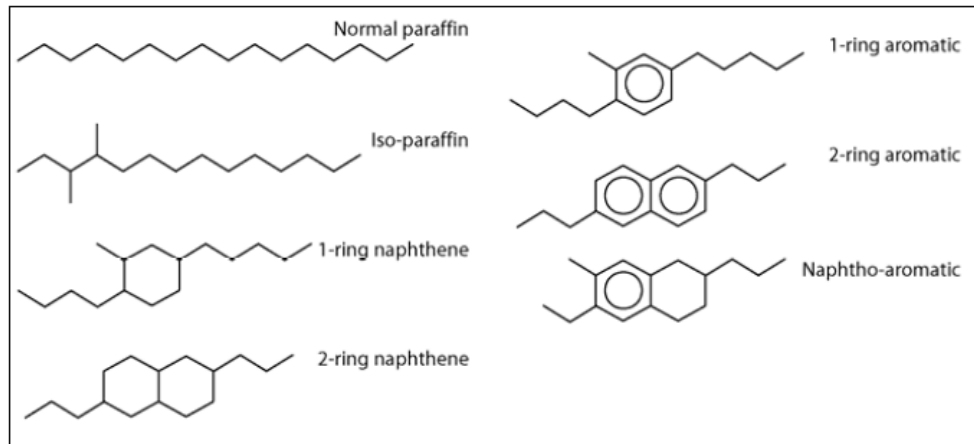
Figure 2.2: Representative examples of the major classes of molecules contained in diesel fuel. Adapted from: Farrell *et al.* (2007)

○ Diesel A: It is a fuel made in refineries, in the core of petrochemical raw materials and makers, or other authorized places. It is made for vehicles equipped with Diesel cycle engines, road use, without the addition of biodiesel;

○ Diesel B: It is diesel A with the addition of biodiesel. Proportion varies according to legislation. Since November 1th 2014, it is 7%. Brazilian biodiesel is regulated by ANP resolution n° 45, from 8/25/2014.

Diesel A and B are classified according to their maximum sulfur:

○ Diesel A S10 and B S10: maximum 10 mg of sulfur/kg of fuel.

○ Diesel A S500 and B S500: maximum 500 mg of sulfur/kg of fuel.

Brazilian urban bus of several cities use diesel B S10 only.

The choice of a surrogate depends on the application target chosen. Farrell *et al.* (2007); Battin-Leclerc (2008); Pitz and Mueller (2011) made extensive reviews of different types of diesel surrogate fuels, and we recommend these works for further information. Dagaut and Cathonnet (2006) presents a review on experimental and kinetic modeling of kerosene. They reviewed the development of surrogates for jet fuels and highlighted the importance of n-decane as a kerosene surrogate or as a component of it.

In the present work, pure n-decane ($C_{10}H_{22}$) was studied. Figure 2.3 presents its 2D structure and 3D conformation. N-decane is a n-alkane and it can be used for the development of higher alkane property models studies. It is an important component of real diesel and it is studied as

a kerosene surrogate and as the major component of diesel surrogates. Blends of n-decane and α-methylnaphthalene are one of the most studied diesel surrogate (Farrell *et al.*, 2007).
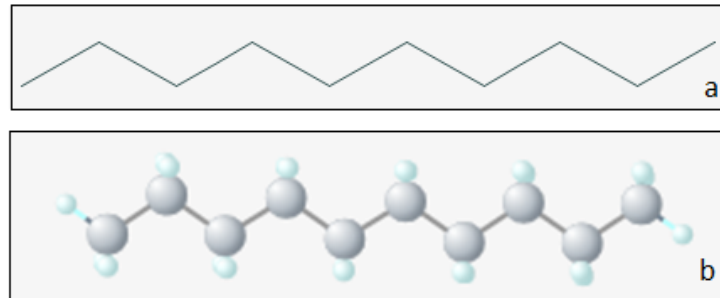
Figure 2.3: N-decane a) 2D structure and b) 3D conformation. Source: National Center for Biotechnology Information (2015)

Barths *et al.* (1999) compared diesel with n-decane and a blend of 70% n-decane and 30% α-methylnaphthalene (volume), called IDEA fuel. Experiments were made in a real motor and a flamelet model was developed for simulations. No difference was observed between vaporization, ignition and heat release of diesel and IDEA fuel. Evaluation of the emissions revealed that the gradient of NO_x and soot emissions for IDEA and diesel is the same, with diesel values about 3-7% higher. On the other hand, n-decane NO_x and soot emissions are significantly (about 30%) smaller. These results are presented in Figure 2.4.
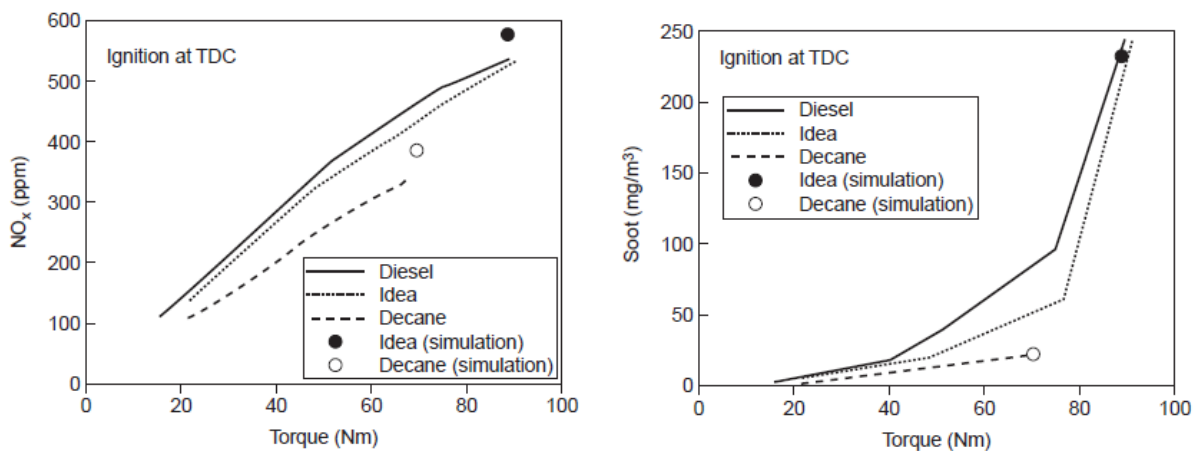
Figure 2.4: Comparison between diesel, n-decane and IDEA fuel (70%n-decane + 30% α-methylnaphthalene) emissions. Source: Barths *et al.* (1999)

Lemaire *et al.* (2009) experimentally compared soot formation of commercial low sulfur diesel, IDEA fuel and a modified IDEA, with 80%n-decane and 20%α-methylnaphthalene (vol-

ume). The modified IDEA mapping of soot volume fraction and fluorescent soot precursors are quite identical to disel's. IDEA fuel emission were higher than diesel's. The composition of the soot differed from the surrogates to diesel.

Ramirez L *et al.* (2010) compared the kinetics of oxidation of diesel and IDEA fuel at 10atm, for temperatures of 560-1030 K and equivalence ratios of 0.25, 0.5, 1, and 1.5. Concentration profiles obtained from CO, CO_2, H_2O and O_2 were very similar between the two fuels. Surrogate produced more C_2H_2 and C_3H_3 and less CH_4.

Several studies have compared the oxidation of kerosene with the oxidation of n-decane. Vovelle *et al.* (1991) used a mass spectrometer to measure different aromatic species in sooting process of n-decane and kerosene. The combustion occurred in a flat flame burner. They concluded that the flame structure of kerosene and decane are very similar, except for benzene formation. This similarity was validated again by Dagaut *et al.* (1994), that used a jet-stirred reactor to compare the oxidation of these two fuels; and by some other works presented in Table 2.1.

Table 2.1 summarizes pure n-decane and n-decane blends kinetic chemical models available in literature. The studies started in the 1990's and most of them were developed to mimic kerosene behavior. Some of them were created from the start, manually or using computer codes; others were generated adding reactions to preexisting models of smaller alkanes. Their ability to describe combustion vary for a wide range of pressures, temperatures and air/fuel ratios. The models were validated measuring flame speed, flame profiles and emissions. Figure 2.5 presents the number of species and reactions of n-decane chemical kinetic models available in literature over the years.
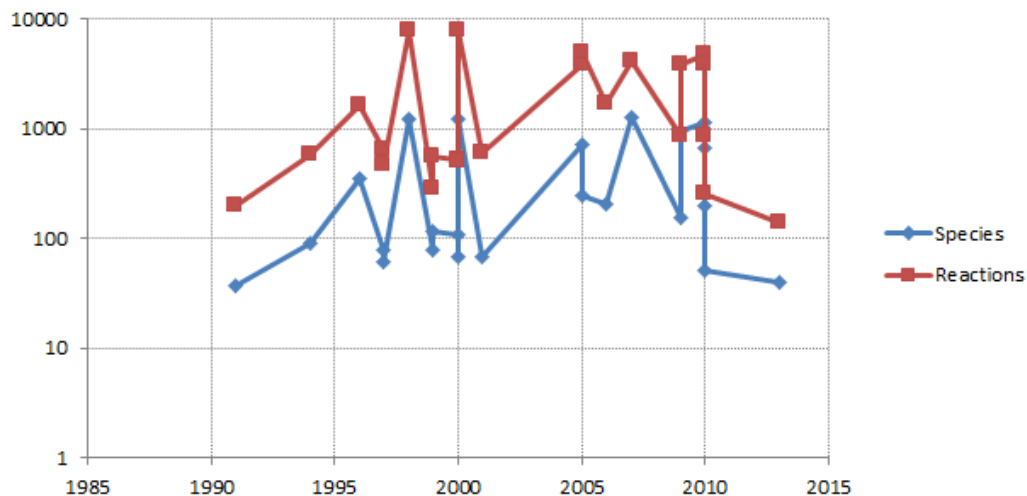
Figure 2.5: Number of species and reactions of n-decane chemical kinetic models available in literature over the years. Source: own elaboration.

Table 2.1: N-decane chemical kinetic models. Source: own elaboration

Studied fuel	Target Fuel	Number of Species and Reactions	Work Developed	Reference
n-decane	n-decane	37 species and 202 reactions	The structure of a premixed sooting decane O_2-Ar flame (ϕ = 1.9) has been simulated using a detailed kinetic mechanism and determined experimentally	Delfau *et al.* (1991)
n-decane	n-decane	not available	Concentration of molecular species in n-decane oxidation in a jet-stirred flow reactor (temperature range 873-1033 K at atmospheric pressure) was measured by gas chromatography. Results were used to develop quasi-global chemical kinetic reaction mechanisms.	Bales-Gueret *et al.* (1992)
90% n-decane +10% toluene	kerosene	not available	Comparison of computed mole fraction profiles with measured profiles of a sooting kerosene-oxygen-argon flame with an equivalence ratio of 2.2	Vovelle *et al.* (1994)
n-decane	kerosene	90 species and 573 reactions	A detailed chemical kinetic reaction mechanism of n-decane was developed to reproduce experimental data of kerosene oxidation.	Dagaut *et al.* (1994)

n-decane	kerosene	not available	Detailed chemical kinetic modeling of the high-temperature oxidation of n-decane	Dagaut *et al.* (1995)
n-decane	n-decane	350 species and 1650 reactions	Reaction mechanism for the oxidation of n-decane and n-heptane was automatically generated by a program developed. The mechanisms are validated for a wide range of pressures, temperatures, and equivalence ratios, covering conditions dictated by potential applications.	Nehse *et al.* (1996)
n-decane	n-decane	1st mechanism: 78 species and 638 reactions; 2nd mechanism: 62 species and 467 reactions	Chemical structure of a premixed n-decane/O_2/N_2 flame (equivalence ratio 1.7, 1atm) has been simulated with two reaction mechanisms. The second mechanism was derived from the first one by successively removing an increasing number of n-decyl radicals. The only species affected are the large intermediate olefins.	Douté *et al.* (1997)

n-decane	n-decane	1216 species and 7920 reactions	Development of a detailed model of the oxidation of n-octane and n-decane in the gas phase by using mechanisms written by means of a software recently developed (EXGAS). Computational data was compared to literature data. Considering that no fitting of any kinetic parameter was done, the agreement between computed and experimental values is satisfactory.	Glaude *et al.* (1998)
78% n-decane, 9.8% cyclohexane and 12.2% toluene by volume	kerosene	not available	Comparison between experimental and simulated concentration profiles for different pressures and equivalence ratios	Cathormet *et al.* (1999)
n-decane	kerosene	78 species and 283 reactions	Reduction of the mechanism for the oxidation of n-decane. Entrance temperature between 300K and 400K. Pressure between 1atm and 40atm and equivalence ratios between 0.3 and 2.5	Cathormet *et al.* (1999)

pure n-decane; diesel 70% (volume) n-decane + 30% α-methylnaphthalene (Idea-fuel)	118 species and 557 reactions	"Representative Interactive Flamelet" (RIF) model was used to simulate the combustion of two fuels. Results were compared to experimental results obtained in a real motor fueled with the two surrogates and diesel. Experimental results showed that both studied fuels are adequate surrogates to diesel, except in NO_x and soot formation, in which n-decane fail to reproduce diesel behavior. Injection rates were the only parameters that differed in simulations.	Barths *et al.* (1999)
70% (volume) diesel n-decane + 30% α-methylnaphthalene (Idea-fuel)	109 species and 519 reactions	Eulerian particle flamelet model is used to simulate combustion. Simulation results were compared to experiments made with diesel in a motor.	Barths *et al.* (2000)

n-decane	n-decane	69 species and 494 reactions	Development of a new partially reduced skeletal chemical kinetic mechanism for the oxidation and pyrolysis of n-decane, based in previous n-heptane model. Validation using n-decane flow reactor data and comparison against n-decane oxidation jet-stirred reactor data and n-decane/air shock tube ignition delay data obtained from the literature	Zeppieri *et al.* (2000)
n-decane	kerosene	Not available	Comparison of n-decane and kerosene premixed flames profiles	Lindstedt and Maurice (2000)
n-decane	n-decane	1216 species and 7920 reactions	Computer package EXGAS was used to automatically generate detailed kinetic mechanisms for n-decane from 550 K to 1600 K, aiming at reproducing experiments performed in a jet-stirred reactor and in a premixed laminar flame. The predictions of the mechanisms were compared to the experimental results without any adjustment of kinetic data.	Battin-Leclerc *et al.* (2000)

89% n-decane + kerosene 11% toluene		14 global reactions to break down the parent molecule into smaller alkyl radicals and olefins	Effect on the structure of counter-flow diffusion flames of increasing both the pressure and the strain rate	Patterson *et al.* (2001)
n-decane	n-decane	67 species and 600 reactions	Development of a chemical kinetic mechanism for the combustion of n-decane. Validation has been performed by using experimental measurements on a premixed flame of n-decane, O_2 and N_2, stabilized at 1 atm on a flat-flame burner, as well as from shock-tube ignition experiments, from jet-stirred reactor experiments and from a freely propagating premixed flame. Special attention is directed towards an accurate description of species relevant to pollutant formation.	Bikas and Peters (2001)
n-decane	n-decane	715 species and 3872 reactions	A kinetic mechanism automatically generated by a software developed at the laboratory (EXGAS) was validated using literature shock tubes and in rapid compression machines data. Temperature ranged from 600 to 1200 K, and pressure ranged from 1 to 50 bar.	Buda *et al.* (2005)

n-decane	n-decane	250 species and 5000 reactions	A new chemical model was developed for n-decane based in previows n-pentane and n-heptane kinetic models, using a lumped approach. Comparison to experimental literature data was made in order to validate the developed model.	Ranzi *et al.* (2005)
74% n-decane, 15% n-propylbenzene, and 11% n-propylcyclohexane	kerosene	209 species and 1673 reactions	A new chemical model was created and evaluated. Ignition delay foreseen agreed with literature data when $\phi = 0.5$. The model fail to predict high pressures behavior	Dagaut and Cathonnet (2006)
77% n-decane and 23% mesitylene (by volume)	kerosene	Not available	Laser extinction, fine wire thermocouples, and mass spectrometric sampling were used to determine soot volume fraction, temperature and mixture fraction. Species are added to a previously developed flamelet-based two-equation model of soot formation used for methane-air flames to describe the studied surrogate	Moss and Aksit (2007)

n-decane	different large hydrocarbons	1253 species and 4177 reactions	Modifications were made in a code that automatically generate chemical mechanisms. Simulations of data available in literature were carried out to validate the developed model.	Muharam and Warnatz (2007)
n-decane and other fuels (n-heptane, iso-octane and n-decane + toluene)	n-decane, n-heptane, iso-octane and kerosene	154 species and 850 reactions	A new chemical model was build adding some reactions to a previous scheme developed to model jet-fuel. The model was validate by JSR experiments at 1.0 and 2.0 MPa and by soot analisys at 0.1, 1.0 and 2.0 MPa.	Marchal *et al.* (2009)
n-alkane hydrocarbons from n-octane to n-hexadecane	n-alkane hydrocarbons from n-octane to n-hexadecane	940 species and 3878 reactions	Development of detailed chemical kinetic reaction mechanisms describing pyrolysis and oxidation of nine n-alkanes from n-octane to n-hexadecane. These mechanisms are validated through extensive comparisons between computed and experimental data from a wide variety of different sources.	Westbrook *et al.* (2009)

80%n-decane + 20% 1,2,4-trimethylbenzene by weight (Aachen surrogate)	kerosene	not available	A chemical-kinetic mechanism was developed assembling previously developed chemical-kinetic mechanisms for the components. The mechanism was validated using experimental data.	Honnet *et al.* (2009)
70% n-decane and 30% α-methylnaphthalene (volume)	diesel	1124 species and 4762 reactions	Surrogate and diesel oxidation were experimentally studied, confirming surrogate's reliability. A chemical kinetic model was developed and simulation results showed reasonable agreement with experimental data.	Ramirez L *et al.* (2010)
70% n-decane and 30% α-methylnaphthalene (volume)	diesel	662 species and 3864 reactions	The auto-ignition of fuel/air mixtures was studied in a heated high-pressure shock tube. A comprehensive kinetic mechanism was developed and showed good agreement with experimental data.	Wang *et al.* (2010)

| n-decane | n-decane | 1st mechanism: 202 species and 846 reactions; 2nd mechanism: 51 species and 256 reactions | Directed relation graph with error propagation and sensitivity analysis (DRGEPSA) was used to reduct a detailed reaction mechanism for n-alkanes to two skeletal mechanisms for n-decane: the first one covered a comprehensive range of temperature, pressure, and equivalence ratio conditions, and the other limited to high temperatures. | Niemeyer *et al.* (2010) |
| n-decane | n-decane | 40 species and 141 reactions | Decoupling methodology was used to develop a new skeletal n-decane oxidation mechanism. Simulations were compared to literature data and used to predict the combustion and emissions of premixed charge compression ignition engines. | Chang *et al.* (2013) |

2.3   Ethanol

Ethanol (C_2H_6O) is a renewable fuel that can be obtained by the fermentation of several vegetable species. It's structure is presented in Figure 2.6. Brazilian ethanol is regulated by ANP resolution n°19. It classifies ethanol in three types: anhydrous ethanol fuel (AEF), that is the one mixed with the gasoline sold in Brazilian gas stations; hydrated ethanol fuel (HYF), that is intended for direct use in internal combustion engines; and premium hydrates ethanol fuel (PYEF), that has a different variation in the specific gravity range.
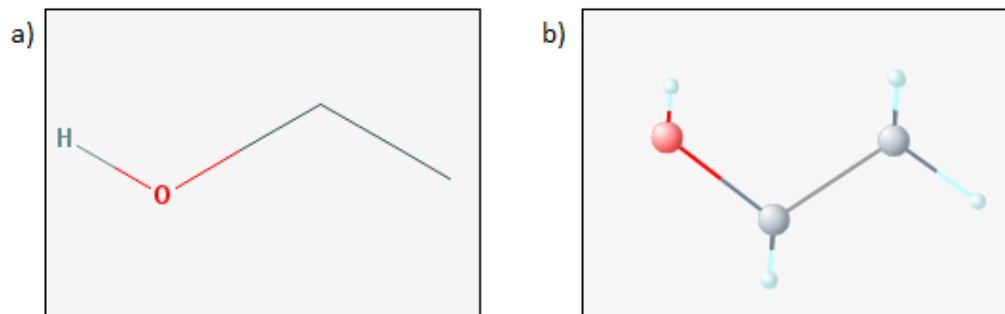
Figure 2.6: Ethanol a) 2D structure and b) 3D conformation. Source: National Center for Biotechnology Information (2015)

There are several chemical kinetic models describing ethanol combustion available in literature. Table 2.2 summarizes them. Ethanol models are simpler than n-decane models because ethanol chain is shorter and its decomposition involves a smaller number of reactions. One model was developed adding reactions to a previous methanol model; the others used experimental data obtained using different equipments, such as a counterflow twin flame, a turbulent flow reactor or shock tubes. Figure 2.7 presents the number of species and reactions of ethanol chemical kinetic models available in literature over the years.

Table 2.2: Ethanol chemical kinetic models. Source: own elaboration

Number of Species and Reactions	Work Developed	Reference
30 species and 97 reactions	A kinetic mechanism for high temperature ethanol oxidation was assembled based on a preview methanol model and adjusted to fit experimental ignition delay time data.	Dunphy *et al.* (1991)
35 species and 196 reactions	A counterflow twin flame technique was used to measure flame speed of ethanol/air mixtures at 1atm and initial temperature varying from 363K and 453K. Data obtained were used to develop a detailed kinetic scheme that was able to describe ethanol, methanol, methane and $C_2 - hydrocarbons$ flame speed. Some sub-reactions speeds numerically predicted significantly differed from experimental literature data.	Egolfopoulos *et al.* (1992)
34 species and 142 reactions	A turbulent flow reactor was used to analyze ethanol combustion with initial temperature near 1100K and equivalence ratio varying from 0.61 to 1.24. Experimental profiles of stable species concentration were used to validate a chemical kinetic model.	Norton and Dryer (1992)
57 species and 387 reactions	A new chemical kinetic scheme was developed based on experimental data acquired by shock tubes, combustion bomb , counterflow twin flame and jet-stirred and turbulent flow reactors. Initial temperature ranged from 1000K to 1700 K, pressure ranged from 1.0atm to 4.5atm and equivalence ratio ranged from 0.5 to 2.0.	Marinov (1999)

36 species and 192 reactions	A new detailed chemical kinetic mechanism was developed based on previous hydrogen, carbon monoxide, methane, ethane, ethylene, acetylene, propane, propene, propyne, allene and methanol mechanisms. Temperature was restricted to below 1000K, pressure to bellow 100bar and equivalence ratio bellow 3. The mechanism was validate experimentally using a counterflow burner, a shock-tube and gas chromatographic analysis.	Saxena and Williams (2007)
136 species and 1349 reactions	A new model for ethanol thermal oxidation was developed and validated using a shock tube in different equivalence ratios ($\phi = 0.3$ and $= 1.0$) and pressures (30, 40 and 50 bar); $650K \leq T \leq 1220K$.	Cancino $et\ al.$ (2010)
36 species and 252 reactions	A new chemical kinetic mechanism was built by thoroughly reviewing the literature. It was validated by measuring mole fraction profiles of chemical species of ne-dimensional laminar premixed flames with equivalence ratio varying from 0.25 to 2.00.	Leplat $et\ al.$ (2011)
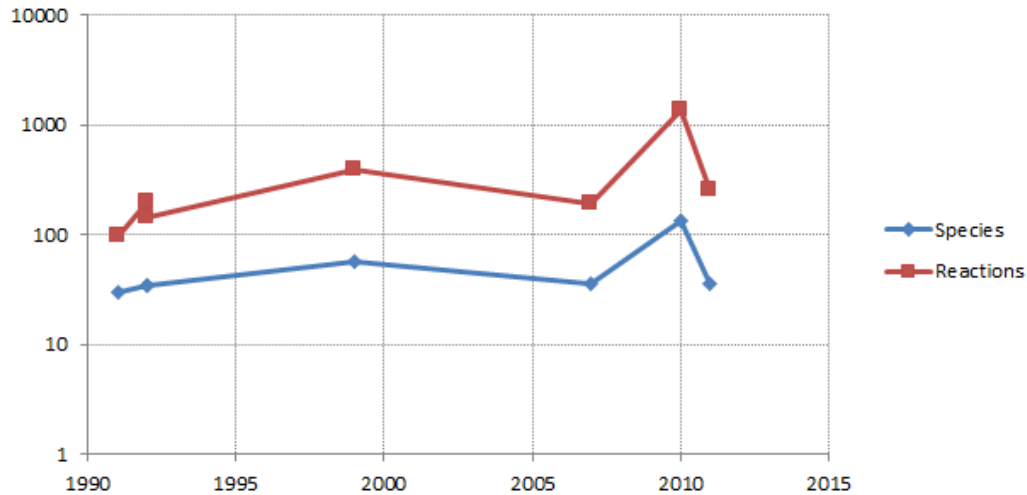
Figure 2.7: Number of species and reactions of ethanol chemical kinetic models available in literature over the years. Source: own elaboration.

2.4 Blends properties

Oil crisis has motivated diesel-ethanol blends to be studied since 1980. These blends are called e-diesel or diesehol. Even thought it was shown that these blends were technically acceptable for existing diesel engines, they were not commercially used because ethanol price was not competitive. It started to change with increasing interest in renewable fuels due to environmental causes. Nowdays, ethanol price is competitive with diesel, and the main interest of e-diesel use is emissions reduction (Hansen *et al.*, 2005). Ethanol diffusion flames product virtually no soot, what makes e-diesel interesting to meet NO_x and particulate matter (PM) emissions legislation (Datta and Mandal, 2016).

Miraglia (2007) simulated the environmental and social impacts from the use of a 91.8% common diesel, 7.7% ethanol, and 0.5% additive (vol) blend in the bus and truck fleet of the city of São Paulo, Brazil. The results are reduction in air pollutants, especially particulated matter (10.79% reduction), and consequent reduction in diseases and deaths. Economic advantages were reported as well. Even thought there are costs involved (Cleaning of diesel storage tanks, installation of vacuum and pressure valve in storage tank and intensive training in safety and handling and periodic maintenance), they are outnumbered for the benefits: the operational costs are reduced due to additive's high lubricity and less contamination of lubricant oil, that increases oil drain intervals for motor maintenance; and the dispersant detergent characteristic of the additive, that reduces the engine residue, providing longer engine maintenance intervals. Furthermore, there are social-economic benefits: job generation (direct and indirect), stability and employment of unskilled workforce, de-

creased national energy dependence (improved balance of payments), sustainable development and potential carbon credits due to probable greenhouse gas reduction. Environmental cost of sugarcane harvesting could not be estimated.

Recently, the interest in biofuels also has grown in the aviation industry. Besides its low energy density, ethanol is considered one of the most promising renewable fuels, but the limited miscibility of it in kerosene at lower temperatures is an obstacle. Hydrous ethanol miscibility in kerosene is even lower than anhydrous ethanol miscibility; but the costs of hydrous ethanol are much lower than anhydrous ethanol costs. Chen *et al.* (2014) studied a blend of n-decane (80% vol.) and 1,2,4-Trimethylbenzene (20% vol.) as a kerosene surrogate, and evaluated the miscibility of ternary surrogate-ethanol-water blends. The results are presented in Figure 2.8, where the separation curves and tie lines calculated can be seen. In the figure, A is an arbitrarily chosen point in the two-phase region, P1 and P2 are the the intersection points and refer to the composition of each phase.
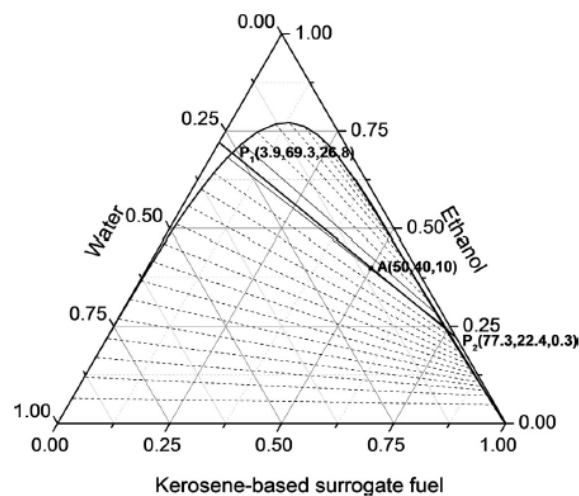
Figure 2.8: Ternary diagram of a kerosene surrogate(80% n-decane + 20% 1,2,4-Trimethylbenzene –vol.) - ethanol - water blends with the separation curve. Source: Chen *et al.* (2014)

2.4.1 Biodiesel use as solubilizer

In order to reduce greenhouse emissions and the use of fossil fuels, Brazil uses 7% biodiesel + 93% diesel blends in diesel engines. Ethanol can be used to produce biodiesel through ethanolysis, but it increases production costs (Lapuerta *et al.*, 2007). It is important to emphasize that using fuels from diverse sources guarantee energy safety; so ethanol and biodiesel can be complementary.

. Diesel-ethanol blends are stable only in restricted conditions: solubility decreases with the

content of water in ethanol, when temperatures decreases and with the increase of the ratio of aromatic compounds. Lapuerta *et al.* (2007) concluded that blends up to 10% in volume of anhydrous ethanol can be used in diesel engines in countries where ambient temperature does not decreases bellow 5°C. It is necessary to prevent contamination with water, especially in places where the humidity is high. In the present work, n-decane was studied as the main component of diesel surrogate. The solubility curve of n-decane - ethanol - water blends can be found in Skrzecz *et al.* (1999)

In order to increase blend stability in lower temperatures or in higher ethanol content blends, a surfactant or a co-solvent additive can be added. A broader discussion of the types of possible additives is out of the scope of this work, but we recommend the review made by Ribeiro *et al.* (2007) for further information. There are several studies of mixtures of diesel, biodiesel and ethanol; and biodiesel can be used to stabilize diesel-ethanol blends that other way would form a biphasic blend (Chotwichien *et al.*, 2009).

Chotwichien *et al.* (2009) studied the effect of palm oil alkyl esters (types of biodiesel) in the stability of diesel-ethanol blends. The ternary diagram developed by them is presented in Figure 2.9.

2.4.2 Methyl decanoate as a biodiesel surrogate

Methyl decanoate ($C_{11}H_{22}O_2$) has been studied as a biodiesel surrogate in several works, as can be seen in Alviso (2013) and references therein. Figure 2.10 presents methyl decanoate 2D structure and 3D conformation.

There are several chemical kinetic models of methyl decanoate combustion available in literature. Some of them are summarized in Table 2.3. Figure 2.11 presents the number of species and reactions of methyl chemical kinetic models available in literature over the years. All works presented there highlights the importance of methyl decanoate as a surrogate for biodiesel.

2.4.3 Physicochemical properties

Due to fuels differences, some aspects need to be evaluated in order to use e-diesel. There are several studies comparing e-diesel's and diesel's properties, emissions, performance and viability.

The three pure substances and the real fuels that they intend to mimic have different physicochemical properties that need to be evaluated. Table 2.4 compares some properties of them. As long as diesel, kerosene and biodiesel properties change depending on how they were obtained, data from Brazilian legislation are presented in the Table. The evaluated properties are not specified for Brazilian ethanol. It is a pure substance, so those data were found in Toxicology Data Net-
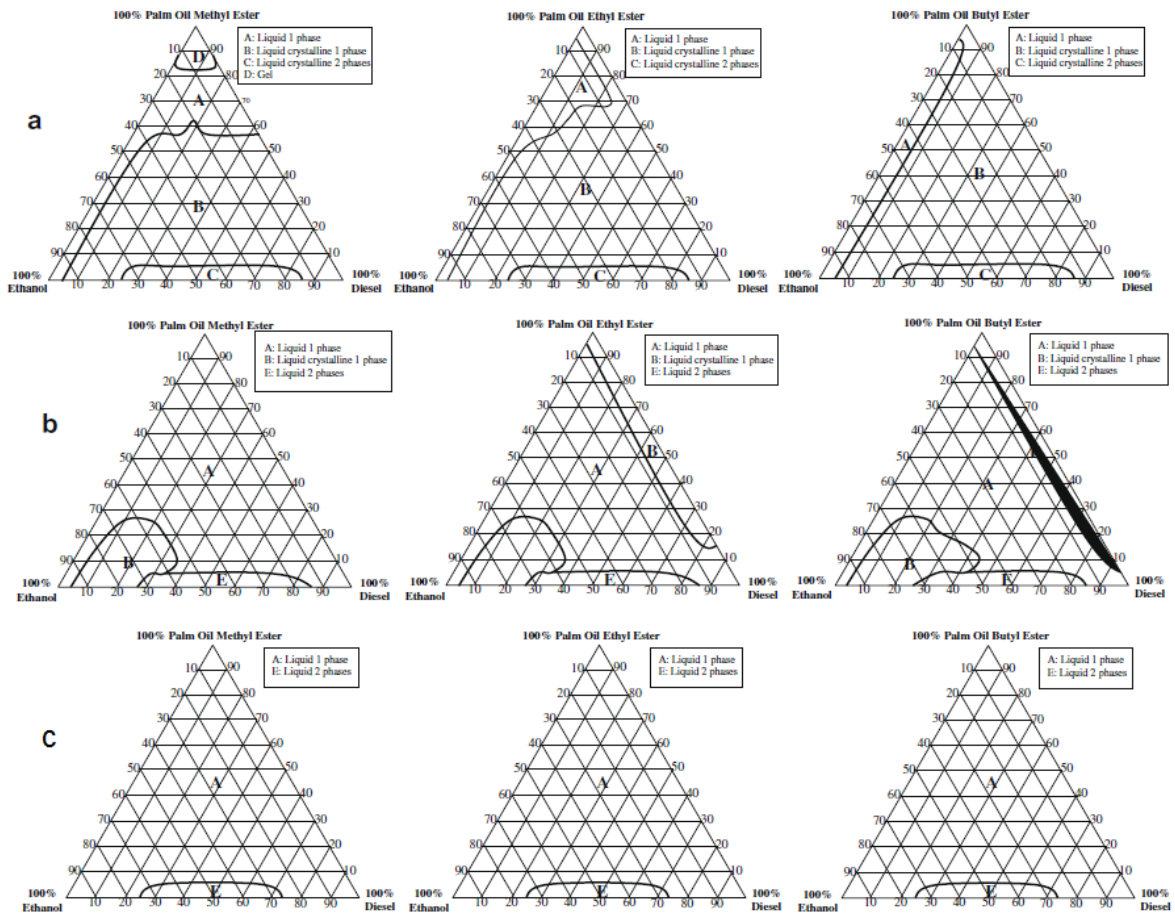
Figure 2.9: Long term stability of diesel–palm oil alkyl ester–ethanol at (a) 10°C (b) 20°C and (c) 30°C. Adapted from: Chotwichien *et al.* (2009)

work (2016); NNOAA's Ocean Service (2016); Yanowitz *et al.* (2014) and Knothe and Steidley (2005). Table 2.4 shows that n-decane density at 20°C and flash point are similar to diesel and kerosene's; but viscosity of n-decane at 40°C is half of diesel's and cetane number of n-decane is higher than diesel's. The same occurs comparing methyl decanoate and biodiesel: density and flash point are close, but methyl decanoate viscosity is much smaller. A adequate surrogate do not need to reproduce all physicochemical properties of the target fuel, and those characteristics do not necessarily affect combustion behavior. Differences between diesel and ethanol and kerosene and ethanol presented in Table 2.4; and the effect of biodiesel addition in this blends are discussed in next subsections.
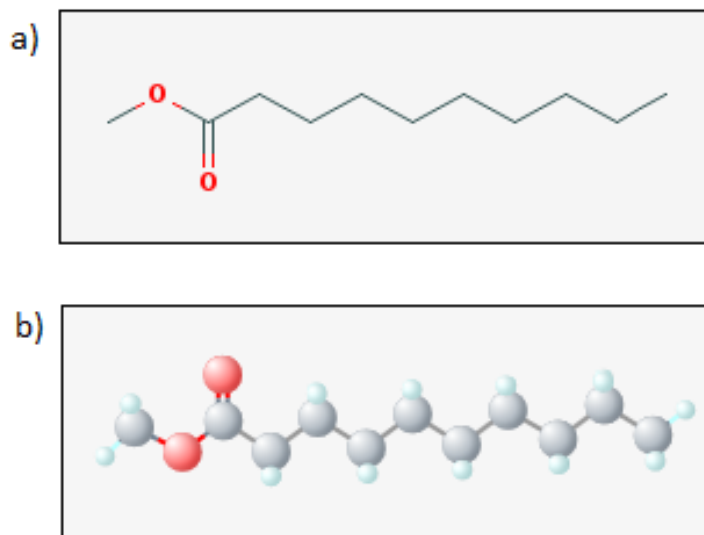
Figure 2.10: Methyl decanoate a) 2D structure and b) 3D conformation. Source: National Center for Biotechnology Information (2015)
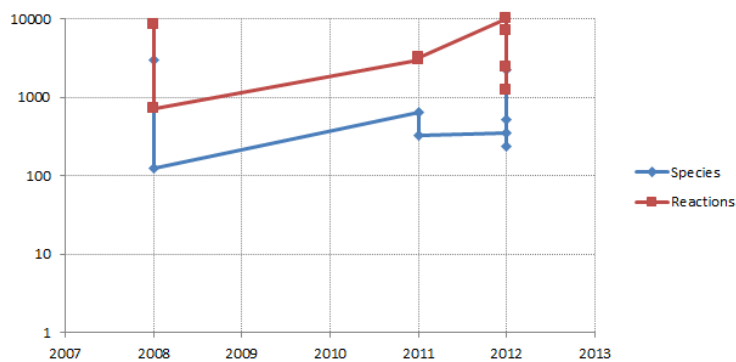
Figure 2.11: Number of species and reactions of methyl chemical kinetic models available in literature over the years. Source: own elaboration

Table 2.3: Methyl decanoate chemical kinetic models. Source: own elaboration

Number of Species and Reactions	Work Developed	Reference
3036 species and 8555 reactions	A chemical kinetic model was developed combining pre-existing models for n-heptane, iso-octane and methyl butanoate and adding some chemical data of methyl decanoate. It was validated using shock tube experiments and jet stirred reactor experiments.	Herbinet *et al.* (2008)
125 species and 713 reactions	"Directed relation graph" method was used to reduce a previous model with 8555 reactions and 3036 species. The new model developed was validated in a counterflow configuration for critical conditions of extinction and ignition.	Seshadri *et al.* (2009)
648 species and 2998 reactions	An opposed-flow diffusion flame was used to obtain data of methyl decanoate combustion. A new chemical kinetic model was developed and validated for temperatures of 900–1800 K, equivalence ratios of 0.25–2.0, and pressures of 101 and 1013 kPa	Sarathy *et al.* (2011)
324 species and 3231 reactions	A new chemical kinetic model was developed using EX-GAS and was validated using data obtained in a jet-stirred reactor at temperatures ranging from 773K to 1123K.	Herbinet *et al.* (2011)
About 350 species and 10 000 reactions	A chemical kinetic model for combustion and pyrolisys of methyl decanoate was developed by lumping methodology using a previous developed methyl butanoate model. It was validated for temperatures of 500-2000K, pressures up to 16 bar and several equivalent ratios.	Grana *et al.* (2012)

2276 species and 7086 reactions; 530 species and 2396 reactions; 238 species and 1244 reactions

A detailed chemical kinetic model for of methyl decanoate was developed by the extension of the chemical kinetic and thermochemical parameters of a methyl butanoate model. It was too large to flame simulations, so two reduced models were generated. Simulations os the reduced models were compared with experimental literature data for premixed flame conditions, high temperature ignition delay and stirred reactor speciation, and the results have a better agreement than previous models available in literature.

Diévart *et al.* (2012)

Table 2.4: Physicochemical Characteristics of n-decane, Brazilian diesel, kerosene Jet A-1, ethanol, methyl decanoate and Brazilian biodiesel. Source: own elaboration, using data from [1] Toxicology Data Network (2016); [2] Nacional Oil Agency (2015b); [3] Nacional Oil Agency (2009); [4] Nacional Oil Agency (2014); [5] NNOAA's Ocean Service (2016); [6] Sigma-Aldrich (2016); [7] Yanowitz *et al.* (2014); [8] Knothe and Steidley (2005)

Characteristic	n-decane	diesel S10	diesel S50	kerosene Jet A-1
Molecular mass $[g/mol]$	142.29	—	—	—
Density at 20°C $[g/cm^3]$	0.7300 [1]	0.815 to 0.850 [2]	0.815 to 0.865 [2]	0.7713 to 0.8366 [3]
Viscosity $[mm^2/s]$ at $40°C$	0.97 [8]	2.0 to 4.5 [2]	2.0 to 5.0 [2]	not specified [3]
Flash Point $[°C]$	46 [1]	min. 38 [2]	min. 38 [2]	min. 38.0 or 40.0 [3]
Cetane number	76 to 78 [7]	min. 48 [2]	min 42 [2]	not specified [3]

Characteristic	ethanol	methyl decanoate	biodiesel
Molecular mass $[g/mol]$	46.07	186.29	—
Density at 20°C $[g/cm^3]$	0.7893 [1]	0.8730 [1]	0.850 to 0.900 [4]
Viscosity $[mm^2/s]$ at $40°C$	1.07 [8]	1.72 [8]	3.0 to 6.0 [4]
Flash Point $[°C]$	12.8 [5]	110 [6]	min. 100 [4]
Cetane number	2 to 12 [7]	47.2 to 52.7 [7]	not specified [4]

Density and viscosity

Density is important because it affects the amount of fuel necessary to obtain some output power: if energetic density is lower, more fuel is needed, which may increase the size and weigh of fuel tanks. Ethanol is less dense and less viscous than diesel. Diesel is less dense and less viscous than biodiesel. (Shahir *et al.*, 2014). E-diesel viscosity is lower than neat diesel viscosity (Hansen *et al.*, 2005). Its a potential problem because lower fuel viscosity can increase pump and injector leakage, hence reducing maximum fuel delivery and power output (Li *et al.*, 2005). On the other hand, a slightly smaller fuel viscosity can increase energy efficiency by helping the formation of small diameter droplets (Moretti, 2013). Li *et al.* (2005) compared kinematic viscosity of neat diesel and diesel-ethanol blends up to 25% with 1.5% solubilizer (volume). The viscosity reduced with the addition of ethanol, as can be seen in Figure 2.12. A similar result was found by Labeckas *et al.* (2014), that compared neat diesel with diesel ethanol fuels up to 15% ethanol and a 80%diesel + 15% ethanol + 5% biodiesel. The blend that contained biodiesel had a kinematic viscosity between the blends of 5% and 10% ethanol.
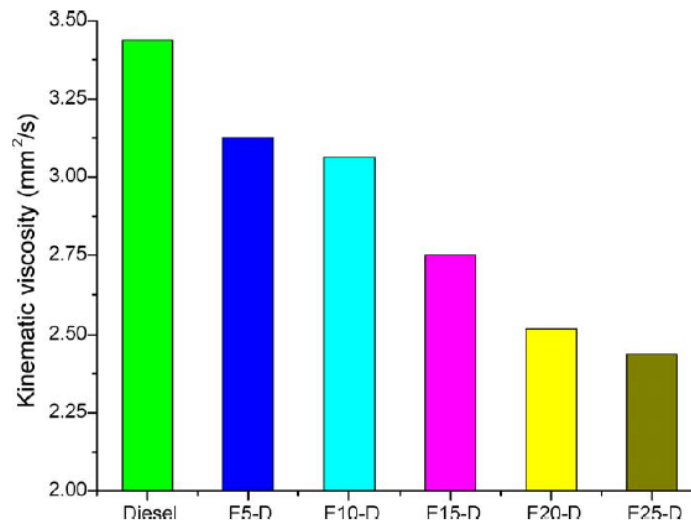
Figure 2.12: Comparison between diesel and different diesel-ethanol blends kinematic viscosities. Source: Li *et al.* (2005)

Cetane number

Cetane number is other important parameter to be evaluated in diesel-ethanol blends. It influences engine-start ability, emissions, peak cilinder pressure, combustion noise and engine life. The type of additive used influences blends cetane number (Li *et al.*, 2005). Labeckas *et al.* (2014) stud-

ied diesel with cetane number = 51.5. As revealed in references therein, the addition of anhydrous ethanol reduces cetane number and the addition of biodiesel to diesel-ethanol blends increases cetane number: A blend with 5% of ethanol had cetane number = 49.9 a blend with 10% ethanol had cetane number = 46.7; a blend with 15% ethanol had cetane number = 44.4; and a blend with 15% ethanol and 5% biodiesel had cetane number = 45.1. Moretti (2013) compared a blend of 5% biodiesel + 95% diesel with blends up to 5% anhydrous ethanol + 4.75% biodiesel + 90.25% diesel (volume) and the cetane number of the blends did not significantly differed.

Flash point

Flash point is the lowest temperature that a fuel's vapor can ignite. It is important for security reasons. In ethanol-diesel blends, the flash point is determined by the fuel that has the smaller flash point: ethanol (Li *et al.*, 2005). This can be seen in Figure 2.13.
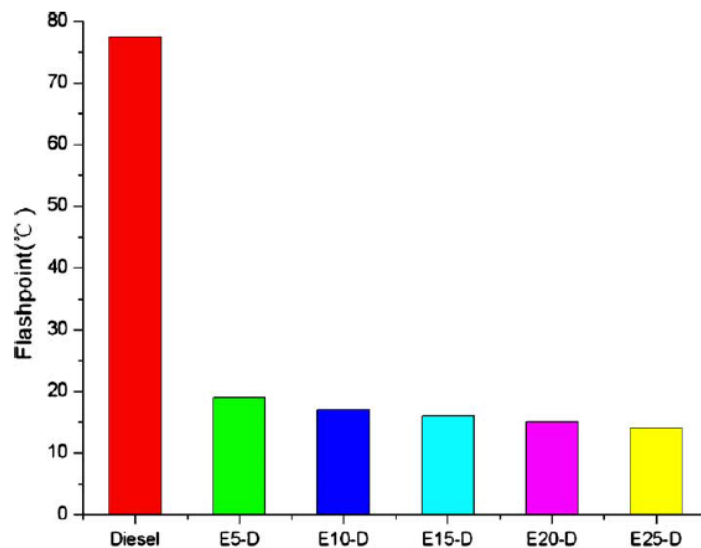
Figure 2.13: Comparison between diesel and different diesel-ethanol blends flash points. Source: Li *et al.* (2005)

Material compatibility

Ethanol is more corrosive than fossil fuels, so it is necessary to study material compatibility to use blends containing ethanol in motors. Studies made for gasoline-ethanol blends can be extrapolated to diesel-ethanol blends. The most impaired motor components are the metal ones, but non-metalic parts are affected as well: seals, o-rings and other elastomeric, resin-bonded and resin-sealed components (Hansen *et al.*, 2005).

Emissions

Finally, emissions and engine performance need to be evaluated. Ajav *et al.* (1999) compared the performance of a low horsepower, constant speed, stationary diesel engines running with neat diesel and 5%, 10%, 15% and 20% ethanol-diesel blends.They evaluated brake horsepower (bhp), brake specific fuel consumption (bsfc), brake thermal efficiency, exhaust gas temperature and lubricating oil temperature, and exhaust emissions. Engine start and bhp did not change significantly with the addition of ethanol. Other parameters maintained its curves, but changed values: bsfc increased with ethanol addition. Brake thermal efficiency, exhaust gas temperature, temperature of the lubricating oil and CO and NO_x emissions decreased with ethanol addition. Li *et al.* (2005) also compared performance and emissions of diesel and e-diesel, using the same blends proportions that Ajav *et al.* (1999), and found similar results to bsfc, CO and NO_x emissions. Besides, they found out that the emissions of total hydrocarbons increased.

2.5 Comparison between chemical kinetic models available for studied fuels

Figure 2.14 relates the number of species and reactions of the chemical kinetic models presented on tables 2.1, 2.2 and 2.3. It shows that there is a tendency of models with more species also have more reactions. It also reveals that ethanol models are the smaller; and methyl decanoate models are the bigger. It happens due to the size of molecules. Ethanol is a simple alcohol and its models can be used as a start point to the development of models to larger alcohols. In the other hand, n-decane and methyl decanoate are more complexes molecules, and some of its models have been built over smaller molecules models.
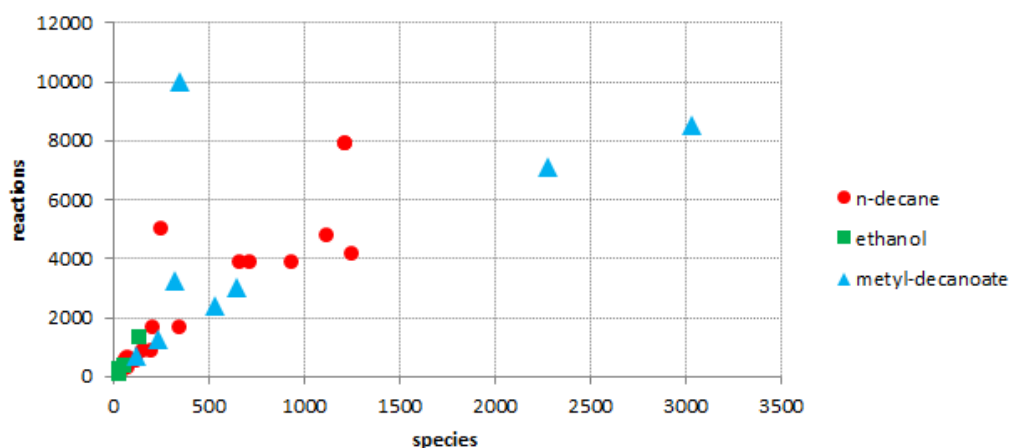
Figure 2.14: Relation between the number of species and reactions of chemical models available in literature. Source: own elaboration.

3 METHODOLOGY

This chapter is divided in two main parts:

1. Physicochemical characterization of the blends, described in section 3.1;

2. Combustion characterization, described in section 3.2.

3.1 Physicochemical characterization of the blends

The first part of this chapter is the physical-chemical characterization of ternary n-decane - ethanol - methyl decanoate blends. No previous study of ternary n-decane - ethanol - methyl decanoate blends or quaternary n-decane - ethanol - methyl decanoate - water blends properties were found in literature. The characteristics evaluated were:

1. Solubility, important to determine the ratio of each fuel that can be used in combustion. Ethanol solubility in diesel and kerosene varies with temperature, presence of water and ethanol ratio (Gerdes and Suppes, 2001). Biodiesel can be used to increase the solubility of ethanol in diesel (Chotwichien *et al.*, 2009).

2. Density, used to compare properties of surrogates and real fuels and important due to energetic density.

3. Flash point, important for safety reasons.

The reagents are described in Table 3.1.

Table 3.1: Reagents used. Source: own elaboration

Reagent	Producer	Purity
Decane	Exodo	99%
Anhydrous ethanol	Exodo	99.9%
Methyl-decanoate	Aldrich	$\geq 99\%$

The tests were made for the proportions presented in Table 3.5. The exact values used are presented in Appendix A. Blends were evaluated in weight basis, but Table 3.5 presents also the equivalent volume ratio of tested blends in Standard Conditions for Temperature and Pressure (SCTP), as a reference. The samples were weighed on a precision scale with error = $\pm 0.0001g$.

Table 3.2: Blends ratio tested. Source: own elaboration

	% Weight basis			% Volumetric basis		
Sample	N-decane	Ethanol	Methyl decanoate	N-decane	Ethanol	Methyl decanoate
1	80.0	10.0	10.0	82.0	9.5	8.6
2	70.0	10.0	20.0	72.9	9.6	17.4
3	70.0	20.0	10.0	72.3	19.1	8.6
4	60.0	10.0	30.0	63.6	9.8	26.6
5	60.0	20.0	20.0	63.0	19.4	17.6
6	60.0	30.0	10.0	62.4	28.9	8.7
7	50.0	10.0	40.0	53.9	10.0	36.1
8	50.0	20.0	30.0	53.4	19.8	26.8
9	50.0	30.0	20.0	52.9	29.4	17.7
10	50.0	40.0	10.0	52.4	38.8	8.8
11	40.0	10.0	50.0	43.9	10.2	45.9
12	40.0	20.0	40.0	43.5	20.1	36.4
13	40.0	30.0	30.0	43.1	29.9	27.0
14	40.0	40.0	20.0	42.7	39.5	17.8
15	40.0	50.0	10.0	42.3	48.9	8.8
16	30.0	10.0	60.0	33.5	10.3	56.1
17	30.0	20.0	50.0	33.2	20.5	46.3
18	30.0	30.0	40.0	32.9	30.4	36.7
19	30.0	40.0	30.0	32.6	40.2	27.2
20	30.0	50.0	20.0	32.3	49.7	18.0
21	30.0	60.0	10.0	32.0	59.1	8.9
22	20.0	10.0	70.0	22.8	10.5	66.7
23	20.0	20.0	60.0	22.6	20.9	56.6
24	20.0	30.0	50.0	22.3	31.0	46.7
25	20.0	40.0	40.0	22.1	40.9	37.0
26	20.0	50.0	30.0	21.9	50.6	27.5
27	20.0	60.0	20.0	21.7	60.2	18.1
28	20.0	70.0	10.0	21.5	69.5	9.0
29	10.0	10.0	80.0	11.6	10.7	77.7
30	10.0	20.0	70.0	11.5	21.3	67.3
31	10.0	30.0	60.0	11.4	31.6	57.1
32	10.0	40.0	50.0	11.3	41.7	47.1
33	10.0	50.0	40.0	11.1	51.6	37.3
34	10.0	60.0	30.0	11.0	61.3	27.7
35	10.0	70.0	20.0	10.9	70.8	18.3
36	10.0	80.0	10.0	10.8	80.1	9.1

3.1.1 Solubility tests

Solubility analysis was visual: homogeneous blends had a translucent appearance, and non-homogeneous blends were cloudy. The blends were mixed and then they were allowed to stand in a water bath for at least 18 hours, using two different temperatures: $T_1 = 25.0 \pm 0.1°C$ and $T_2 = 5.0 \pm 0.1°C$, at atmospheric pressure.

Solubility analysis was made for two conditions: first, using anhydrous ethanol presented in Table 3.1. Samples tested were 1, 9, 17, 20, 29 and 36. These samples were chosen because they are critical points of the solubility triangle: the edges and the middle. Then, all the samples presented in Table 3.5 were tested using hydrated ethanol, obtained by adding milli-q water to anhydrous ethanol in proportion = $93.3 \pm 0.4\%$ ethanol $+6.8 \pm 0.4\%$ water (mass fraction), which is equivalent to $94.5 \pm 0.4\%$ ethanol $+5.5 \pm 0.4\%$ water in volumetric fraction at SCTP. This proportion was chosen because Brazilian legislation determines that the minimum ethanol content in hydrated ethanol fuel is 94.5% (vol) and maximum water content is 7.5% (mass) (Nacional Oil Agency, 2015a). The exact values of each component used in sample are presented in Appendix A. Each blend weighed about 4.0g.

3.1.2 Density test

Density test was performed in samples 1, 3 and 6 (presented in Table 3.5; exact values of each component used can be found in Appendix A). Each blend weighed about 30g. These samples were chosen because they have the biggest proportions of n-decane (80%, 70% and 60%, respectively) and a constant proportion of methyl decanoate (10%), what makes them more similar to real possibilities of combinations of target fuels. Tests were performed using a density meter Anton-Paar DMA 4500. It uses the method of oscillating U-shaped tube. Temperatures tested were $20.00 \pm 0.03°C$, $40.00 \pm 0.03°C$ and $60.00 \pm 0.03°C$. All samples were double-checked and measurement errors were in the order of $10^{-5}g/cm^3$. The difference observed between measurements were $\leq 0.00007g/cm^3$.

3.1.3 Flash Point tests

Flash point tests were made in samples 7, 10, 11 and 22 (presented in Table 3.5; exact values of each component used can be found in Appendix A). Each blend weighed about 4.0g. Tests were mad using the Miniflash flph, that uses the Grabner flash detection method. Each sample were triple-checked. The measurement that deviated more was despised. The value considered was the average between the two more close measurements. Results for samples 7, 10 and 11 were the same

at both used tests. Results for sample 22 differed $1.0°C$.

3.2 Combustion characterization

The second part of this work was developed using numerical package REGATH, described in the subsection 3.2.1.

The numerical description of combustion consists on the following steps:

1. Development of a chemical kinetic model that describes n-decane - ethanol - methyl decanoate blends combustion, explained in subsection 3.2.2;

2. Numerical characterization of n-decane - ethanol - methyl decanoate blends combustion, described in 3.2.3.

3.2.1 Numerical Package: REGATH

REGATH (Candel *et al.*, 2011) is a numerical package written mainly in FORTRAN used to study chemical kinetic models in combustion problems. It was developed in EM2C lab (Centrale Supelec, France) and courteously provided to be used in the present work. REGATH's input data are similar to commercial package CHEMKIN, meaning that chemical kinetic models developed to be read at CHEMKIN can be read for REGATH.

A chemical kinetic model read by REGATH consists in:

1. The Mechanism file, that contains the chemical elements, the chemical species and the reactions with its respective rate coefficients of empirical Arrhenius equation (eq. 3.1):

$$k_{fi} = A_i T^{\beta_i} exp(\frac{-E_i}{RT})$$ (3.1)

Where k_f is the rate constant of a chemical reaction, A_i is pre-exponential factor , β_i is temperature exponent and E_i is activation energy. The subscript i is relative to each reaction.

2. The Thermodynamic file, that contains the 14 polynomial coefficients (7 for each temperature; 2 temperatures are used) necessary to determine specific heat, enthalpy and entropy, obtained by equations 3.2, 3.4 3.3.

$$\frac{C^o_{pk}}{R} = a_{1k} + a_{2k}T_k + a_{3k}T_k^2 + a_{4k}T_k^3 + a_{5k}T_k^4$$ (3.2)

$$\frac{H_k^o}{RT_k} = a_{1k}T_k + \frac{a_{2k}}{2}T_k + \frac{a_{3k}}{3}T_k^2 + \frac{a_{4k}}{4}T_k^3 + \frac{a_{5k}}{5}T_k^4 + \frac{a_{6k}}{T_k} \tag{3.3}$$

$$\frac{S_k^o}{R} = a_{1k}lnT_k + a_{2k}T_k + \frac{a_{3k}}{2}T_k^2 + \frac{a_{4k}}{3}T_k^3 + \frac{a_{5k}}{4}T_k^4 + a_{7k} \tag{3.4}$$

Where C_{pk} is specific heat, R is Gas Constant, H_k is enthalpy, S_k in entropy, T_k is temperature and a are the coefficients used by REGATH. The subscript k is relative to each specie. The superscript o refers to the standard-state 1 atmosphere.

3. The Transport file, that contains:

   ○ An index that represents the molecule geometrical configuration: 0 means that it is monoatomic; 1 means that it is linear and 2 means that it is nonlinear;

   ○ The Lennard-Jones potential in Kelvin (K);

   ○ The Lennard-Jones collision diameter in Angstroms (Å);

   ○ The dipole moment in Debye (D);

   ○ The polarizability in $Å^3$;

   ○ The rotational relaxation collision number at 298K.

All these data are empirical, based on experimental works or guessed from similar studies. Values used in this work were found in literature.

Figure 3.1 presents an scheme of a chemical kinetic model.

REGATH can solve different geometries problems. In the present work, two geometries are studied: a 1D premixed laminar flame, that uses a tube where fuel and air are inserted premixed, as presented in Figure 3.2; and a counterflow laminar diffusion flame, that uses a burner where fuel and air are fed in separately, as presented in Figure 3.3. For further information about the real counterflow burner simulated, we recommend the papers of Rolon *et al.* (1991, 1995), where it was first described. The two geometries studied are simple, but they are important first steps for future studies in more complex problems. Simple geometries are easier to model and control in lab, neglecting other physic effects.

There are several real application of premixed laminar flames, such as cooktop burners and heatings appliances. In chemical combustion studies, this configuration is important because it allows the understanding of physical phenomenon that are present also in turbulent flows; and laminar
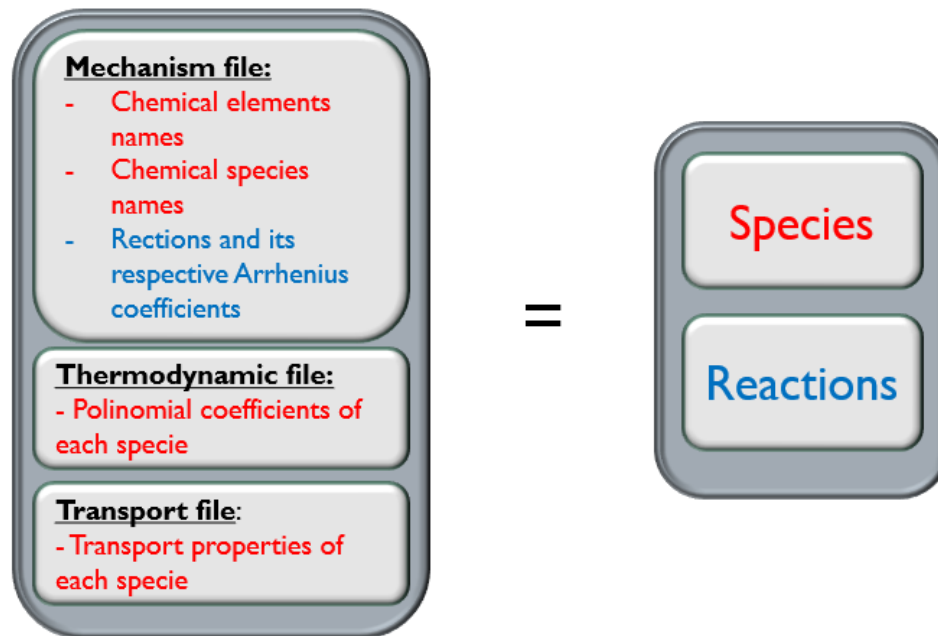
Figure 3.1: Scheme of a chemical kinetic model. Data in red and non-italic are species properties; data in blue and italic are reactions properties. Source: own elaboration.

Figure 3.2: Simulated geometry: 1D premixed flame. Source: Own Elaboration

flame speed and flame thickness model and measurements. The counterflow configuration is important because it simplifies chemical combustion modeling by considering the analysis 1D, allowing measurements of temperature and species conservation to be made in a single line. Extinction characteristics and the detailed structure of diffusion flames can be understand using this configuration (Turns *et al.*, 1996).

REGATH uses Newton's method to solve the following five basic equations for each specie:Mass Conservation, Momentum Conservation, Energy Conservation, Species Conservation and Ideal Gas Law. Aguerre (1994) presents in detail the equations used to unveil the properties of the flame: first, he presents the general equations, then he presents the simplifying assumptions and finally he presents the formulation used. This formulation is explained bellow.

General basic equations are: General Continuity Equation (eq. 3.5) , General Conservation of Momentum (eq. 3.6), General Conservation of Energy (eq. 3.7), General Conservation of
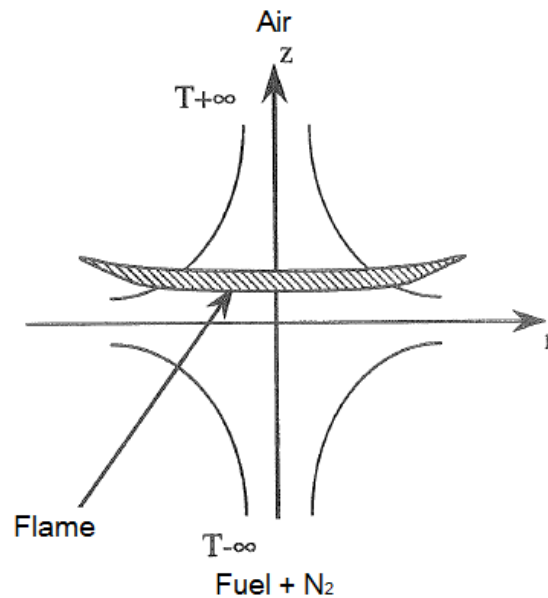
Figure 3.3: Simulated geometry: Counterflow diffusion flame. Source: adapted from Aguerre (1994)

Species (eq. 3.8) and Ideal Gas Law (eq. 3.9).

$$\frac{\partial \rho}{\partial t} + \nabla.(\rho v) = 0 \tag{3.5}$$

$$\frac{\partial (\rho v)}{\partial t} + \nabla.(\rho v v) = f_v + \nabla.\sigma \tag{3.6}$$

$$\rho \frac{\partial e_t}{\partial t} + \rho (v.\nabla) e_t = -\nabla.q + (\dot{Q}) + (\nabla.\sigma).v + f_v.v \tag{3.7}$$

$$\rho \frac{\partial Y_k}{\partial t} + \rho (v.\nabla) Y_k = -\nabla (\rho Y_k V_k) + \omega_k W_k, k = 1, ..., N \tag{3.8}$$

$$p = \rho \frac{RT}{W} \tag{3.9}$$

Where ρ is density, t is time, v is velocity, ω is molar production rate and W is molar mass. Other terms are better explained while the necessary simplifications are made.

Eqs 3.5 and 3.8 are analyzed in their general form. Other basic equations can be simplified. In eq 3.6, f_v are the forces acting on the body and are neglected. σ is the surface stress tensor,

calculated by eq 3.10.

$$\sigma = -pI + \tau \tag{3.10}$$

Where τ is the viscous stress tensor.

p is pressure, and it can be decomposed in two terms, as shown in eq. 3.11:

$$p = p_o + \tilde{p} \tag{3.11}$$

$\tilde{p}$ is a low pressure variation. Spacial pressure variation is neglected, and only time variations are considered.

So, eq. 3.6 can be rewrite as eq. 3.12

$$\rho\frac{\partial v}{\partial t} + \rho(v.\nabla)v = -\nabla\tilde{p} + \nabla.\tau \tag{3.12}$$

In eq. 3.7, e_t is total energy, that can be expressed as eq. 3.13

$$e_t = e + \frac{v^2}{2} \tag{3.13}$$

Where e is internal energy.

The last term of eq. 3.7 can be presented as a function of mass fraction of each component Y_k (presented in eq 3.14), diffusion velocity of each component V_k and the forces acting in each component f_{uk}. This relation is presented in eq. 3.15

$$Y_k = \frac{W_k}{W} \tag{3.14}$$

$$f_v.v = \rho\sum_{k=1}^{N} Y_k(g_i v_i)_k \tag{3.15}$$

Energy conservation also can be presented as a function of total enthalpy, as presented in eq. 3.16

$$h = e + \frac{p}{\rho} \tag{3.16}$$

Heat flow, presented in eq. 3.17, is composed by two effects: conduction (first term), measured by Fourrier Law, and diffusion (second term).

$$q = -\lambda \nabla T + \sum_{k=1}^{N} \rho Y_k h_k V_k \tag{3.17}$$

λ is thermal conductivity of the mixture. The subscript k is related to each specie evaluated.

Putting together eqs. 3.7, 3.15, 3.16 and 3.17; energy conservation can be expressed as eq. 3.18.

$$\rho \frac{\partial h}{\partial t} + \rho(v.\nabla)h = -\nabla.(-\lambda \nabla T + \rho \sum_{k=1}^{N} Y_k h_k V_k) + \dot{(Q)} + \rho \sum_{k=1}^{N} Y_k f_{vk} V_k + \tau : \nabla v + \frac{\partial p}{\partial t} + (v\nabla)p \tag{3.18}$$

Mass enthalpy h also can be presented as eq. 3.19:

$$h_k = \frac{C_{pk} T}{W} \tag{3.19}$$

Terms $\tau : \nabla v$ and $(v.\nabla)p$ can be neglected. Finally, we have the simplified equation of energy conservation, Eq. 3.20

$$\rho C_p \frac{\partial T}{\partial t} + \rho C_p(v.\nabla)T = \nabla.(\lambda \nabla T) - \sum_{k=1}^{N} h_k \omega_k W_k + \frac{\partial p_0}{\partial t} \tag{3.20}$$

Ideal Gas Law is reordered and rewrite as eq. 3.21.

$$\rho = \frac{p_o W}{RT} \tag{3.21}$$

Eq. 3.5, eq. 3.12, eq. 3.20, eq. 3.8 and eq. 3.21 are the equations to be solved by REGATH.

In the counterflow burner presented the flame geometry is cylindrical, because the nozzle are round. So the equations can be rewrite in cylindrical coordinates, and became eq. 3.22, eq. 3.24, eq. 3.25 and eq. 3.26. Eq. 3.21 does not change because it does not depend on the problem coordinates.

$$\frac{\partial \rho}{\partial t} + \frac{1}{r}\frac{\partial(r\rho u)}{r \partial r} + \frac{\partial(\rho v)}{\partial z} = 0 \tag{3.22}$$

$$\rho \frac{\partial u}{\partial t} + \rho(u\frac{\partial u}{\partial r} + v\frac{\partial u}{\partial z}) = -\frac{\partial \tilde{p}}{\partial r} + \frac{1}{r}\frac{\partial(r\tau_{\tau\tau})}{\partial r} - \frac{1}{r}\tau_{\theta\theta} + \frac{\partial \tau_{rz}}{\partial z} \tag{3.23}$$

$$\rho \frac{\partial v}{\partial t} + \rho(u\frac{\partial v}{\partial r} + v\frac{\partial v}{\partial z}) = -\frac{\partial \tilde{p}}{\partial z} + \frac{1}{r}\frac{\partial(r\tau_{\tau z})}{\partial r} + \frac{\partial \tau_{zz}}{\partial z} \tag{3.24}$$

$$\rho c_p \frac{\partial T}{\partial t} + \rho c_p (u \frac{\partial T}{\partial r} + v \frac{\partial T}{\partial z}) = \nabla.(\lambda \nabla T) - \sum_{k=1}^{N} h_w \omega_k W_k + \frac{\partial p_0}{\partial t} \tag{3.25}$$

$$\rho \frac{\partial Y_k}{\partial t} + \rho (u \frac{\partial Y_k}{\partial r} + v \frac{\partial Y_k}{\partial z}) = -\frac{1}{r} \frac{\partial (r \rho Y_k V_{kr})}{\partial z} + + \omega_k W_k \tag{3.26}$$

V_{kr} and V_{kz} are the radial and axial velocity components, respectively.

To reduce computational cost, the flow is considered unidimensional, and it's properties are analyzed only in the axial direction. Then, temperature and mass fraction of each specie are considered function only of axial distance z and time.

The radial pressure gradient presented in eq. 3.27 is considered constant.

$$J = -\frac{1}{r} \frac{\partial p}{\partial r} \tag{3.27}$$

Other mathematical relations are necessary beyond the basic equations: chemical production rate (eq. 3.28), viscous stress tensor (eq. 3.30), heat flow (eq. 3.17); thermodynamic properties; and transport coefficients as a function of state variables (eq. 3.31).

The chemical production rate equation is:

$$\omega_k = \sum_{i=1}^{I} (\nu''_{ki} k_{fi} \prod_{j=1}^{N} [X_j]^{\nu'_{ji}} - \nu'_{ki} k_{ri} \prod_{j=1}^{N} [X_j]^{\nu''_{ji}}) \tag{3.28}$$

At 3.28 the subscript i is related to each reaction that is being evaluated. The subscript f is used when the rate is evaluated in the forward direction, and the subscript r is used when it is evaluated in reverse direction. $k_{f}i$ is forward reaction rate constant, calculated by Arrhenius equation 3.1.

k_{fi} and k_{ri} are related by eq. 3.29.

$$\frac{k_{fi}}{k_{ri}} = \left(\frac{P_{atm}}{RT}\right)^{\sum_{j=1}^{N} \nu_{ji}} exp \left(\frac{\delta S^0_i}{R} - \frac{\delta H^0_i}{RT}\right) \tag{3.29}$$

P_{atm} is atmospheric pressure, $\nu_{ji} = \nu''_{ji} - \nu'_{ji}$; δS^0_i is entropy difference between reagents and products in standard conditions and δH^0_i is enthalpy difference between reagents and products in standard conditions.

Viscous stress tensor is calculated by equation 3.30, considering a Newtonian fluid.

$$\tau = -\mu \frac{2}{3} (\nabla.v) I + \mu ((\nabla v) + (\nabla v)^T) \tag{3.30}$$

μ is dynamic viscosity.

Diffusion speed is approximate by 3.31. The last term is called correction speed and is added to the equation to ensure mass conservation.

$$V_k = \frac{1}{X_k W} \sum_{j=1, j \neq k}^{N} W_j D_{kj} \left(\nabla X_j + (X_j + Y_j) \frac{1}{p} \nabla p \right) - \frac{D_k^T}{\rho Y_k T} \nabla T \qquad (3.31)$$

3.2.2 Development of the new chemical kinetic model

A chemical kinetic model is a list of chemical reactions with its reactions rate constants, transport and thermodynamic properties. There are different possible ways to develop a new chemical kinetic model: it can be build analytically from the start, as described by Frenklach *et al.* (1992), by generating an list of elementary chemical reactions, determining reaction rates constants, and comparing computational and experimental results. It can be build using a program, as described in Chevalier *et al.* (1992). Or it can be build using previous developed models, by adding reactions in order to be able describe more species combustion.

In the present work, a new chemical model was build by putting together 3 previous validated literature chemical models. The steps of the development of the new model are described bellow:

1. **Review of previous chemical kinetic models available in literature for the studied fuels.** The result of this step is summarized in Literature Review, in Tables 2.1 (n-decane) and 2.2 (ethanol) and 2.3 (methyl-decanoate) . Not all the papers present their developed model.

2. **Evaluation of literature chemical kinetic models available in literature and choice of which would be used to develop the new model.** For n-decane, the model presented by Marchal *et al.* (2009) was chosen primarily because it is able to predict satisfactorily the combustion of n-decane and several other hydrocarbons that can be used as surrogate components for oil fuels, such as n-heptane and toluene. It is also considerably simple, with 154 species and 850 reactions. For ethanol, the model presented by Marinov (1999) was chosen because it was the most detailed ethanol model found in literature, but still not computational expensive: it has 57 species and 387 reactions and has proved itself to be able to predict experimental data. For methyl decanoate, the model developed by Seshadri *et al.* (2009), with125 species and 713 reactions, was chosen due to its good results. Alviso (2013) added some species and reactions to this model, in order to describe CO* and OH* behavior. This modified model was used.

   129 species and 741 reactions, was chosen due to its good results.

3. **Chemical kinetic models fusion and 1D validation.** The fusion of the chemical kinetic models was made by parts. The 3 models used are independent, but have common reactions and species. The rate coefficients of empirical Arrhenius equation for the same reactions, and the polynomial coefficients and the transport properties for the same species change between models. So it is necessary to choose which ones should be used when species or reactions are repeated. The model that prevails is called skeleton, the other one is the complimentary. The fusion process is diagrammed in Figure 3.4.
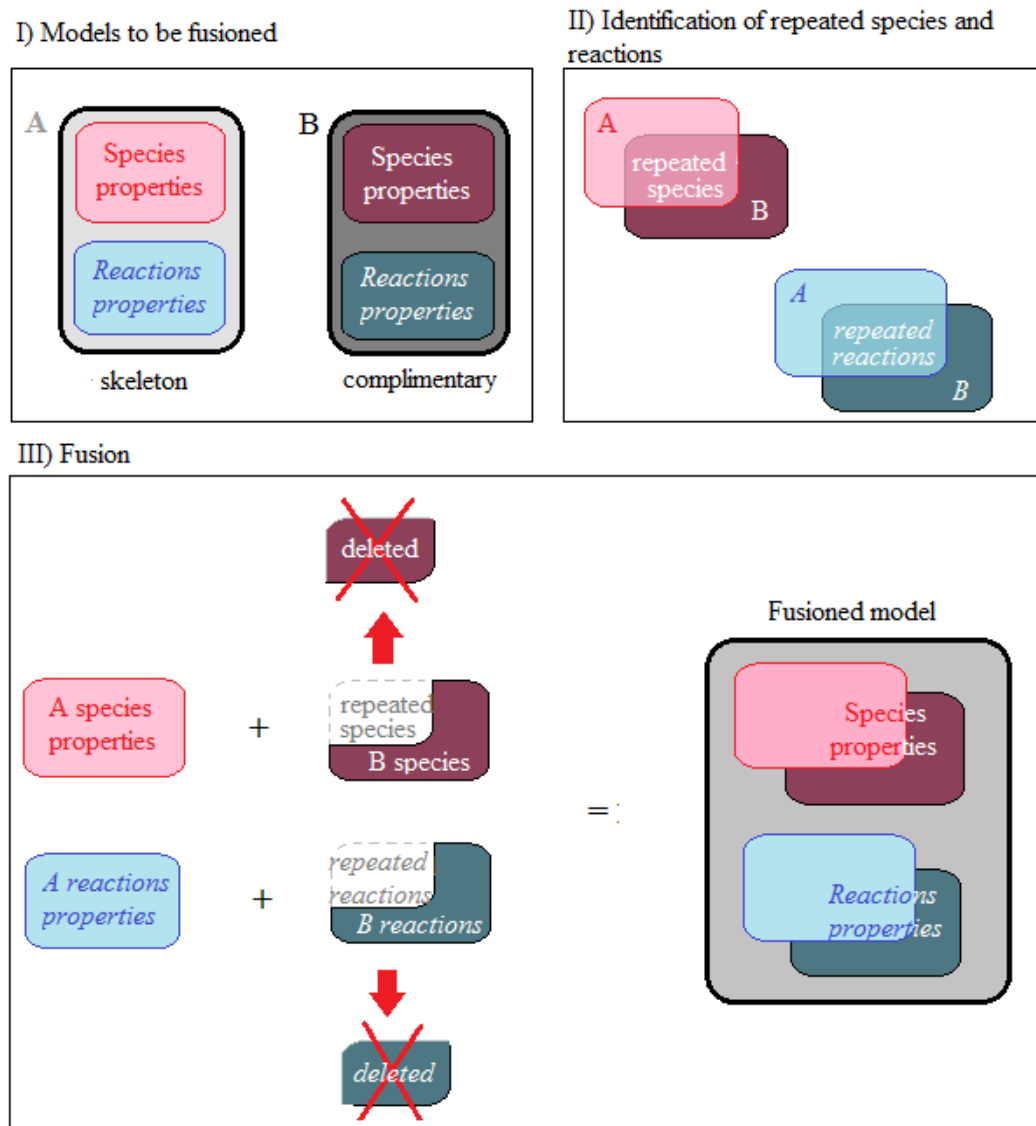
Figure 3.4: Diagram of the fusion of models. Source: own elaboration.

The fusion processes follows the steps above:

- ○ Copy of all reactions from complimentary model to skeleton model;

- ○ Identification of chemical reactions that are present in both schemes;

- ○ Elimination of repeated chemical reactions: the repeated reactions of complimentary model are deleted;

- ○ Identification of missing species in skeleton model;

- ○ Copy of non-repeated species and its thermodynamic and transport properties from complimentary model to skeleton model;

- ○ Simulation of developed model and comparison with literature laminar flame speed data for different air/fuel ratios.

Three fusions were made. First, the n-decane model was merged with the ethanol model. When the n-decane + ethanol model was properly validated, this intermediate model was fusioned with the methyl decanoate model. The first two-models fusion was made twice: first using n-decane model as skeleton and ethanol as complimentary; then changing places - the ethanol model became skeleton and vice-versa. The model developed using ethanol as skeleton showed better results comparing with literature data. The second fusion was made only once, using the intermediate ethanol (skeleton) + decane (complimentary) model as skeleton model and the methyl decanoate model as complimentary. The results found by this fusion satisfactorily approached literature data. The validation was made comparing laminar flame speed data predicted using a 1D premixed flame (Figure 3.2) with experimental and computational laminar flame speed data available in literature for surrogates and target fuels. Laminar flame speed is a fundamental flame property because it is a function of preheat temperature, pressure and fuel composition; and its behavior reflects effects of diffusivity, exothermicity and reactivity of the fuel (Hui and Sung, 2013). Table 3.6 summarizes the experimental data from literature used to validate the developed model.

3.2.3 Numerical characterization of n-decane - ethanol - methyl decanoate blends combustion

After the validation of the new chemical kinetic model developed, pure fuel combustion were compared with the combustion of three samples studied in physicochemical characterization: sample 1, also called E10 (80% n-decane + 10% ethanol + 10% MD); sample 3, also called E20 (70% n-decane + 20% ethanol + 10% MD); and sample 6, also called E30 (60% n-decane + 30% ethanol + 10% MD). 1D premixed flame configuration (Figure 3.2) was simulated to determine laminar flame speed.

Counterflow diffusion flame configuration (Figure 3.3) was simulated to determine flame structure, flame speed, flame temperature and some species profiles: O_2, HCO, H_2O, CO and CO_2. Besides the effect of ethanol and methyl decanoate addition, the influence of equivalence ratio and injection velocity were studied as well. Pure n-decane and blends combustion were simulated at 5 different conditions of fuel-air equivalence ratio (ϕ, defined in equation 3.32) and velocity: $\phi = 4.0$ and $v = 30m/s$; $\phi = 3.0$ and $v = 30m/s$; $\phi = 5.0$ and $v = 30m/s$; $\phi = 4.0$ and $v = 40m/s$; $\phi = 4.0$ and $v = 50m/s$. Pure ethanol and pure methyl decanoate were simulated only using $\phi = 4.0$ and $v = 30m/s$.

$$\phi = \frac{n_{fuel}/n_{air}}{(n_{fuel}/n_{air)}stech} \tag{3.32}$$

Table 3.3: Experimental data of laminar flame speed used to validate the developed model. Source: own elaboration

Fuel(s)	Experiment	Reference
n-decane	A counterflow burner and a Laser Doppler Velocimetry were used to perform the experiments and measure the flow velocities at atmospheric pressure and T = 403K.	Ji *et al.* (2010)
n-decane and jet-A1	A counterflow twin-flame configuration was used to measure the flame speed at T=400K, atmospheric pressure.	Kumar and Sung (2007); **?**
n-decane and jet-A1	Flame speed was determined by linear extrapolation using data obtained in a counterflow configuration twin flame, T= 400K and atmospheric pressure.	Hui *et al.* (2012)
n-decane	A nearly constant pressure spherical combustion bomb was used. Measurements were made at T=400K and atmospheric pressure	Kim *et al.* (2013)
n-decane	A jet-wall apparatus was used for the measurements. The geometry generates stable flames and allows precise knowledge of the stagnation-point location and its associated boundary conditions. Heat loss can be neglect. Temperature was 400K and the tests were made in atmospheric pressure.	Munzar *et al.* (2013)
n-decane	Laminar flame speed was measured in spherically expanding premixed flames, T= 400K, atmospheric pressure. Linear and non-linear extrapolation values were compared.	Singh *et al.* (2011)

n-decane	Measures were made in a spherical bomb, that consists of a spherical stainless steel vessel equipped with quartz windows. Temperature was 403K and the tests were made at initial pressure of 1 bar.	Comandini *et al.* (2015)
Ethanol	A constant volume bomb was used to investigate laminar flame speed of ethanol-gas mixtures, T=300K, P= 1atm.	Gulder (1982) apud Marinov (1999)
Ethanol	A constant volume combustion bomb was used to determine laminar flame speed. Measurements of spherically expanding flames using schlieren photography technique were made. Tests were made at T=358K, 1atm and extrapoled to others temperatures.	Liao *et al.* (2007)
Methyl decanoate	A counterflow configuration at atmospheric pressure was used to determine laminar flame speed of methyl decanoate.	Wang *et al.* (2011)
Jet-A1, diesel, palm methyl esters (43.1% methyl oleate, 39.5% methyl palmitate, 10.4% methyl linoleate and 5% methyl stearate) and blends	The jet-wall stagnation flame configuration and particle imaging velocimetry (PIV) technique were used to determine laminar flame speed at T=470K and P= 1atm	Chong and Hochgreb (2011)

4 RESULTS

4.1 Physicochemical characterization of the blends

4.1.1 Solubility tests

Solubility tests were made for two conditions: anhydrous ethanol and hydrated ethanol ($93.3 \pm 0.4\%$ ethanol $+6.8 \pm 0.4\%$ water - mass fraction), as described in subsection 3.1.1. Exact values of each component used can be found in Appendix A.

All the samples tested using anhydrous ethanol were monophasic at both temperatures ($25°C$ and $5°C$). Phase behavior of samples tested using hydrated ethanol is presented in Figure 4.1. The analysis was visual. The difference between monophasic blends (translucent) and biphasic or multiphasic blends (cloudy) can be seen in Figure 4.2.
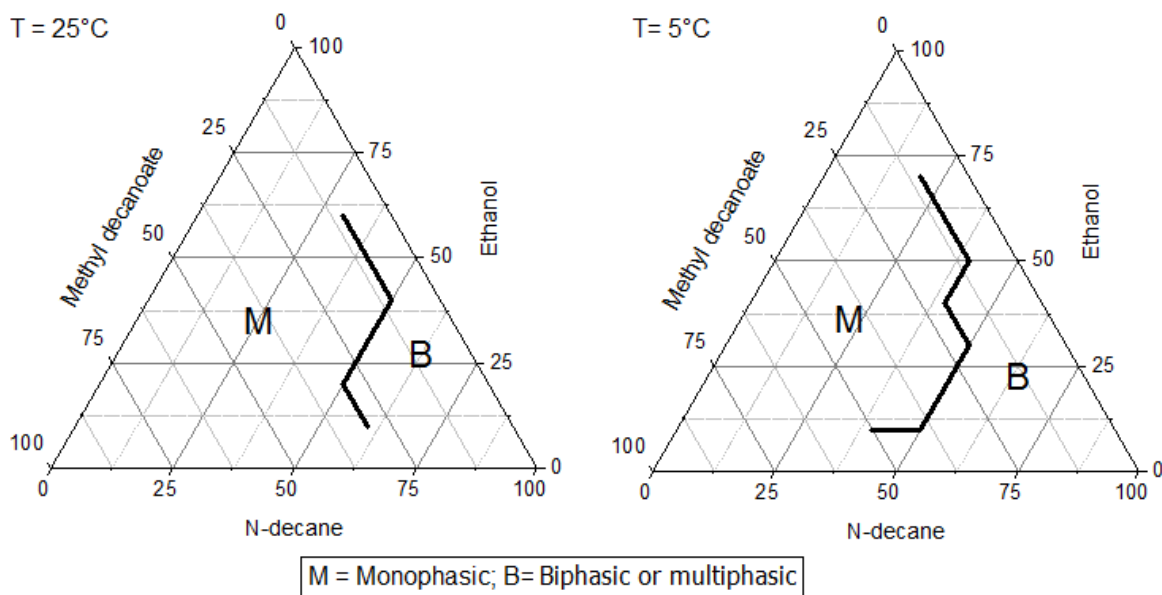
Figure 4.1: Solubility diagram of ternary n-decane + hydrated ethanol + methyl decanoate blends for $T = 25°C$ and $T = 5°C$ (mass fraction). Blends at right side of the line were biphasic or multiphasic (B); blends at left side of the line were monophasic (M). Source: Own Elaboration

Anhydrous ethanol solubility in n-decane is higher than anhydrous ethanol solubility in diesel, as can be seen comparing experimental data results (total solubility) with the data presented by Chotwichien *et al.* (2009) reproduced in Figure 2.9. N-decane's chemical class (n-alkane) is responsible for only a small fraction of diesel fuel (Pitz and Mueller, 2011), what explains this difference. The increase of the content of aromatics in diesel decreases ethanol solubility in it (Shahir

Figure 4.2: Visual difference between 1) a monophasic blend (translucent) and 2) a biphasic or multiphasic blend (cloudy). Source: Own Elaboration

et al., 2014).

The results found confirm the effect of water addition and temperature reduction in the blends: both factors reduce solubility, and water addition affects solubility more than temperature reduction. This result is relevant because Brazil uses hydrated ethanol as fuel in Otto cycle motors. Also, water contamination is a problem that need to be avoided when anhydrous ethanol is blended with diesel (Chotwichien *et al.*, 2009; Lapuerta *et al.*, 2007) or kerosene (Chen *et al.*, 2014). It is important to highlight that blends simulated in numerical combustion study are monophasic with anhydrous ethanol (as simulated), but biphasic or multiphasic with hydrated ethanol at both temperatures.

Maximum solubility observed in blends using hydrated ethanol at $T = 25°C$ was 10% ethanol + 40% methyl decanoate in 50% n-decane. Reducing temperature to $T = 5°C$, no blend with 50% or more n-decane was monophasic.

4.1.2 Density test

Density test was performed in sample 1 (80% n-decane + 10% ethanol + 10% methyl decanoate, mass fraction, now identified as E10), sample 3 (70% n-decane + 20% ethanol + 10% methyl decanoate, mass fraction, now identified as E20) and sample 6 (60% n-decane + 30% ethanol + 10% methyl decanoate, mass fraction, now identified as E30) at $T = 20.00 \pm 0.03°C$, $T = 40.00 \pm 0.03°C$ and $T = 60.00 \pm 0.03°C$. Data obtained is presented is Figure 4.3. Exact values of each component used can be found in Appendix A.

Figure 4.3 reveals that the addition of ethanol increases blend density, while the increase
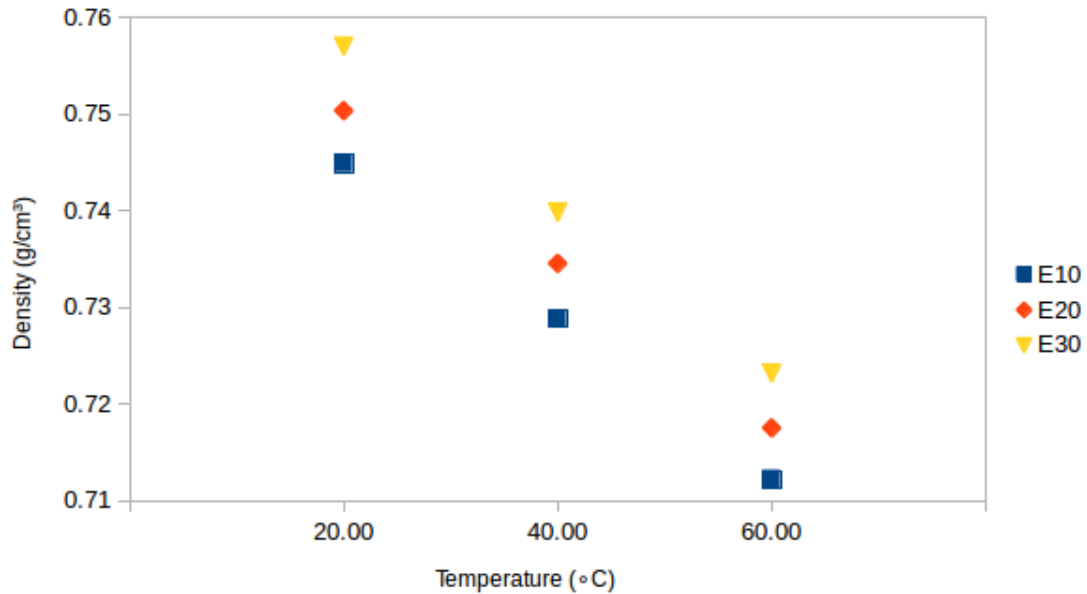
Figure 4.3: Densities of E10 (80% n-decane + 10% ethanol + 10% methyl decanoate, mass fraction), E20 ((70% n-decane + 20% ethanol + 10% methyl decanoate, mass fraction) and E30 ((60% n-decane + 30% ethanol + 10% methyl decanoate, mass fraction) at $T = 20.00 \pm 0.03°C$, $T = 40.00 \pm 0.03°C$ and $T = 60.00 \pm 0.03°C$. Source: Own Elaboration

of temperature decreases blend density. That behavior is coherent because ethanol is more dense than n-decane and temperature decreases fluids density because mass is constant and the volume increases. If the real fuels were studied, ethanol addition would be expected to decrease blends density, as long as diesel and kerosene are more dense than n-decane.

4.1.3 Flash point tests

Flash point tests were performed in samples 7; 10; 12 and 22 (20% n-decane + 10% ethanol + 70% methyl decanoate, mass fraction). Exact values of each component used can be found in Appendix A. Table 4.1 compares the flash point results found for samples with literature data for pure fuels.

Results presented in Table 4.1 reveal that blends flash point are low and close to pure ethanol flash point. This result is also seen in the real fuels, as presented in figure 2.13. The most ethanol the blend has, the lowest is the flash point; but even small ethanol ratios drastically decreases this property. Sample 10 has the biggest ethanol ratio and the lowest flash point. Sample 22 has only $10.84 \pm 0.01\%$ of ethanol and $69.18 \pm 0.01\%$ of methyl decanoate (mass fraction), and it's flash point is much smaller than methyl decanoate's.

Table 4.1: Comparison between measured flash points for the blends and literature data for pure fuels. References: [1]Toxicology Data Network (2016); [2] NNOAA's Ocean Service (2016); [3]Sigma-Aldrich (2016). Source: own elaboration

Sample	% n-decane	% ethanol	% methyl decanoate	Flash point [$°C$]
N-decane	99%	—	—	46 [1]
Ethanol	—	99.9%	—	12.8 [2]
Methyl-decanoate	—	—	$\geq 99\%$	110 [3]
7	49.94 ± 0.01	10.14 ± 0.01	39.92 ± 0.01	20.5 ± 0.1
10	49.78 ± 0.01	40.01 ± 0.01	10.21 ± 0.01	15.4 ± 0.1
12	40.09 ± 0.01	19.99 ± 0.01	39.92 ± 0.01	17.5 ± 0.1
22	19.97 ± 0.01	10.84 ± 0.01	69.18 ± 0.01	23.0 ± 0.5

4.2 Combustion characterization

4.2.1 Freely propagating flames

New Model development and validation

In order to be able to simulate n-decane-methyl decanoate-ethanol/air flames, species representing these three fuels must be present in a single model. The kinetic model proposed here is designed from the original ethanol oxidation framework of Marinov (1999). This latter chemical scheme is used as a starting base model. Then additional species found in kinetic scheme of Marchal *et al.* (2009) (n-decane) and the corresponding reactions are added. For the common species, reactions present in Marchal *et al.* (2009) model and not present in Marinov (1999) model are also added. The reactions of Marchal *et al.* (2009) model that already were present in Marinov (1999) model are neglected. Then, this combined ethanol/n-decane model was used as template. Additional species found in kinetic scheme of Seshadri *et al.* (2009) modified by Alviso (2013) (methyl decanoate) and the corresponding reactions are added. For the common species, reactions present in Seshadri *et al.* (2009) modified by Alviso (2013) model and not present in the combined ethanol/n-decane model are also added. The other reactions are neglected. Thus, the new combined ethanol/n-decane/methyl decanoate scheme, consists of 258 species and 1586 elementary reactions. This guarantees reproducing the principal features of the three fuels combustion characteristics.

The new developed model was validated comparing laminar flame speed data from experimental works found in literature and presented in Table 3.6 with simulations using the New Model and others chemical kinetic models from literature in the 1D premixed flame configuration presented in Figure 3.2. All data were measured or simulated in atmospheric pressure, using different temperatures: Figure 4.4 compares pure n-decane data at T=400K. Figure 4.5 compares pure

ethanol data at T=300K and T=358K. Figure 4.6 compares pure methyl decanoate data at T=400K.
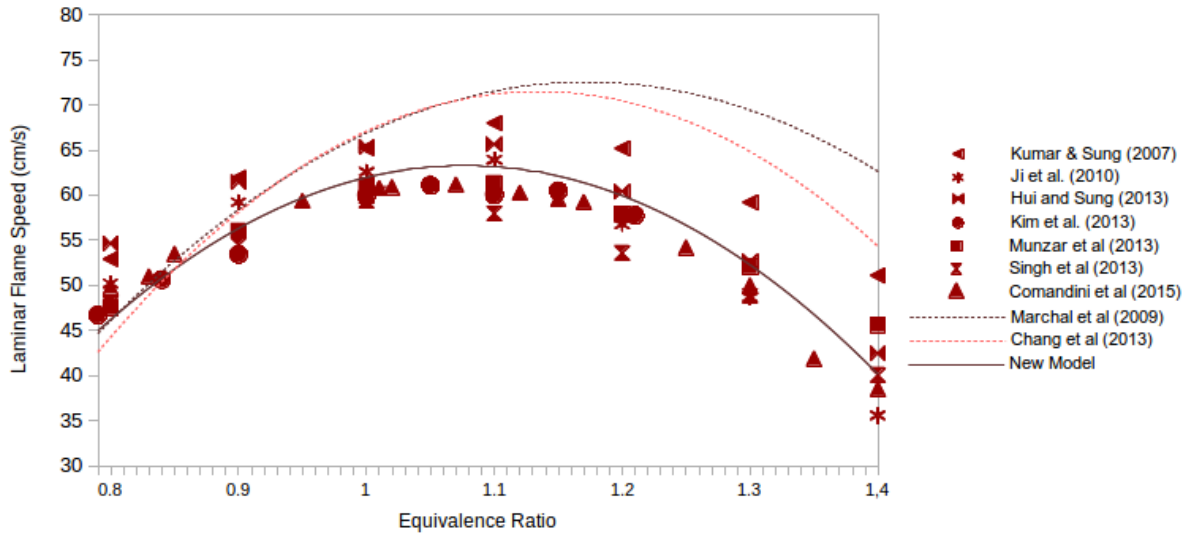
Figure 4.4: Comparison between experimental data (no line points) and numerical data (solid and dashed lines) of laminar flame speed of pure n-decane at T=400K. Source: Own Elaboration
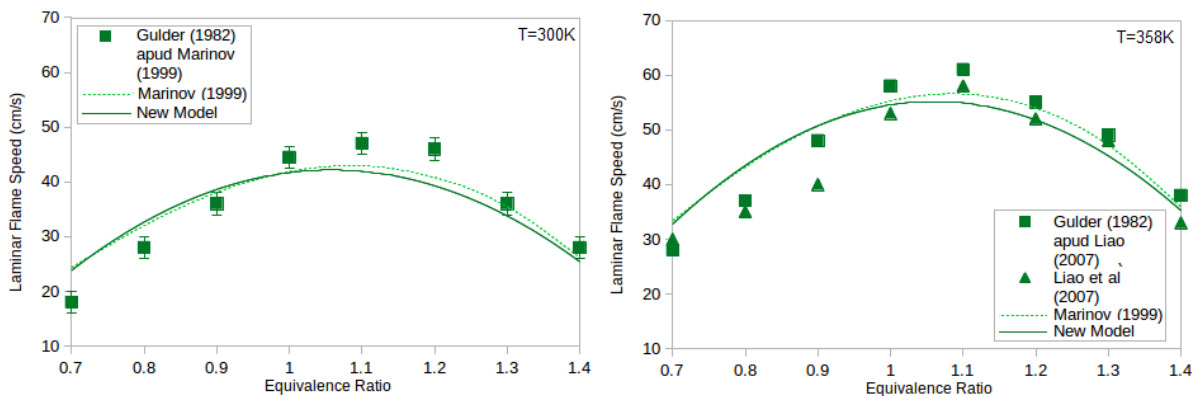
Figure 4.5: Comparison between experimental data (no line points) and numerical data (solid and dashed lines) of laminar flame speed of pure ethanol at T=300K and T=358K. Source: Own Elaboration

Figures 4.4, 4.5 and 4.6 reveal that the developed model has a good agreement with experimental laminar flame speed data of pure fuels. Ethanol model (Marinov, 1999) was used as skeleton, so the simulation of the New Model was expected to be close to it, as observed in Figure 4.5. Figures 4.4 and 4.6 reveal that the New Model simulated data is closer to experimental data than the models used as complimentary - Decane model (Marchal *et al.*, 2009) and Methyl decanoate model Seshadri *et al.* (2009) modified by Alviso (2013) - and other decane model found
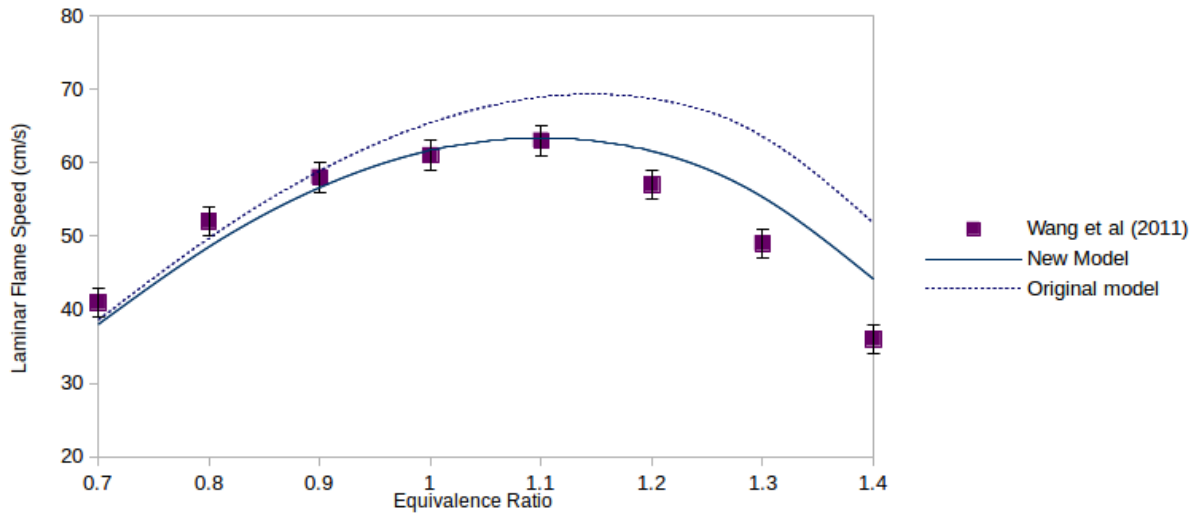
Figure 4.6: Comparison between experimental data (no line points) and numerical data (solid and dashed lines) of laminar flame speed of pure methyl decanoate at T=400K. Source: Own Elaboration

in literature (Chang *et al.*, 2013). The New Model is validated for the studied fuels, and it can be used to predict combustion properties of their blends.

There was not found in literature any study of laminar flame speed of n-decane + ethanol + methyl decanoate blends.

Comparison between laminar flame speed of surrogates and target fuels

After the model validation for the studied fuels, laminar flame speeds of surrogates were simulated and compared with target fuels experimental data found in literature (Table 3.6) using 1D premixed flame configuration presented in Figure 3.2.

Figure 4.7 compares n-decane simulated data using the New Model with experimental data of diesel (Chong and Hochgreb, 2011) and kerosene Jet A1 (Chong and Hochgreb, 2011; Kumar *et al.*, 2011; Hui *et al.*, 2012) at T=470 K and atmospheric pressure. It reveals that for lean or stoichiometric equivalence ratios ($\phi \leq 1$) laminar flame speed of n-decane approaches significantly to both diesel and kerosene. When equivalence ratio increases, diesel laminar flame speed becomes higher than n-decane's and the surrogate behavior approaches to kerosene behavior only. This result is consistent with studies found in literature that use n-decane as the main component of diesel's surrogate but add an aromatic compound to get closer to real fuel behavior, because pure n-decane do not match it properly (Barths *et al.*, 1999, 2000; Ramirez L *et al.*, 2010; Wang *et al.*, 2010). Results also agrees with studies that use pure n-decane as kerosene surrogate (Dagaut

et al., 1994, 1995; Cathormet *et al.*, 1999; Lindstedt and Maurice, 2000). Adding more components to surrogate composition can improve the similarities between surrogate and target fuel, but also increase computational cost of simulations, because more chemical reactions are necessary to describe combustion.
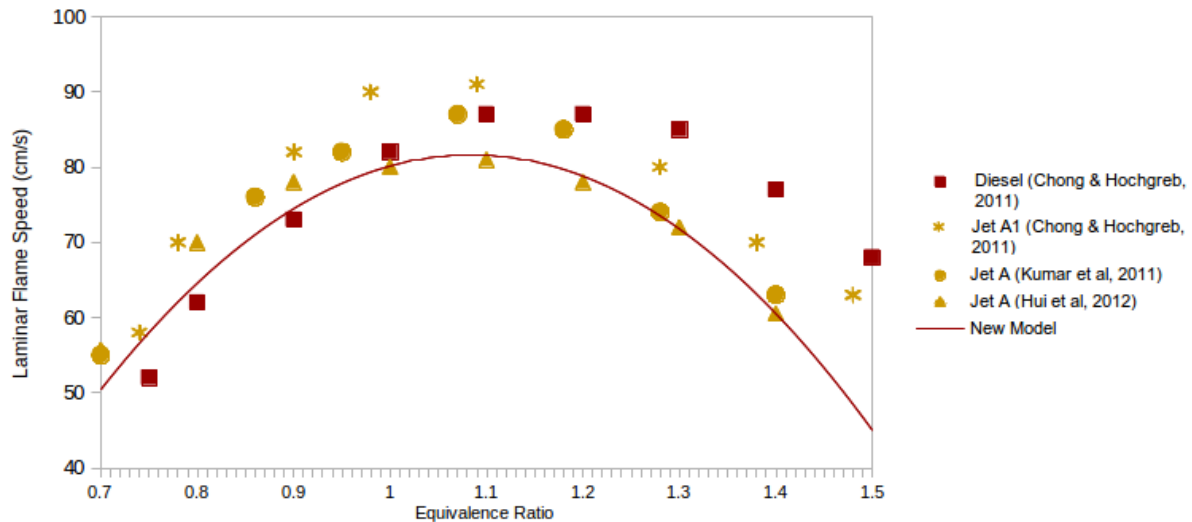
Figure 4.7: Comparison between laminar flame speed of n-decane (simulated), diesel (experimental) and kerosene Jet A1 (experimental) at T=470K and P=1atm. Source: Own Elaboration

Figure 4.8 compares laminar flame speed simulated for pure methyl decanoate with laminar flame speed of biodiesel (palm methyl ester) experimentally found by Chong and Hochgreb (2011) at T=470 K and P=1 atm. Methyl decanoate laminar flame speed approaches a little to biodiesel laminar flame speed, suggesting that more tests are necessary to validate if methyl decanoate is an adequate surrogate to biodiesel. It is important to remember that biodiesel's composition changes depending on the vegetable chosen, where it was produced and the legislation of each country. Other studies have used methyl decanoate as an appropriate biodiesel surrogate, as can be seen in Alviso (2013) and references therein.

Figure 4.9 compares laminar flame speed simulated for pure n-decane, pure methyl decanoate and blends of these species with laminar flame speed for biodiesel (palm methyl ester) and diesel and biodiesel and kerosene experimentally found by Chong and Hochgreb (2011) at T=470K and P=1atm. Methyl decanoate and decane have a similar chemical composition and its laminar flame speed are really close, so the addition of methyl decanoate in n-decane do not significantly affects the laminar flame speed. Differences between those fuels flame speeds can be seen only in richer equivalence ratios ($\phi \geq 1.3$), when methyl decanoate laminar flame speed stars to be slightly higher than n-decane laminar flame speed. Blends simulation approached real data only when $\phi \leq 1.1$,
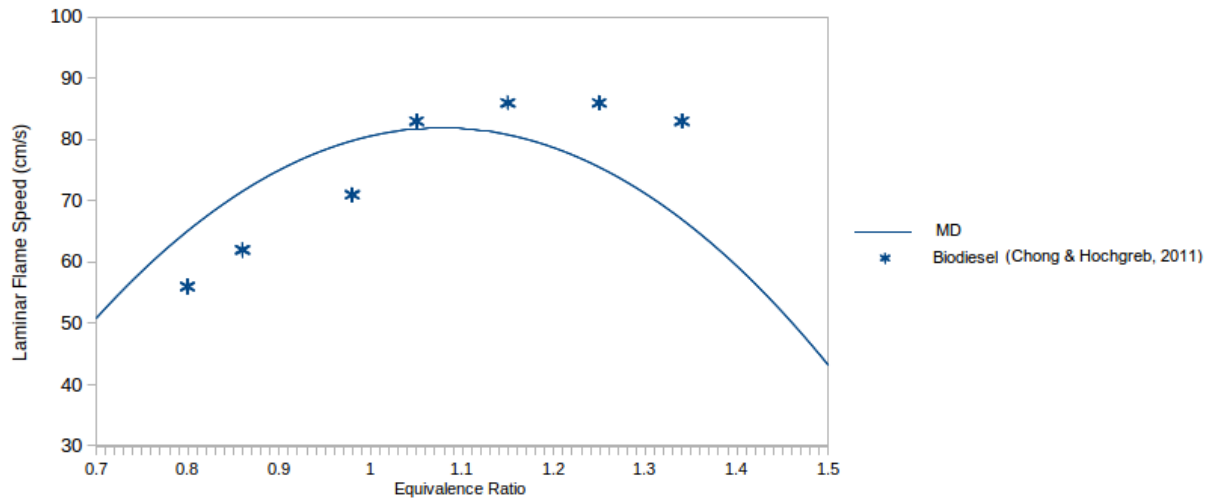
Figure 4.8: Comparison between simulated laminar flame speed of pure methyl decanoate with experimental data from Chong and Hochgreb (2011) of laminar flame speed of biodiesel at T=470K and P=1atm. Source: Own Elaboration

what can be explained by the difference observed between surrogates and target fuels.
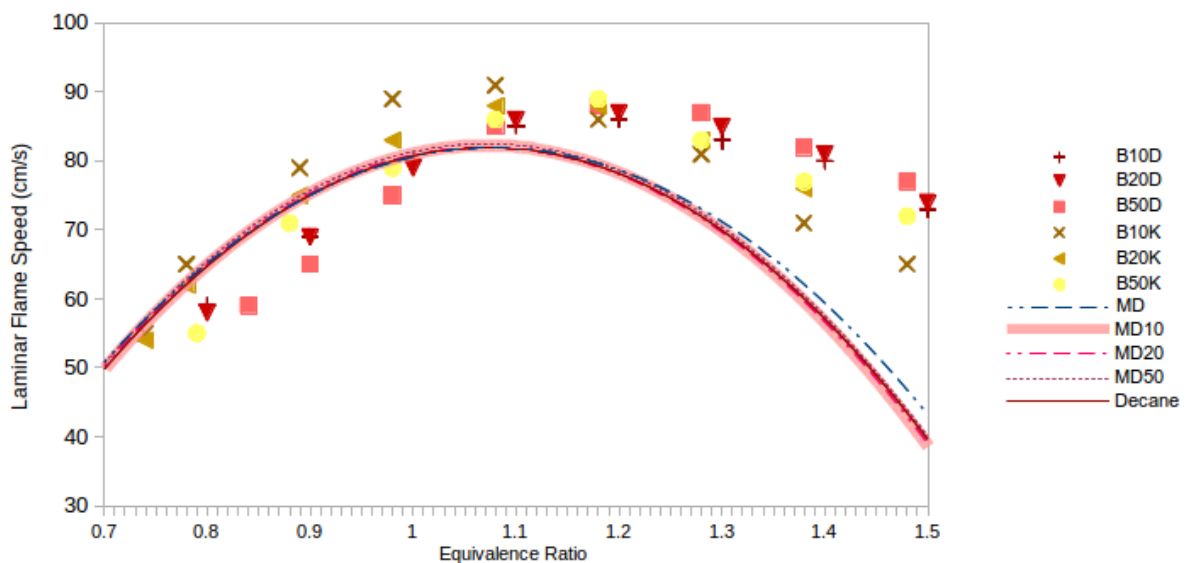
Figure 4.9: Comparison between simulated laminar flame speed of pure n-decane, pure methyl decanoate and blends with 10% methyl decanoate (MD10), 20% methyl decanoate (MD20) and 50% methyl decanoate (MD50) (vol) with experimental data from Chong and Hochgreb (2011) of laminar flame speed of blends with 10% biodiesel + 90% diesel (B10D), 20% biodiesel + 80% diesel (B20D), 50% biodiesel + 50% diesel (B50D), 10% biodiesel + 90% kerosene (B10K), 20% biodiesel + 80% kerosene (B20K) and 50% biodiesel + 50% kerosene (B50K) (vol) at T=470K and P=1atm. Source: Own Elaboration

There was not found in literature any study of laminar flame speed of diesel + ethanol, kerosene + ethanol, biodiesel + ethanol, diesel + ethanol + biodiesel nor kerosene + ethanol + biodiesel.

Comparison between laminar flame speed of blends and pure fuels

Three blends studied in physicochemical characterization were chosen to be studied in the final part of the present work: E10 (80% n-decane + 10% ethanol + 10% MD, weight basis), E20 (70% n-decane + 20% ethanol + 10% MD, weight basis) and E30 (60% n-decane + 30% ethanol + 10% MD, weight basis). All data presented in this section were simulated using the New Model developed and, even thought the model has been validate using experimental literature data for pure fuels, it is still necessary to experimentally validate it for the blends, which we suggest as a future work.

Figure 4.10 presents laminar flame speed of pure fuels and blends E10, E20 and E30 simulated at T=300K, P=1atm. It reveals that the addition of ethanol up to 30% in weigth basis do not change significantly n-decane laminar flame speed.
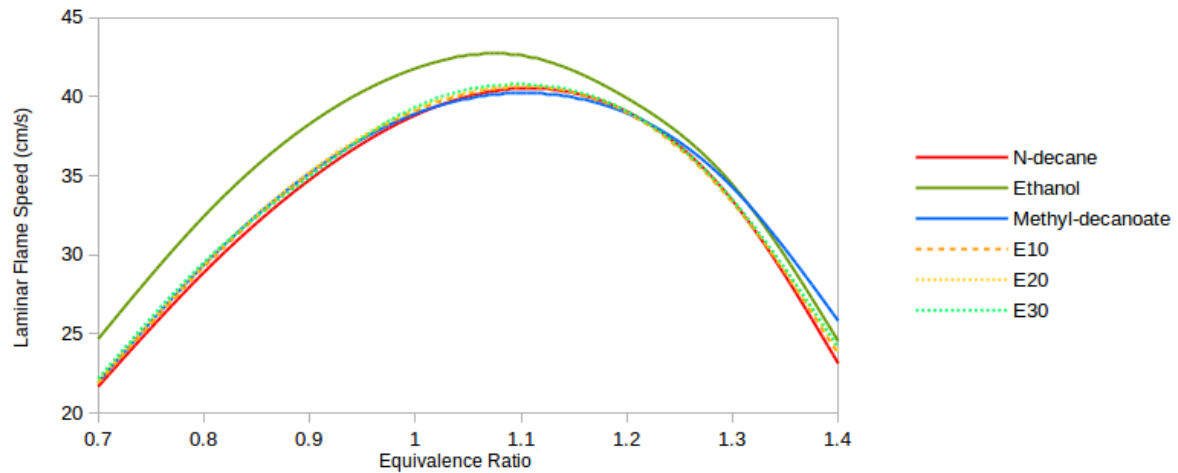
Figure 4.10: Comparison between simulated laminar flame speed of pure n-decane, pure ethanol, pure methyl decanoate and blends E10 (80% n-decane + 10% ethanol + 10% MD, weight basis), E20 (70% n-decane + 20% ethanol + 10% MD, weight basis) and E30 (60% n-decane + 30% ethanol + 10% MD, weight basis) at T=300K, P=1atm. Source: Own Elaboration

4.2.2 Counterflow diffusion flames

The combustion of blends E10, E20 and E30 were also simulated using counterflow configuration and compared with pure n-decane, pure ethanol and pure methyl decanoate. Comparisons

between blends and pure n-decane were made in five different operations conditions ($\phi = 4.0$ and $v = 30m/s$; $\phi = 3.0$ and $v = 30m/s$; $\phi = 5.0$ and $v = 30m/s$; $\phi = 4.0$ and $v = 40m/s$; $\phi = 4.0$ and $v = 50m/s$). Ethanol and methyl decanoate were simulated only at $\phi = 4.0$ and $v = 30m/s$. The results of these simulations are presented in this section. Some simulations results were the same for different operation conditions or for different blends. In this case, only one graph is presented, and the similarity is explained in the text.

Figure 4.11 presents n-decane flame structure and temperature at different equivalence ratios and different injection speeds. The flame stabilizes at same point for all conditions. The increase of equivalence ratio increases maximum temperature. Changing the injection speed do not significantly affect this parameter. This behavior was observed in studied blends as well.

Figure 4.12 presents pure ethanol and pure methyl decanoate flame structure and temperature at equivalence ratio $\phi = 4.0$ and injection velocity at both left and right sides $v = 30m/s$ in a counterflow diffusion flame configuration. Ethanol molecule is lighter than methyl decanaote molecule (see Table 2.4), so ethanol mass fraction is higher then methyl decanaote mass fraction for the same equivalence ratio. In a counteflow diffusion configuration, the flame stabilizes at the stoichiometric condition. The flame position is almost constant in all simulated conditions. Ethanol and methyl decanoate maximum temperature are close, and smaller then n-decane maximum temperature.

Figure 4.13 presents blends flame structure and temperature at $\phi = 4.0$ and injection velocity $v = 30m/s$. Blends maximum temperature are close to each other and close to n-decane's, revealing that the addition of ethanol and methyl decanoate do not change this parameter. Changes in equivalence ratio and injection speed have the same effect in the blends and in pure n-decane.

Figure 4.14 presents n-decane axial velocity and H_2O profile at different equivalence ratios and different injection speeds. The point $v = 0m/s$ is the stagnation point. The axial velocity profile depends on the injection velocity at both sides, and there is an acceleration and deceleration of the gas when approaching to the reaction zone. This behavior was observed in blends as well. H_2O is a main product of combustion and its profile is very similar to that of temperature. The fact that its profile do not change significantly with the increase of equivalence ratio indicates that the extra fuel is producing other compounds.

Figure 4.15 presents pure ethanol and pure methyl decanoate axial velocities and H_2O profile at $\phi = 4.0$ and $v = 30m/s$. Velocity profiles are similar. Ethanol produces more water then methyl decanoate because, for the same equivalence ratio, ethanol mass fraction is higher than methyl decanoate mass fraction in a mixture. Besides, hydrogen ratio is higher in ethanol than in methyl decanoate.

Figure 4.16 presents blends axial velocity and H_2O profile at $\phi = 4.0$ and $v = 30m/s$. The profiles are very similar. The addition of ethanol slightly increases H_2O production.
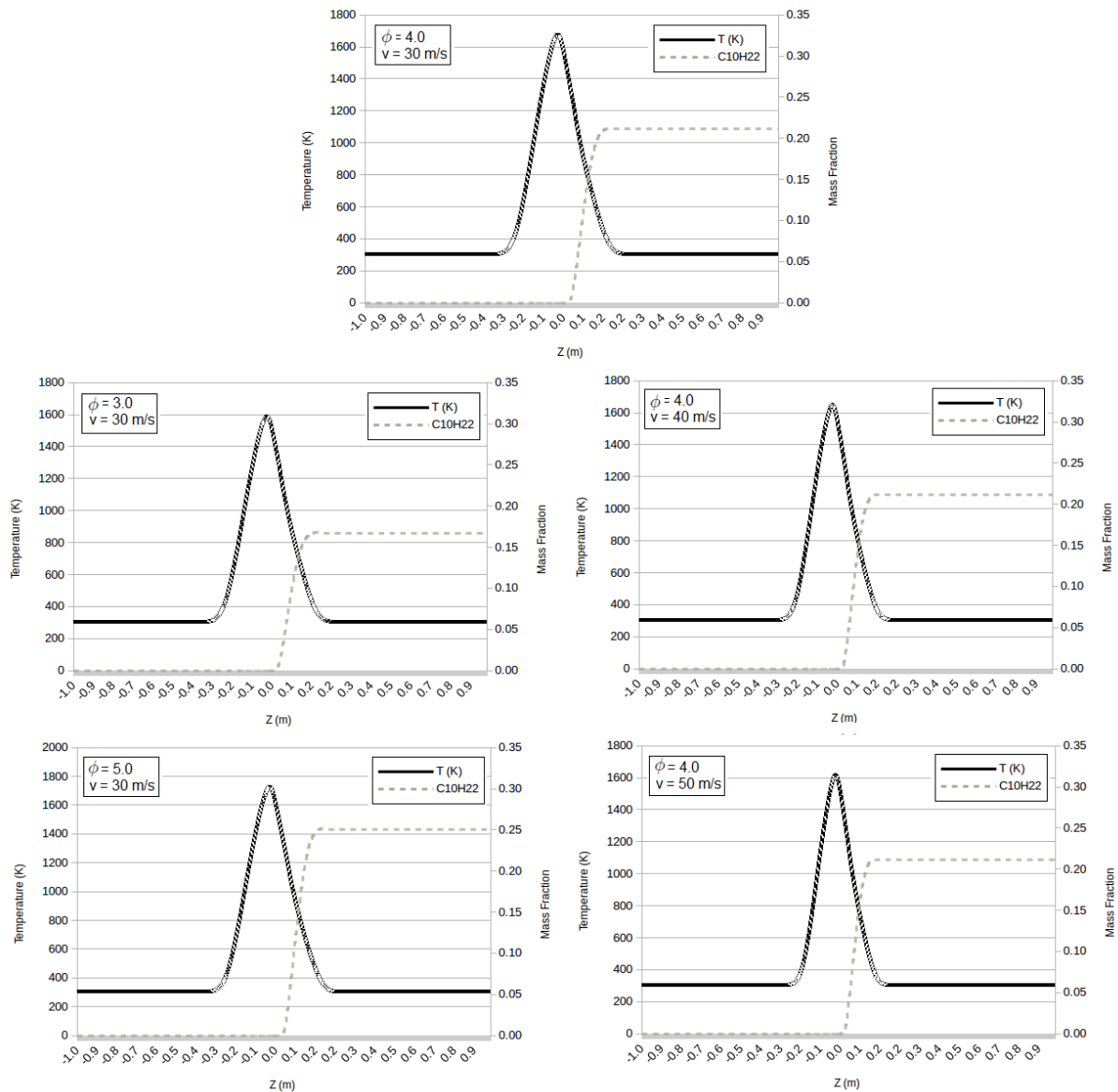
Figure 4.11: N-decane flame structure and temperature at different equivalence ratios and different injection speeds. Source: Own Elaboration

Figure 4.17 presents n-decane, O_2 and HCO profiles at different equivalence ratios and different injection speeds. O_2 in consumed in combustion and its initial mass fraction varies with the equivalence ratio. HCO is an indicator of flame front, revealing if the stoichiometric position varies with the operating conditions. In addition, its thickness reveals if the flame is more or less stretched (smaller thickness means more stretched flames). HCO mass fraction decreases with the increase of equivalence ratio and increases with the increase of injection speed.

Figure 4.18 presents pure ethanol and pure methyl decanoate O_2 and HCO profiles at $\phi = 4.0$
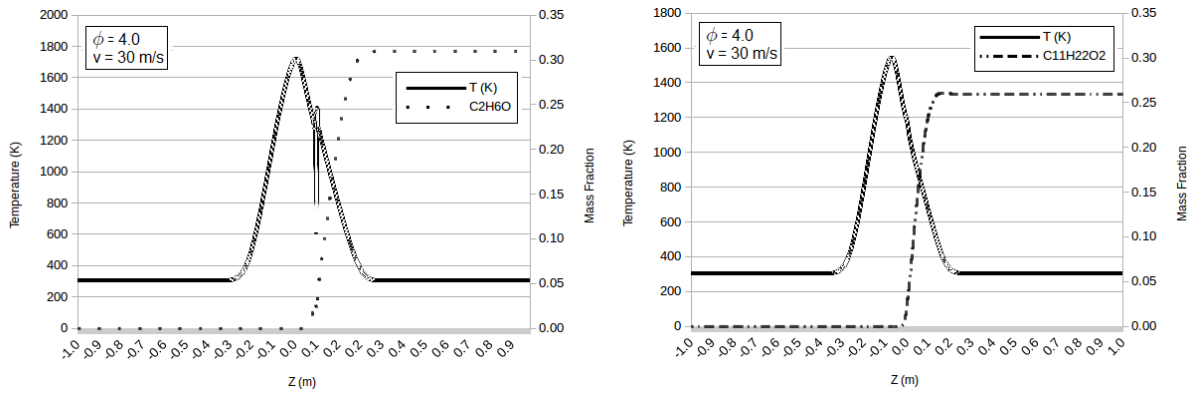
Figure 4.12: Pure ethanol and pure methyl decanoate flame structure and temperature at $\phi = 4.0$ and $v = 30m/s$. Source: Own Elaboration
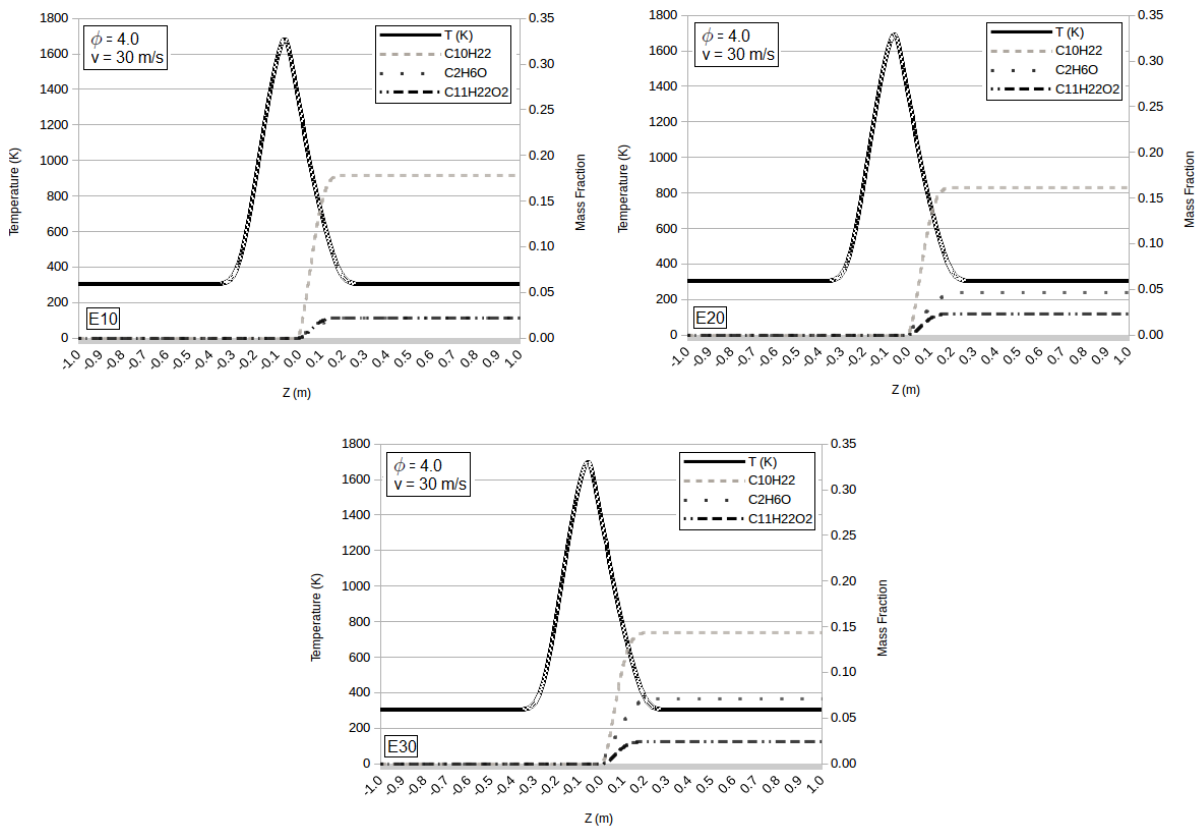
Figure 4.13: Blends E10 (80% n-decane + 10% ethanol + 10% MD, weight basis), E20 (70% n-decane + 20% ethanol + 10% MD, weight basis) and E30 (60% n-decane + 30% ethanol + 10% MD, weight basis) flame structure and temperature at $\phi = 4.0$ and $v = 30m/s$. Source: Own Elaboration
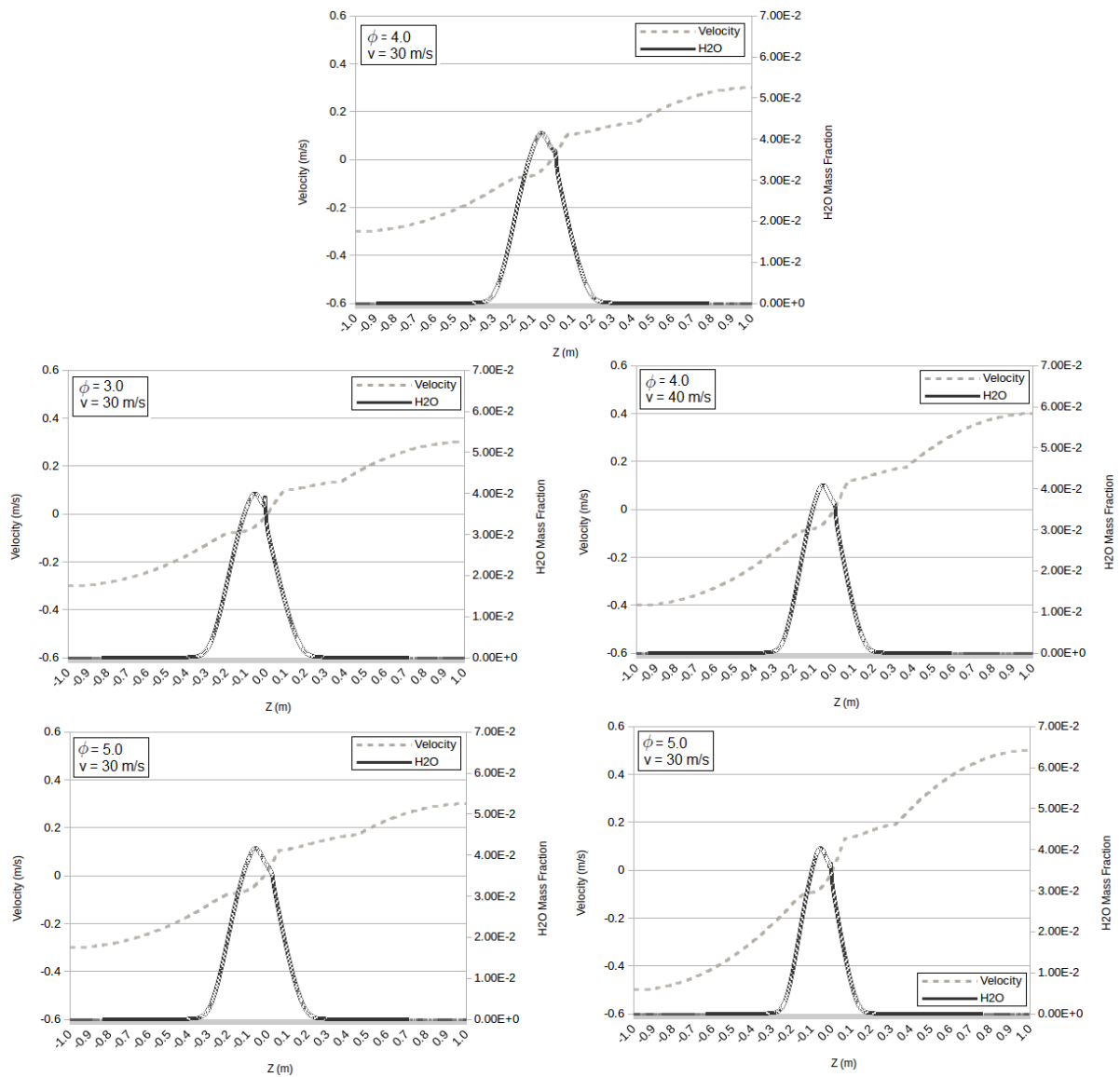
Figure 4.14: N-decane axial velocity and H_2O profile at different equivalence ratios and different injection speeds. Source: Own Elaboration

and $v = 30m/s$. HCO profile is wider in ethanol flame than in n-decane flame, indicating that ethanol flame is less stretched than methyl decanoate flame.

Figure 4.19 presents blends. O_2 and HCO profiles at $\phi = 4.0$ and $v = 30m/s$. They are very similar to each other and to the profiles observed in n-decane, revealing that the addition of ethanol and methyl decanaote do not affect these profiles.

Figure 4.20 presents n-decane CO and CO_2 profiles at different equivalence ratios and different injection speeds. Both compounds are products of combustion and air pollutants. The increase
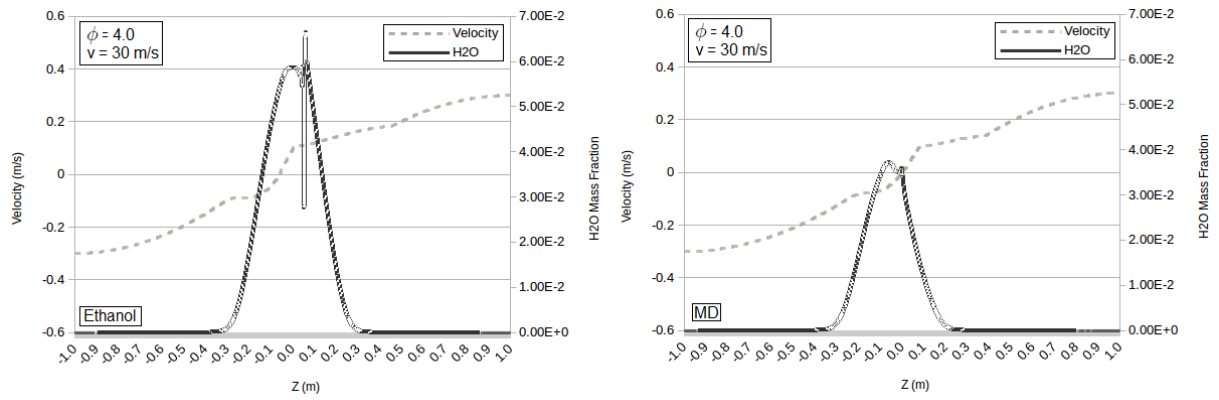
Figure 4.15: Pure ethanol and pure methyl decanoate axial velocity and H_2O profile at $\phi = 4.0$ and $v = 30 m/s$. Source: Own Elaboration
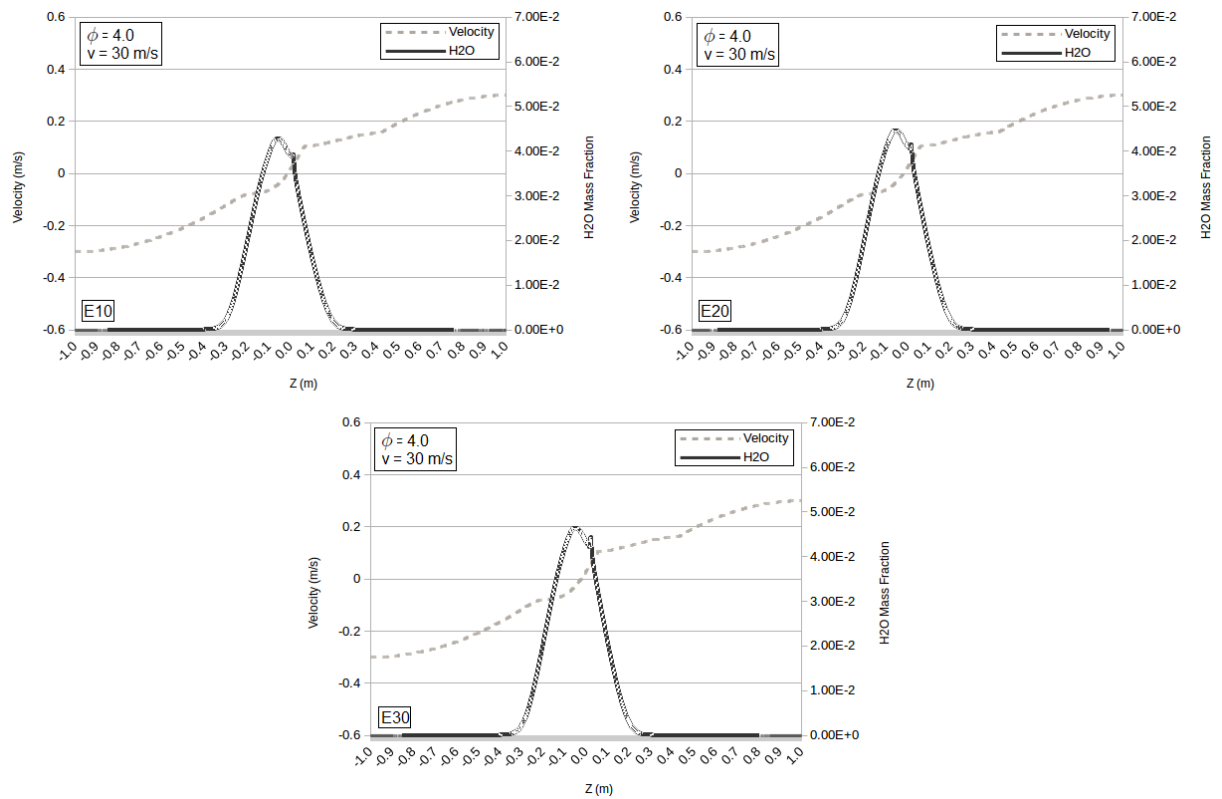
Figure 4.16: Blends E10 (80% n-decane + 10% ethanol + 10% MD, weight basis), E20 (70% n-decane + 20% ethanol + 10% MD, weight basis) and E30 (60% n-decane + 30% ethanol + 10% MD, weight basis) axial velocity and H_2O profile at $\phi = 4.0$ and $v = 30 m/s$. Source: Own Elaboration
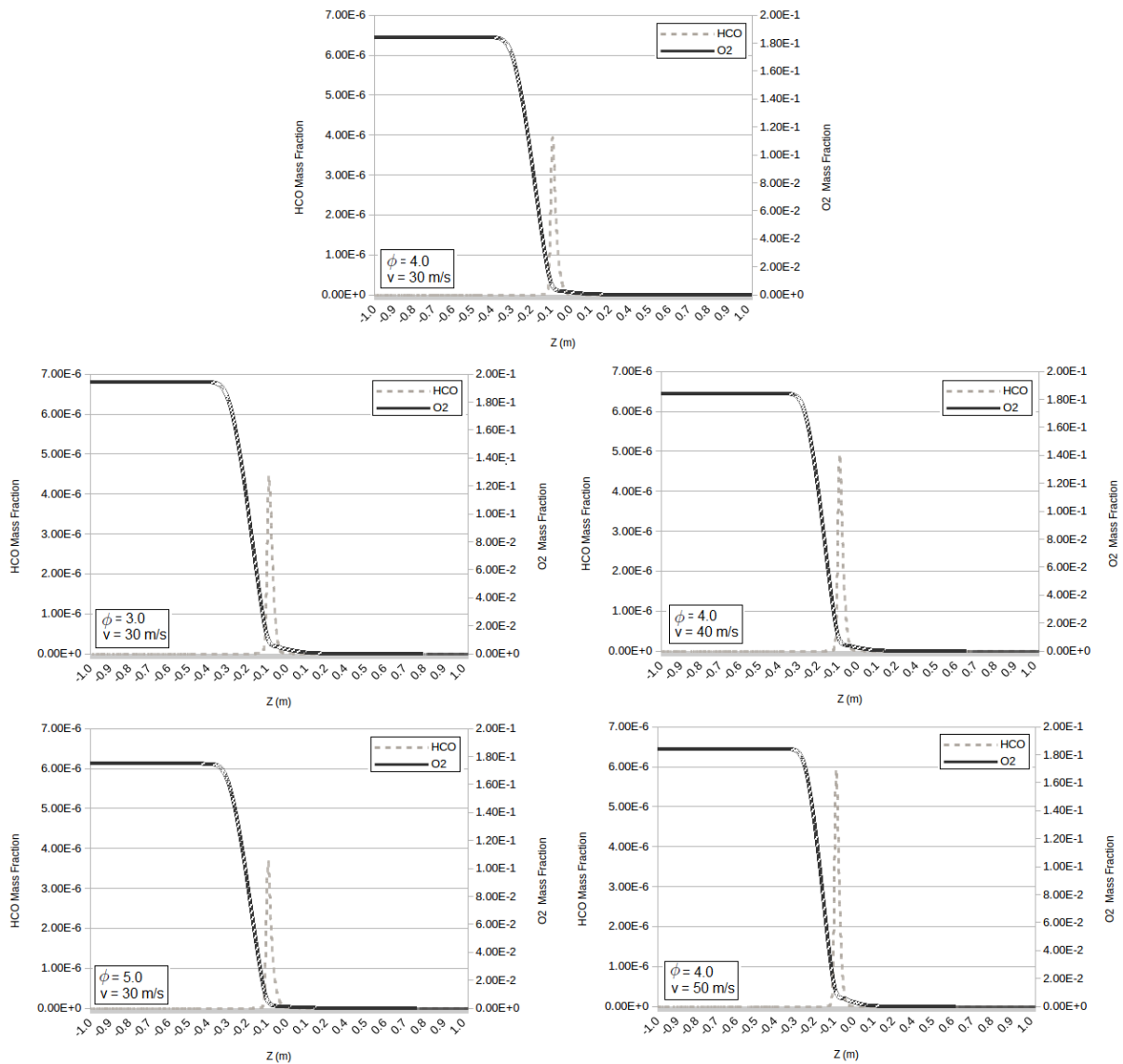
Figure 4.17: N-decane O_2 and HCO profiles at different equivalence ratios and different injection speeds. Source: Own Elaboration

of equivalence ratio increases CO production, but do not affects significantly CO_2 production, what can be justified by the fact that CO_2 is a product of complete combustion and CO, of incomplete. In a rich mixture, there is no sufficient air to completely burn all the fuel.

Figure 4.21 presents pure ethanol and pure methyl decanoate CO and CO_2 profiles at $\phi = 4.0$ and $v = 30m/s$. Profiles are similar. CO production of ethanol is higher then CO production of methyl decanoate because ethanol mass fraction is higher than methyl decanoate mass fraction in mixtures with the same equivalence ratio.
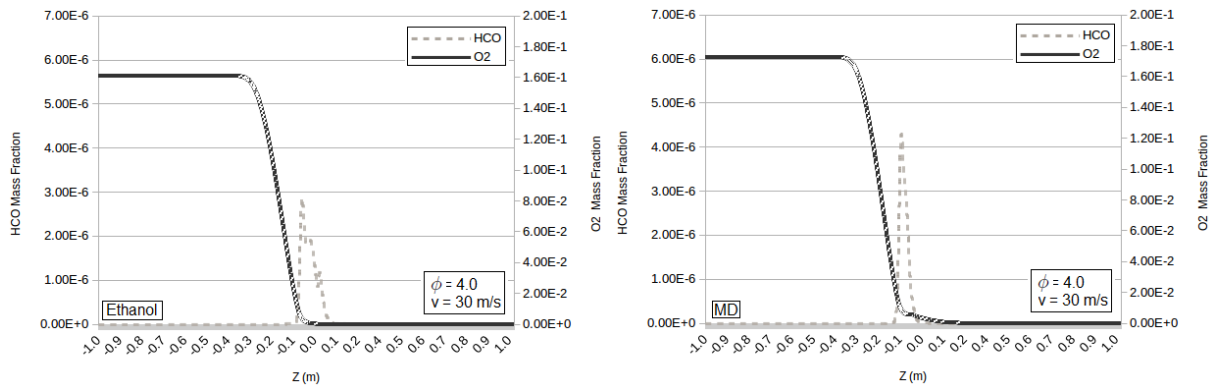
Figure 4.18: N-decane O_2 and HCO profiles at $\phi = 4.0$ and $v = 30m/s$s. Source: Own Elaboration
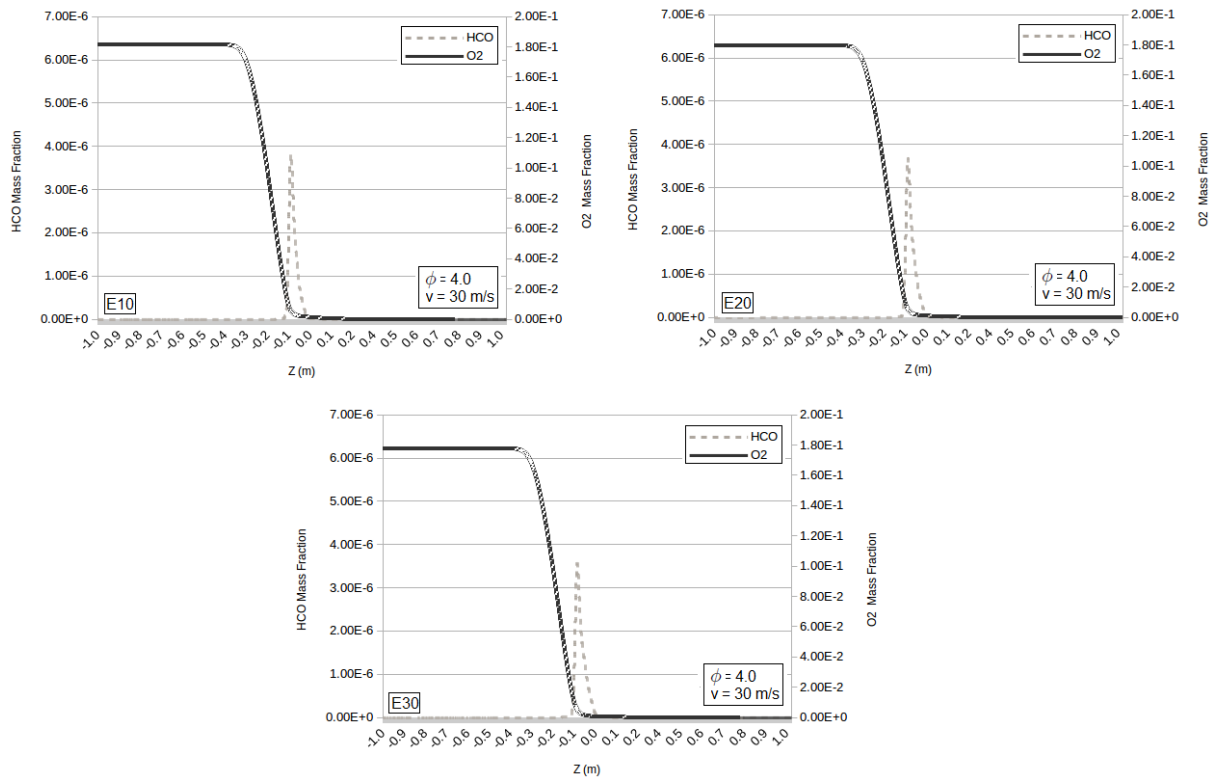
Figure 4.19: Blends E10 (80% n-decane + 10% ethanol + 10% MD, weight basis), E20 (70% n-decane + 20% ethanol + 10% MD, weight basis) and E30 (60% n-decane + 30% ethanol + 10% MD, weight basis) O_2 and HCO profiles at $\phi = 4.0$ and $v = 30m/s$. Source: Own Elaboration

Figure 4.22 presents blends CO and CO_2 profiles at $\phi = 4.0$ and $v = 30m/s$. The profiles are almost the same. CO is one of the pollutants which production is reduced by the addition of ethanol in diesel (Miraglia, 2007). This behavior was not observed in n-decane, suggesting that another component need to be added to it to reproduce target fuel behavior. Ramirez L *et al.* (2010)
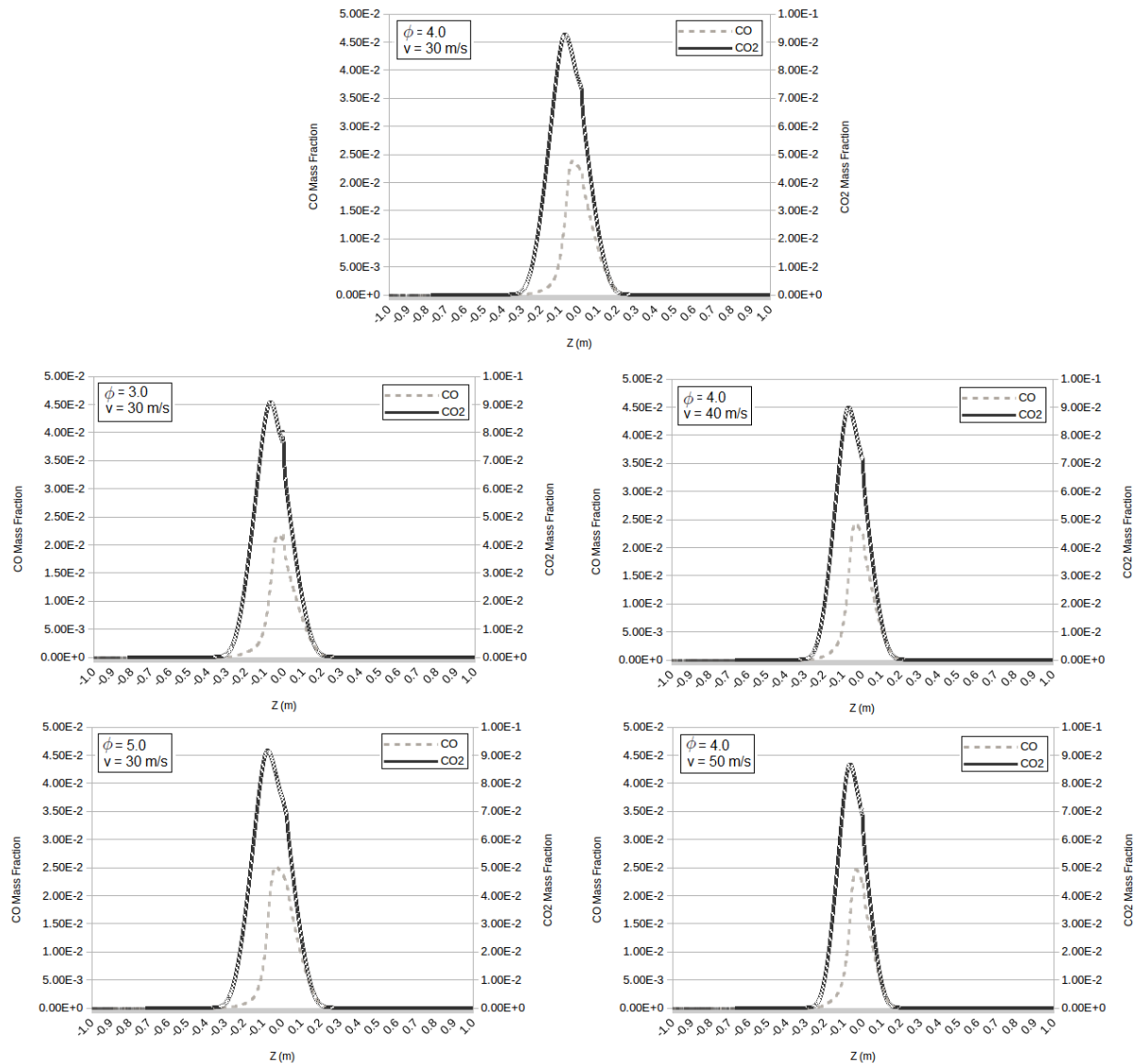
Figure 4.20: N-decane CO and CO_2 profiles at different equivalence ratios and different injection speeds. Source: Own Elaboration

reveled that IDEA fuel and diesel had similar CO profiles in a higher pressure (10atm) and smaller equivalence ratios (from 0.25 to 1.5).

Finally, the effect of the addition of ethanol and methyl decanoate in formation of aldehydes (acetaldehyde, CH_3CHO and formaldeyde, CH_2O) and one carboxylic acid (formic acid, $HCOOC$) were studied. Figure 4.23 presents CH_3CHO, CH_2O and $HCOOC$ profiles for pure n-decane, pure ethanol, pure metyhl decanoate and samples E10, E20 and E30 at $\phi = 4.0$ and $v = 30m/s$. It reveals that n-decane production of CH_3CHO, CH_2O and $HCOOC$ is small.
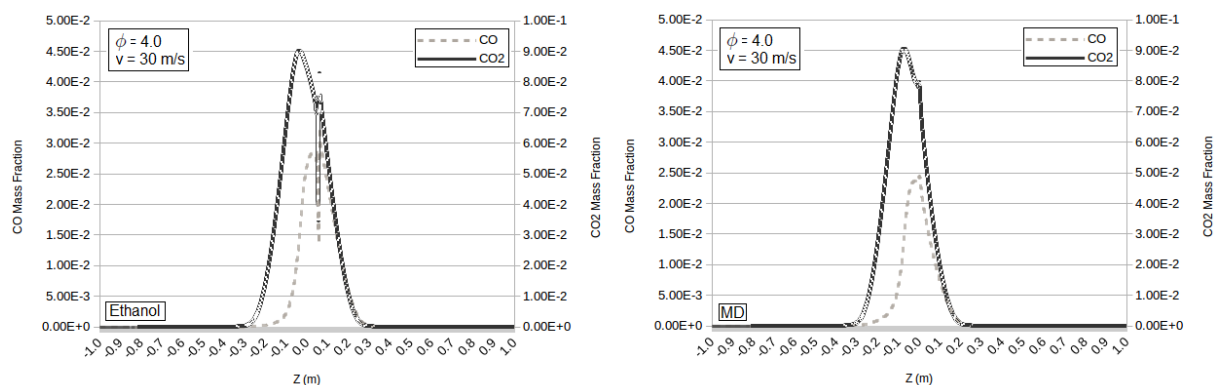
Figure 4.21: N-decane CO and CO_2 profiles at $\phi = 4.0$ and $v = 30m/ss$. Source: Own Elaboration
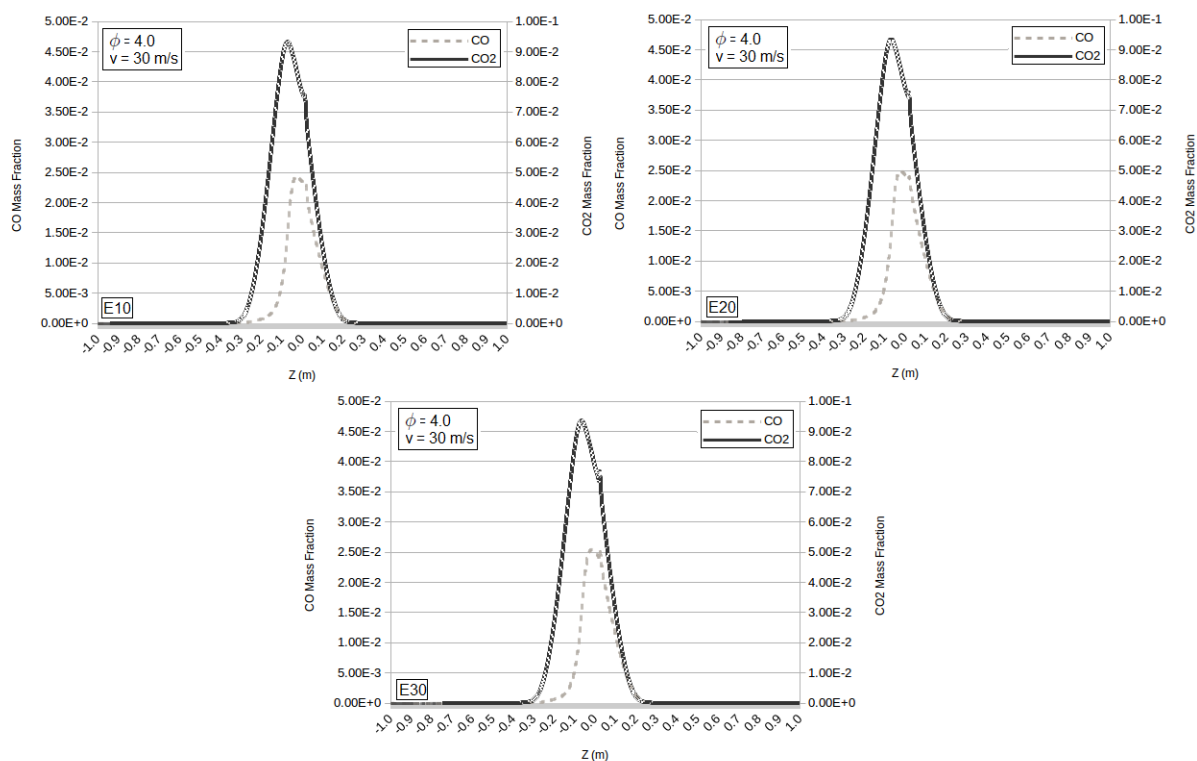
Figure 4.22: Blends E10 (80% n-decane + 10% ethanol + 10% MD, weight basis), E20 (70% n-decane + 20% ethanol + 10% MD, weight basis) and E30 (60% n-decane + 30% ethanol + 10% MD, weight basis) CO and CO_2 profiles at $\phi = 4.0$ and $v = 30m/s$. Source: Own Elaboration

Pure ethanol produces more formic acid; pure methyl decanoate produces more acetaldehyde and both ethanol and methyl decanoate produce formaldeyde.The production of CH_3CHO, CH_2O and $HCOOC$ in samples is proportional to the ratio of ethanol and methyl decanoate in then. This information is relevant because these compounds can cause damages to health, but in Brazil aldehy-
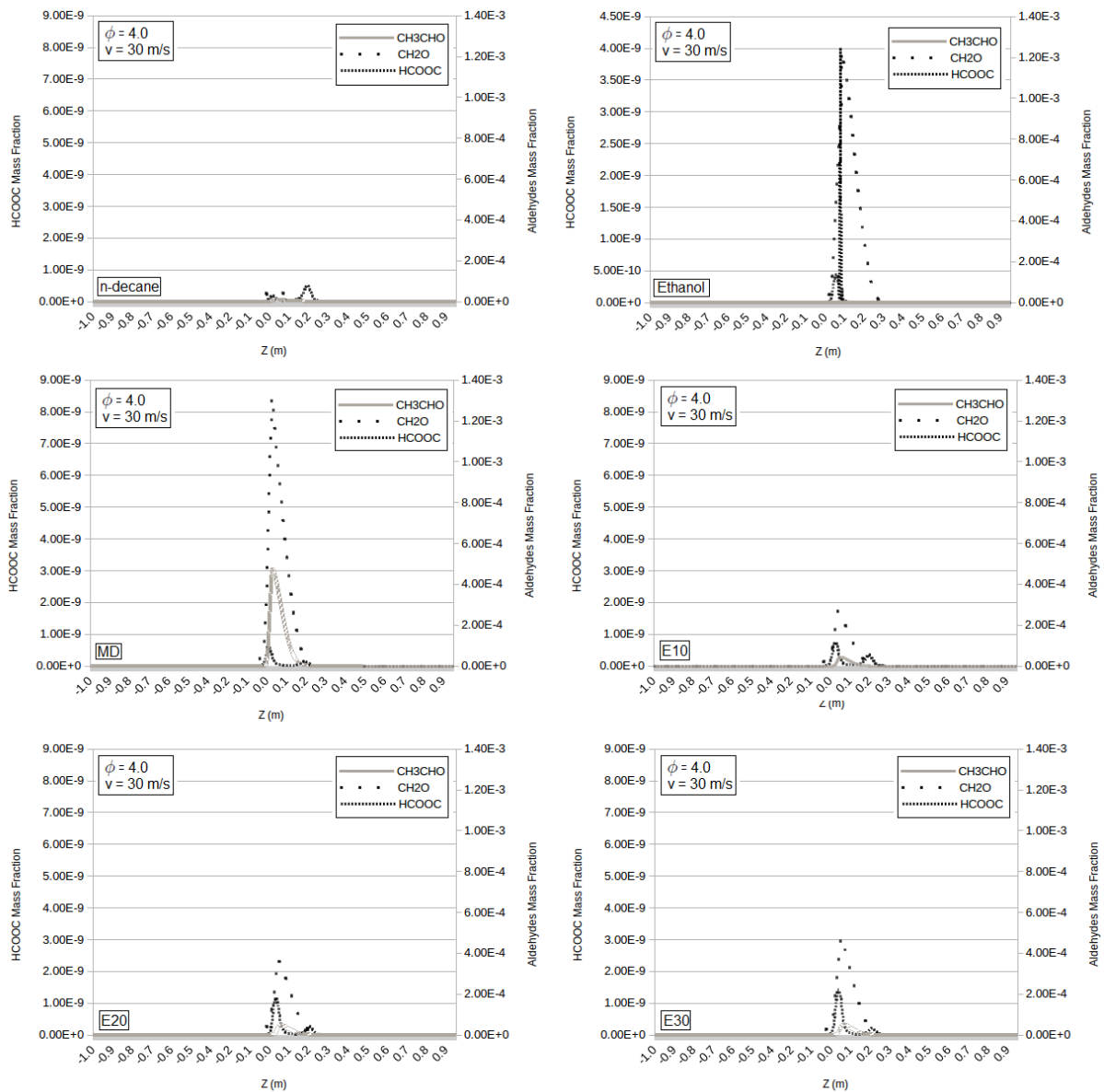
Figure 4.23: Pure n-decane, pure ethanol, pure metyhl decanoate and blends E10 (80% n-decane + 10% ethanol + 10% MD, weight basis), E20 (70% n-decane + 20% ethanol + 10% MD, weight basis) and E30 (60% n-decane + 30% ethanol + 10% MD, weight basis) CH_3CHO, CH_2O and $HCOOC$ profiles at $\phi = 4.0$ and $v = 30m/s$. Source: Own Elaboration

des emissions are regulated for Otto cycle motors only (Elpidio Neto, 2009). No study comparing the emissions of this compounds in diesel or kerosene and n-decane in the same work conditions was found in literature, so it is not possible to determine if the surrogate behavior is similar to the target fuel behavior, which we suggest to a future work. It is also important to study the formation

of other pollutants that are not represented in the New Model, such as NO and NO_x.

5 CONCLUSIONS AND FUTURE WORKS PERSPECTIVES

5.1 Conclusions

The objective of this work was to unveil some physicochemical and combustion characteristics of blends of three pure fuels: n-decane (presented in literature as a kerosene surrogate, or as the main component of diesel surrogates), ethanol and methyl decanoate (presented in literature as a biodiesel surrogate). In the first part of this work (physicochemical characterization), blends solubility and density were studied. In the second part (numerical combustion characterization), a new chemical kinetic model was developed and validated, and then used to obtain some combustion characteristics.

Solubility tests were made for blends from 80% n-decane + 10% ethanol + 10% methyl decanoate up to 10% n-decane + 80% ethanol + 10% methyl decanoate and 10% n-decane + 10% ethanol + 80% methyl decanoate ,weight basis, 10% step. Two types of ethanol were used: anhydrous ethanol (99.9% pure) and hydrated ethanol ($94.5 \pm 0.4\%$ ethanol $+5.5 \pm 0.4\%$ water in volumetric fraction at SCTP). Two temperatures were studied: $T_1 = 25.0 \pm 0.1°C$ and $T_2 = 5.0 \pm 0.1°C$. The effects of temperature decrease and water addition in surrogates blends solubility were similar to the effects reported in real fuels at literature (Chotwichien *et al.*, 2009; Lapuerta *et al.*, 2007; Chen *et al.*, 2014), but ethanol solubility in surrogate is higher than ethanol solubility in real fuels. All the blends tested using anhydrous ethanol were stable in both temperatures. The addition of water drastically decreased solubility: maximum solubility observed in blends using hydrated ethanol at $T = 25°C$ was 10% ethanol + 40% methyl decanoate in 50% n-decane. Reducing temperature to $T = 5°C$, no blend with 50% or more n-decane was stable.

Density tests were made for blends E10 (80% n-decane + 10% ethanol + 10% methyl decanoate, weight basis), E20 (70% n-decane + 20% ethanol + 10% methyl decanoate, weight basis) and E30 (60% n-decane + 30% ethanol + 10% methyl decanoate, weight basis). Those samples were chosen because they have the biggest proportions of n-decane and a constant proportion of methyl decanoate, what makes them more similar to real possibilities of combinations of real fuels. N-decane is less dense than diesel, kerosene and ethanol, so the effect of the addition of ethanol in the surrogate was opposite to the effect observed in real fuels: E10 was more dense than E20, that was more dense than E30. Three temperatures were tested: $20.00 \pm 0.03°C$, $40.00 \pm 0.03°C$ and $60.00 \pm 0.03°C$. The increase of temperature decreased densities.

The numerical part of this work was developed using REGATH, a numerical package written mainly in FORTRAN that uses Finite Difference Method and Newton Method to solve combustion problems.

The new chemical kinetic model was developed by the combination of models found in literature for the studied fuels. The development process consisted in the review of previous chemical kinetic models available in literature for the studied fuels; evaluation of literature chemical kinetic models available in literature and choice of which would be used to develop the new model; and chemical kinetic models fusion and 1D validation. The models chosen were: n-decane model presented by Marchal *et al.* (2009), that have 154 species and 850 reactions; ethanol model presented by Marinov (1999), that have 57 species and 387 reactions; and methyl decanoate model presented by Seshadri *et al.* (2009) modified by Alviso (2013), that have 129 species and 741 reactions. Ethanol model was used as skeleton and n-decane model was used as complimentary in an intermediate chemical kinetic model. Then, this intermediate model was used as skeleton and methyl decanoate model was used as complimentary. The New Model developed has 258 species and 1586 reactions.

Laminar flame speed was the parameter chosen to validate the New Model. A 1D premixed freely propagating flame was simulated at atmospheric pressure and different temperatures and different equivalence ratios. Simulation results were compared with experimental data found in literature and simulations using the original models. The New Model simulation was closer to experimental data than the original models for n-decane ($T = 400K, 0.8 \leq \phi \leq 1.4$) and methyl decanoate simulations ($T = 400K, 0.7 \leq \phi \leq 1.4$). For ethanol (used as New Model skeleton), New Model simulations data were close both to the original model simulation and the experimental data found in literature ($T = 300K$ and $358K$, $0.7 \leq \phi \leq 1.4$).

After validating the model, laminar flame speed simulated for surrogates was compared with experimental laminar flame speed data of real fuels found in literature at T=470K, atmospheric pressure. N-decane reproduces both diesel and kerosene behavior when $0.7 \leq \phi \leq 1$. When the equivalence ratio increases, diesel laminar flame speed get away from n-decane. Kerosene laminar flame speed is close to n-decane flame speed up to the maximum equivalence ratio simulated, $\phi \leq 1.5$. Those result agree with literature works that use n-decane as a kerosene surrogate; and add other compounds to it in order to reproduce diesel behavior. Methyl decanoate simulation approached little biodiesel experimental data, suggesting that more experimental works are necessary to validate methyl decanoate as an adequate surrogate for biodiesel. Blends of n-decane and methyl decanoate were compared with blends of diesel and biodiesel and kerosene and biodiesel. Results were close only when $0.7 \leq \phi \leq 1.1$. Differences probably occurs because n-decane and methyl decanoate laminar flame speeds are close to each other and methyl decanoate laminar flame speed do not reproduce biodiesel behavior.

The final part of the work was the use of the New Model to unveil some combustion properties. Samples E10, E20 and E30 were compared with pure fuels. 1D premixed flame was simulated

to predict laminar flame speed of the blends at T=300K, atmospheric pressure. Blends results are close to pure decane. The counterflow configuration was simulated at different injection velocities and equivalence ratios for n-decane and blends ($\phi = 3.0$ and $v = 30m/s$; $\phi = 4.0$ and $v = 30m/s$; $\phi = 4.0$ and $v = 40m/s$; $\phi = 4.0$ and $v = 50m/s$; $\phi = 5.0$ and $v = 30m/s$). Pure ethanol and pure methyl decanaote were simulated only in $\phi = 4.0$ and $v = 30m/s$. Flame profiles, temperature profiles, axial velocities profiles and O_2, HCO, H_2O, O_2, CO, CO_2, CH_3CHO, CH_2O and $HCOOC$ profiles were analyzed. The flame stabilizes at same point for all conditions. The increase of equivalence ratio increases maximum flame temperature and the generation of some combustion products for both n-decane and blends: CO, $HCOOC$. In blends, CH_2O and CH_3CHO production also increases with the increase of equivalence ratio. H_2O and CO_2 are total combustion products, but their generation do not varies with equivalence ratio. This indicates that the extra carbons and hydrogen are producing other compounds. The increase of injection speed changes maximum axial velocity, but not change the velocity profile. Blends maximum temperature, velocity profile, HCO, CO and CO_2 profile were the same observed for n-decane at same equivalence ratio and injection velocity.The addition of ethanol slightly increases H_2O production. The addition of ethanol increases $HCOOC$ formation. Methyl decanoate increases CH_3CHO production and both ethanol and methyl decanoate increase CH_2O production.

5.2 Future work perspectives

The development of a surrogate that properly describes blends of fossil fuels and biofuels combustion is a fascinating challenge that this work started to solve. It was able to find some important answers, but there are much more open questions in the subject. Some suggestions for future works are:

○ To measure others physicochemical properties of the blends, such as viscosity, flash point and cetane number;

○ Experimentally validate the developed model by measuring laminar flame speed of simulated fuels in simulated conditions (premixed flame and diffusion flame). Other parameters can be used to the validation as well, such as species profiles and ignition time;

○ To measure other types of biodiesel (specially Brazilian biodiesel) laminar flame speed, in order to compare this data with methyl decanoate laminar flame speed and confirm its ability to reproduce real fuel behavior;

○ To add more pure components to the surrogate, in order to reproduce pure diesel and diesel blends physicochemical properties and combustion characteristics;

- ○ To add NO and NO_x reactions to th model, in order to predict the formation of those pollu-tants;

- ○ To reduce the model, in order to obtain a model that could be used in numerical simulation of combustion systems.

REFERENCES

AGUERRE, Frédéric. **Etude expérimentale et numérique des flammes laminaires étirees stationnaires et instationnaires**. 1994. Thesis (PhD). Ecole Centrale Paris.

AJAV, E.; SINGH, B. and BHATTACHARYA, T. Experimental study of some performance parameters of a constant speed stationary diesel engine using ethanol–diesel blends as fuel. **Biomass and Bioenergy**, v. 17, n. 4, 357–365, 1999.

ALVISO, Dario. **Experimental and numerical characterization of the biodiesel combustion in a counterflow burner**. 2013. Thesis (PhD). École Centrale Paris - Universidad Nacional de Asunción.

BALES-GUERET, C.; CATHONNET, M.; BOETTNER, J.C. and GAILLARD, F. Experimental study and kinetic modeling of higher hydrocarbon oxidation in a jet-stirred flow reactor. **Energy & Fuels**, v. 6, n. 2, 189–194, 1992.

BARTHS, H.; HASSE, C.; BIKAS, G. and PETERS, N. Simulation of combustion in direct injection diesel engines using a eulerian particle flamelet model. **Proceedings of the combustion Institute**, v. 28, n. 1, 1161–1168, 2000.

BARTHS, H.; PITSCH, H. and PETERS, N. 3d simulation of di diesel combustion and pollutant formation using a two-component reference fuel. **Oil & Gas Science and Technology**, v. 54, n. 2, 233–244, 1999.

BATTIN-LECLERC, F. Detailed chemical kinetic models for the low-temperature combustion of hydrocarbons with application to gasoline and diesel fuel surrogates. **Progress in Energy and Combustion Science**, v. 34, n. 4, 440–498, 2008.

BATTIN-LECLERC, F.; FOURNET, R.; GLAUDE, P.; JUDENHERC, B.; WARTH, V.; CÔME,

G. and SCACCHI, G. Modeling of the gas-phase oxidation of n-decane from 550 to 1600 k. **Proceedings of the Combustion Institute**, v. 28, n. 2, 1597–1605, 2000.

BIKAS, G. and PETERS, N. Kinetic modelling of n-decane combustion and autoignition: Modeling combustion of n-decanem. **Combustion and Flame**, v. 126, n. 1, 1456–1475, 2001.

BUDA, F.; BOUNACEUR, R.; WARTH, V.; GLAUDE, P.A.; FOURNET, R. and BATTIN-LECLERC, F. Progress toward a unified detailed kinetic model for the autoignition of alkanes from c 4 to c 10 between 600 and 1200 k. **Combustion and flame**, v. 142, n. 1, 170–186, 2005.

CANCINO, L.; FIKRI, M.; OLIVEIRA, A. and SCHULZ, C. Measurement and chemical kinetics modeling of shock-induced ignition of ethanol- air mixtures. **Energy & Fuels**, v. 24, n. 5, 2830–2840, 2010.

CANDEL, S.; SCHMITT, T. and DARABIHA, N. Progress in transcritical combustion: experimentation, modeling and simulation. **Proceedings of 23rd ICDERS, Irvine USA**, p. 27, 2011.

CATHORMET, M.; VOISIN, D.; ETSORDI, A.; SFERDEAN, C.; REUILLON, M.; BOETTNER, J. and DAGAUT, P. Kerosene combustion modeling using detailed and reduced chemical kinetic mechanisms. In **RTO Meeting Proceedings 14, Gas Turbine Engine Combustion, Emissions and Alternative Fuels**, pp. 12–16. 1999.

CHANG, Y.; JIA, M.; LIU, Y.; LI, Y. and XIE, M. Development of a new skeletal mechanism for n-decane oxidation under engine-relevant conditions based on a decoupling methodology. **Combustion and Flame**, v. 160, n. 8, 1315–1332, 2013.

CHEN, L.; SUN, P.; DING, S. and YANG, S. Miscibility of ternary systems containing kerosene-based surrogate fuel and hydrous ethanol: Experimental data+ thermodynamic modeling. **Fluid Phase Equilibria**, v. 379, 1–9, 2014.

CHEVALIER, C.; PITZ, W.; WARNATZ, J.; WESTBROOK, C. and MELENK, H. Hydrocarbon ignition: automatic generation of reaction mechanisms and applications to modeling of engine

knock. In **Symposium (International) on Combustion**, v. 24, pp. 93–101. Elsevier, 1992.

CHONG, C.T. and HOCHGREB, S. Measurements of laminar flame speeds of liquid fuels: Jet-a1, diesel, palm methyl esters and blends using particle imaging velocimetry (piv). **Proceedings of the Combustion Institute**, v. 33, n. 1, 979–986, 2011.

CHOTWICHIEN, A.; LUENGNARUEMITCHAI, A. and JAI-IN, S. Utilization of palm oil alkyl esters as an additive in ethanol–diesel and butanol–diesel blends. **Fuel**, v. 88, n. 9, 1618–1624, 2009.

COMANDINI, A.; DUBOIS, T. and CHAUMEIX, N. Laminar flame speeds of n-decane, n-butylbenzene, and n-propylcyclohexane mixtures. **Proceedings of the Combustion Institute**, v. 35, n. 1, 671–678, 2015.

DAGAUT, P. and CATHONNET, M. The ignition, oxidation, and combustion of kerosene: A review of experimental and kinetic modeling. **Progress in energy and combustion science**, v. 32, n. 1, 48–92, 2006.

DAGAUT, P.; EL BAKALI, A. and RISTORI, A. The combustion of kerosene: Experimental results and kinetic modelling using 1-to 3-component surrogate model fuels. **Fuel**, v. 85, n. 7, 944–956, 2006.

DAGAUT, P.; REUILLON, M.; BOETTNER, J.C. and CATHONNET, M. Kerosene combustion at pressures up to 40 atm: Experimental study and detailed chemical kinetic modeling. In **Symposium (International) on Combustion**, v. 25, pp. 919–926. Elsevier, 1994.

DAGAUT, P.; REUILLON, M.; CATHONNET, M. and VOISIN, D. High pressure oxidation of normal decane and kerosene in dilute conditions from low to high temperature. **Journal de chimie physique**, v. 92, n. 1, 47–76, 1995.

DATTA, A. and MANDAL, B.K. Impact of alcohol addition to diesel on the performance combustion and emissions of a compression ignition engine. **Applied Thermal Engineering**, 2016.

DELFAU, J.L.; BOUHRIA, M.; REUILLON, M.; SANOGO, O.; AKRICH, R. and VOVELLE, C. Experimental and computational investigation of the structure of a sooting decane-o 2-ar flame. In **Symposium (International) on Combustion**, v. 23, pp. 1567–1572. Elsevier, 1991.

DIETLER, M. Alcohol: anthropological/archaeological perspectives. **Annu. Rev. Anthropol.**, v. 35, 229–249, 2006.

DIÉVART, P.; WON, S.H.; DOOLEY, S.; DRYER, F.L. and JU, Y. A kinetic model for methyl decanoate combustion. **Combustion and Flame**, v. 159, n. 5, 1793–1805, 2012.

DOUTÉ, C.; DELFAU, J.L. and VOVELLE, C. Modeling of the structure of a premixed n-decane flame. **Combustion science and technology**, v. 130, n. 1-6, 269–313, 1997.

DUNPHY, M.P.; PATTERSON, P.M. and SIMMIE, J.M. High-temperature oxidation of ethanol. part 2.—kinetic modelling. **J. Chem. Soc., Faraday Trans.**, v. 87, n. 16, 2549–2559, 1991.

EGOLFOPOULOS, F.; DU, D. and LAW, C. A study on ethanol oxidation kinetics in laminar premixed flames, flow reactors, and shock tubes. In **Symposium (international) on combustion**, v. 24, pp. 833–841. Elsevier, 1992.

ELPIDIO NETO, Edson. **Caracterizacao preliminar das emissoes de aldeidos e acidos carbox-ilicos em veiculos do ciclo Otto e do ciclo Diesel com uso de combustiveis fosseis e renovaveis**. 2009. Dissertation (Master). Universidade de Sao Paulo.

EMPRESA DE PESQUISA ENERGÉTICA, E.P.E. Balanço energético nacional (ben). v. 01, 2014.

EMPRESA DE PESQUISA ENERGÉTICA, E.P.E. Balanço energético nacional (ben). v. 01, 2015.

FARRELL, J.; CERNANSKY, N.; DRYER, F.; LAW, C.; FRIEND, D.; HERGART, C.; MC-DAVID, R.; PATEL, A.; MUELLER, C.J. and PITSCH, H. Development of an experimental database and kinetic models for surrogate diesel fuels. Technical report, SAE Technical Paper, 2007.

FRENKLACH, M.; WANG, H. and RABINOWITZ, M.J. Optimization and analysis of large chemical kinetic mechanisms using the solution mapping method—combustion of methane. **Progress in Energy and Combustion Science**, v. 18, n. 1, 47–73, 1992.

GERDES, K. and SUPPES, G. Miscibility of ethanol in diesel fuels. **Industrial & engineering chemistry research**, v. 40, n. 3, 949–956, 2001.

GLASSMAN, I.; YETTER, R.A. and GLUMAC, N.G. **Combustion**. Academic press, 2014.

GLAUDE, P.; WARTH, V.; FOURNET, R.; BATTIN-LECLERC, F.; SCACCHI, G. and CÔME, G. Modeling of the oxidation of n-octane and n-decane using an automatic generation of mechanisms. **International journal of chemical kinetics**, v. 30, n. 12, 949–959, 1998.

GRANA, R.; FRASSOLDATI, A.; SAGGESE, C.; FARAVELLI, T. and RANZI, E. A wide range kinetic modeling study of pyrolysis and oxidation of methyl butanoate and methyl decanoate–note ii: Lumped kinetic model of decomposition and combustion of methyl esters up to methyl decanoate. **Combustion and Flame**, v. 159, n. 7, 2280–2294, 2012.

GULDER, O.L. In **Nineteenth Symposium (International) on Combustion; The Combustion Institute**, p. 275. 1982.

HANSEN, A.C.; ZHANG, Q. and LYNE, P.W. Ethanol–diesel fuel blends—-a review. **Bioresource technology**, v. 96, n. 3, 277–285, 2005.

HERBINET, O.; GLAUDE, P.A.; WARTH, V. and BATTIN-LECLERC, F. Experimental and modeling study of the thermal decomposition of methyl decanoate. **Combustion and flame**, v. 158, n. 7, 1288–1300, 2011.

HERBINET, O.; PITZ, W.J. and WESTBROOK, C.K. Detailed chemical kinetic oxidation mechanism for a biodiesel surrogate. **Combustion and Flame**, v. 154, n. 3, 507–528, 2008.

HONNET, S.; SESHADRI, K.; NIEMANN, U. and PETERS, N. A surrogate fuel for kerosene.

Proceedings of the Combustion Institute, v. 32, n. 1, 485–492, 2009.

HUI, X.; KUMAR, K.; SUNG, C.J.; EDWARDS, T. and GARDNER, D. Experimental studies on the combustion characteristics of alternative jet fuels. **Fuel**, v. 98, 176–182, 2012.

HUI, X. and SUNG, C.J. Laminar flame speeds of transportation-relevant hydrocarbons and jet fuels at elevated temperatures and pressures. **Fuel**, v. 109, 191–200, 2013.

INSTITUTO DE PESQUISA ECONÔMICA APLICADA, I.D.P.E.A. Petróleo – da crise aos carros flex. **Desafios do desenvolvimento**, v. 59, 2010.

INTERNATIONAL ENERGY AGENCY, I.E.A. Key world energy statistics 2011. v. 01, 2011.

JI, C.; DAMES, E.; WANG, Y.L.; WANG, H. and EGOLFOPOULOS, F.N. Propagation and extinction of premixed c 5–c 12 n-alkane flames. **Combustion and Flame**, v. 157, n. 2, 277–287, 2010.

KIM, H.H.; WON, S.H.; SANTNER, J.; CHEN, Z. and JU, Y. Measurements of the critical initiation radius and unsteady propagation of n-decane/air premixed flames. **Proceedings of the Combustion Institute**, v. 34, n. 1, 929–936, 2013.

KNOTHE, G. and STEIDLEY, K.R. Kinematic viscosity of biodiesel fuel components and related compounds. influence of compound structure and comparison to petrodiesel fuel components. **Fuel**, v. 84, n. 9, 1059–1065, 2005.

KUMAR, K. and SUNG, C.J. Laminar flame speeds and extinction limits of preheated n-decane/o 2/n 2 and n-dodecane/o 2/n 2 mixtures. **Combustion and Flame**, v. 151, n. 1, 209–224, 2007.

KUMAR, K.; SUNG, C.J. and HUI, X. Laminar flame speeds and extinction limits of conventional and alternative jet fuels. **Fuel**, v. 90, n. 3, 1004–1011, 2011.

LABECKAS, G.; SLAVINSKAS, S. and MAŽEIKA, M. The effect of ethanol–diesel–biodiesel blends on combustion, performance and emissions of a direct injection diesel engine. **Energy Conversion and Management**, v. 79, 698–720, 2014.

LAPUERTA, M.; ARMAS, O. and GARCIA-CONTRERAS, R. Stability of diesel–bioethanol blends for use in diesel engines. **Fuel**, v. 86, n. 10, 1351–1357, 2007.

LEMAIRE, R.; FACCINETTO, A.; THERSSEN, E.; ZISKIND, M.; FOCSA, C. and DESGROUX, P. Experimental comparison of soot formation in turbulent flames of diesel and surrogate diesel fuels. **Proceedings of the Combustion Institute**, v. 32, n. 1, 737–744, 2009.

LEPLAT, N.; DAGAUT, P.; TOGBÉ, C. and VANDOOREN, J. Numerical and experimental study of ethanol combustion and oxidation in laminar premixed flames and in jet-stirred reactor. **Combustion and Flame**, v. 158, n. 4, 705–725, 2011.

LI, D.G.; ZHEN, H.; XINGCAI, L.; WU-GAO, Z. and JIAN-GUANG, Y. Physico-chemical properties of ethanol–diesel blend fuel and its effect on performance and emissions of diesel engines. **Renewable energy**, v. 30, n. 6, 967–976, 2005.

LIAO, S.; JIANG, D.; HUANG, Z.; ZENG, K. and CHENG, Q. Determination of the laminar burning velocities for mixtures of ethanol and air at elevated temperatures. **Applied Thermal Engineering**, v. 27, n. 2, 374–380, 2007.

LINDSTEDT, R. and MAURICE, L. Detailed chemical-kinetic model for aviation fuels. **Journal of Propulsion and Power**, v. 16, n. 2, 187–195, 2000.

MARCHAL, C.; DELFAU, J.L.; VOVELLE, C.; MORÉAC, G.; MOUNAı, C.; MAUSS, F. *et al.* Modelling of aromatics and soot formation from large fuel molecules. **Proceedings of the Combustion Institute**, v. 32, n. 1, 753–759, 2009.

MARINOV, N.M. A detailed chemical kinetic model for high temperature ethanol oxidation. **shock**, v. 3, n. 2, 257–263, 1999.

MAURICE, L.Q.; LANDER, H.; EDWARDS, T. and HARRISON, W. Advanced aviation fuels: a look ahead via a historical perspective. **Fuel**, v. 80, n. 5, 747–756, 2001.

MIRAGLIA, S.G.E.K. Health, environmental, and economic costs from the use of a stabilized diesel/ethanol mixture in the city of são paulo, brazil. **Cadernos de saude publica**, v. 23, S559–S569, 2007.

MORETTI, R.R. Mistura diesel, biodiesel e etanol anidro: uma possibilidade para reduzir o custo de produção da cadeia da cana-de-açúcar. 2013.

MOSS, J. and AKSIT, I. Modelling soot formation in a laminar diffusion flame burning a surrogate kerosene fuel. **Proceedings of the Combustion Institute**, v. 31, n. 2, 3139–3146, 2007.

MUHARAM, Y. and WARNATZ, J. Kinetic modelling of the oxidation of large aliphatic hydro-carbons using an automatic mechanism generation. **Physical Chemistry Chemical Physics**, v. 9, n. 31, 4218–4229, 2007.

MUNZAR, J.; AKIH-KUMGEH, B.; DENMAN, B.; ZIA, A. and BERGTHORSON, J. An exper-imental and reduced modeling study of the laminar flame speed of jet fuel surrogate components. **Fuel**, v. 113, 586–597, 2013.

NACIONAL OIL AGENCY, N.O.A. ANP technical regulation 6/2009. `http://nxt.anp.gov.br/NXT/gateway.dll/leg/resolucoes_anp/2006/janeiro/ranp%203%20-%202006.xml?f=templates$fn=default.htm&sync=1&vid=anp:10.1048/enu`, 2009. [Online; accessed 14-May-2016].

NACIONAL OIL AGENCY, N.O.A. ANP technical regulation 3/2014. `http://nxt.anp.gov.br/nxt/gateway.dll/leg/resolucoes_anp/2014/agosto/ranp%2045%20-%202014.xml`, 2014. [Online; accessed 14-May-2016].

NACIONAL OIL AGENCY, N.O.A. ANP resolution 19. `http://nxt.anp.gov.br/nxt/gateway.dll/leg/resolucoes_anp/2015/abril/ranp%2019%20-%202015.`

`xml`, 2015a. [Online; accessed 24-January-2016].

NACIONAL OIL AGENCY, N.O.A. ANP resolution 50. `http://nxt.anp.gov.br/` `NXT/gateway.dll/leg/resolucoes_anp/2013/dezembro/ranp%2050%20-%` `202013.xml?f=templates$fn=document-frame.htm$3.0`, 2015b. [Online; accessed 12-December-2015].

NATIONAL CENTER FOR BIOTECHNOLOGY INFORMATION, P.U.B.C.H.E.M. PubChem Compound Database; CID=15600. `https://pubchem.ncbi.nlm.nih.gov/`, 2015. [Online; accessed 07-November-2015].

NEHSE, M.; WARNAT, J. and CHEVALIER, C. Kinetic modeling of the oxidation of large aliphatic hydrocarbons. In **Symposium (International) on Combustion**, v. 26, pp. 773–780. Elsevier, 1996.

NIEMEYER, K.E.; SUNG, C.J. and RAJU, M.P. Skeletal mechanism generation for surrogate fuels using directed relation graph with error propagation and sensitivity analysis. **Combustion and flame**, v. 157, n. 9, 1760–1770, 2010.

NNOAA'S OCEAN SERVICE, N.N.O.A.A.S. Cameo Chemicals. `http://` `cameochemicals.noaa.gov/`, 2016. [Online; accessed 17-January-2016].

NORTON, T. and DRYER, F. An experimental and modeling study of ethanol oxidation kinetics in an atmospheric pressure flow reactor. **International Journal of Chemical Kinetics**, v. 24, n. 4, 319–344, 1992.

OWEN, K. and COLEY, T. Automotive fuels reference book. 1995.

PATTERSON, P.; KYNE, A.; POURKASHANIAN, M.; WILLIAMS, A. and WILSON, C. Combustion of kerosene in counterflow diffusion flames. **Journal of Propulsion and Power**, v. 17, n. 2, 453–460, 2001.

PITZ, W.J. and MUELLER, C.J. Recent progress in the development of diesel surrogate fuels. **Progress in Energy and Combustion Science**, v. 37, n. 3, 330–350, 2011.

RAHEMAN, A. Biofuel (alcohol and biodiesel) applications as fuel for internal combustion engines. **Prog. Energ. Combust**, v. 33, 233–271, 2007.

RAMIREZ L, H.; HADJ-ALI, K.; DIEVART, P.; MOREAC, G. and DAGAUT, P. Kinetics of oxidation of commercial and surrogate diesel fuels in a jet-stirred reactor: Experimental and modeling studies. **Energy & Fuels**, v. 24, n. 3, 1668–1676, 2010.

RANZI, E.; FRASSOLDATI, A.; GRANATA, S. and FARAVELLI, T. Wide-range kinetic modeling study of the pyrolysis, partial oxidation, and combustion of heavy n-alkanes. **Industrial & engineering chemistry research**, v. 44, n. 14, 5170–5183, 2005.

RIBEIRO, N.M.; PINTO, A.C.; QUINTELLA, C.M.; DA ROCHA, G.O.; TEIXEIRA, L.S.; GUARIEIRO, L.L.; DO CARMO RANGEL, M.; VELOSO, M.C.; REZENDE, M.J.; SERPA DA CRUZ, R. *et al.* The role of additives for diesel and diesel blended (ethanol or biodiesel) fuels: a review. **Energy & fuels**, v. 21, n. 4, 2433–2445, 2007.

ROLON, J.; AGUERRE, F. and CANDEL, S. Experiments on the interaction between a vortex and a strained diffusion flame. **Combustion and Flame**, v. 100, n. 3, 422–429, 1995.

ROLON, J.; VEYNANTE, D.; MARTIN, J. and DURST, F. Counter jet stagnation flows. **Experiments in fluids**, v. 11, n. 5, 313–324, 1991.

ROSILLO-CALLE, F. and CORTEZ, L.A. Towards proalcool ii—a review of the brazilian bioethanol programme. **Biomass and Bioenergy**, v. 14, n. 2, 115–124, 1998.

SARATHY, S.; THOMSON, M.; PITZ, W. and LU, T. An experimental and kinetic modeling study of methyl decanoate combustion. **Proceedings of the Combustion Institute**, v. 33, n. 1, 399–405, 2011.

SARATHY, S.M.; OßWALD, P.; HANSEN, N. and KOHSE-HÖINGHAUS, K. Alcohol combustion chemistry. **Progress in Energy and Combustion Science**, v. 44, 40–102, 2014.

SAXENA, P. and WILLIAMS, F.A. Numerical and experimental studies of ethanol flames. **Proceedings of the Combustion Institute**, v. 31, n. 1, 1149–1156, 2007.

SESHADRI, K.; LU, T.; HERBINET, O.; HUMER, S.; NIEMANN, U.; PITZ, W.J.; SEISER, R. and LAW, C.K. Experimental and kinetic modeling study of extinction and ignition of methyl decanoate in laminar non-premixed flows. **Proceedings of the Combustion Institute**, v. 32, n. 1, 1067–1074, 2009.

SHAHIR, S.; MASJUKI, H.; KALAM, M.; IMRAN, A.; FATTAH, I.R. and SANJID, A. Feasibility of diesel–biodiesel–ethanol/bioethanol blend as existing ci engine fuel: An assessment of properties, material compatibility, safety and combustion. **Renewable and Sustainable Energy Reviews**, v. 32, 379–395, 2014.

SIGMA-ALDRICH, S.A. Methyl decanoate. `http://www.sigmaaldrich.com/catalog/product/aldrich/299030?lang=pt&region=BR`, 2016. [Online; accessed 14-May-2016].

SINGH, D.; NISHIIE, T. and QIAO, L. Experimental and kinetic modeling study of the combustion of n-decane, jet-a, and s-8 in laminar premixed flames. **Combustion Science and Technology**, v. 183, n. 10, 1002–1026, 2011.

SKRZECZ, A.; SHAW, D.G. and MACZYNSKI, A. Iupac-nist solubility data series 69. ternary alcohol–hydrocarbon–water systems. **Journal of Physical and Chemical Reference Data**, v. 28, n. 4, 983–1235, 1999.

TOXICOLOGY DATA NETWORK, T. Toxicology Data Network. `http://toxnet.nlm.nih.gov/`, 2016. [Online; accessed 17-January-2016].

TURNS, S.R. *et al.* **An introduction to combustion**, v. 287. McGraw-hill New York, 1996.

VOVELLE, C.; DELFAU, J.L. and REUILLON, M. Formation of aromatic hydrocarbons in decane and kerosene flames at reduced pressure. In **Soot formation in combustion**, pp. 50–65. Springer, 1994.

VOVELLE, C.; DELFAU, J.L.; REUILLON, M.; ACKRICH, R.; BOUHRIA, M. and SANOGO, O. Comparison of aromatics formation in decane and kerosene flames. In **Proceedings of the ACS national meeting, New York, NY**, v. 36, pp. 1456–63. 1991.

WANG, H.; WARNER, S.J.; OEHLSCHLAEGER, M.A.; BOUNACEUR, R.; BIET, J.; GLAUDE, P.A. and BATTIN-LECLERC, F. An experimental and kinetic modeling study of the autoignition of α-methylnaphthalene/air and α-methylnaphthalene/n-decane/air mixtures at elevated pressures. **Combustion and Flame**, v. 157, n. 10, 1976–1988, 2010.

WANG, Y.L.; FENG, Q.; EGOLFOPOULOS, F.N. and TSOTSIS, T.T. Studies of c 4 and c 10 methyl ester flames. **Combustion and Flame**, v. 158, n. 8, 1507–1519, 2011.

WESTBROOK, C.K. and DRYER, F.L. Chemical kinetic modeling of hydrocarbon combustion. **Progress in Energy and Combustion Science**, v. 10, n. 1, 1–57, 1984.

WESTBROOK, C.K.; PITZ, W.J.; HERBINET, O.; CURRAN, H.J. and SILKE, E.J. A comprehensive detailed chemical kinetic reaction mechanism for combustion of n-alkane hydrocarbons from n-octane to n-hexadecane. **Combustion and Flame**, v. 156, n. 1, 181–199, 2009.

YANOWITZ, J.; RATCLIFF, M.; MCCORMICK, R.; TAY, J. and MURPHY, M. Compendium of experimental cetane numbers. 2014.

ZEPPIERI, S.P.; KLOTZ, S.D. and DRYER, F.L. Modeling concepts for larger carbon number alkanes: a partially reduced skeletal mechanism for n-decane oxidation and pyrolysis. **Proceedings of the Combustion Institute**, v. 28, n. 2, 1587–1595, 2000.

ZHAO, Z.; LI, J.; KAZAKOV, A.; DRYER, F.L. and ZEPPIERI, S.P. Burning velocities and a high-temperature skeletal kinetic model for n-decane. **Combust. Sci. and Tech.**, v. 177, n. 1, 89–106,

2004.

APPENDIX A – Samples used in experimental tests

Table A.1: Blends used in solubility tests with anhydrous ethanol. Source: own elaboration

	Mass [$\pm 0.0001g$]			% Weight basis		
Sample	N-decane	Ethanol	Methyl decanoate	N-decane	Ethanol	Methyl decanoate
1	3.2150	0.4143	0.4109	79.6	10.3	10.2
9	2.0311	1.2021	0.8217	52.9	29.4	17.7
17	1.2067	0,8144	2.0120	29.9	20.2	49.9
20	1.2076	2.0051	0.8034	30.1	49.9	20.0
29	0.4051	0.4033	3.2040	10.1	10.1	79.9
36	0.4019	3.2064	0.4205	10.0	79.6	10.4

Table A.2: Blends used in solubility tests with hidrated ethanol. Source: own elaboration

	Mass [$\pm 0.0001g$]			% Weight basis		
Sample	N-decane	Ethanol	Methyl decanoate	N-decane	Ethanol	Methyl decanoate
1	3.2824	0.4281	0.4141	79.6	10.4	10.0
2	2.7938	0.4016	0.8002	69.9	10.1	20.0
3	2.8299	0.8148	0.4049	69.9	20.1	10.0
4	2.4012	0.4131	1.2162	59.6	10.2	30.2
5	2.4308	0.8549	0.8159	59.3	20.8	19.9
6	2.4522	1.3213	0.4554	58.0	31.2	10.8
7	2.0360	0.4210	1.6409	49.7	10.3	40.0
8	2.0592	0.8068	1.2114	50.5	19.8	29.7
9	2.0753	1.2189	0.8782	49.7	29.2	21.0
10	2.0212	1.7150	0.4414	48.4	41.1	10.6
11	1.6174	0.4080	2.0185	40.0	10.1	49.9
12	1.6840	0.8446	1.6575	40.2	20.2	39.6
13	1.6133	1.2094	1.2124	40.0	30.0	30.0
14	1.6408	1.6196	0.8615	39.8	39.3	20.9
15	1.6246	2.0362	0.4056	40.0	50.1	10.0
16	1.2301	0.4465	2.4157	30.1	10.9	59.0
17	1.2002	0.8159	2.0366	29.6	20.1	50.3
18	1.2336	1.3233	1.6988	29.0	31.1	39.9
19	1.2498	1.6466	1.2538	30.1	39.7	30.2
20	1.2343	2.0040	0.8132	30.5	49.5	20.1
21	1.2239	2.4310	0.4472	29.8	59.3	10.9
22	0.8266	0.4282	2.8392	20.2	10.5	69.4
23	0.8307	0.8052	2.4625	20.3	19.6	60.1
24	0.8174	1.2218	2.0587	19.9	29.8	50.2
25	0.8294	1.6331	1.6025	20.4	40.2	39.4
26	0.8386	2.0283	1.2577	20.3	49.2	30.5
27	0.8392	2.4401	0.8421	20.4	59.2	20.4
28	0.8285	2.8114	0.4184	20.4	69.3	10.3
29	0.4420	0.4674	3.2348	10.7	11.3	78.1
30	0.4425	0.8281	2.8530	10.7	20.1	69.2
31	0.4418	1.2891	2.4299	10.6	31.0	58.4
32	0.4115	1.6020	2.0692	10.1	39.2	50.7
33	0.4116	2.0500	1.6064	10.1	50.4	39.5
34	0.4377	2.4210	1.2494	10.7	58.9	30.4
35	0.4112	2.8771	0.8353	10.0	69.8	20.3
36	0.4458	3.3097	0.4615	10.6	78.5	10.9

Table A.3: Blends used in density test. Source: own elaboration

	Mass [$\pm 0.0001g$]			% Weight basis		
Sample	N-decane	Ethanol	Methyl decanoate	N-decane	Ethanol	Methyl decanoate
1	24.0067	3.0049	3.0166	79.9	10.0	10.0
3	21.0013	6.0283	3.0052	69.9	20.1	10.0
6	18.0052	9.0109	3.0045	60.0	30.0	10.0

Table A.4: Blends used in flash point test. Source: own elaboration

	Mass [$\pm 0.0001g$]			% Weight basis		
Sample	N-decane	Ethanol	Methyl decanoate	N-decane	Ethanol	Methyl decanoate
7	2.0030	0.4068	1.6009	49.9	10.1	39.9
10	2.0036	1.6104	0.4110	49.8	40.0	10.2
12	1.6079	1.6012	1.6012	40.1	20.0	39.9
22	0.8196	0.4450	2.8391	20.0	10.8	69.2